A PROBABILISTIC PROCEDURE FOR DETERMINING THE SEISMIC LOAD AGAINST RETAINING WALLS THAT ACCOUNTS FOR STRENGTH VARIABILITY

by

D.A. Grivas and S. Slomski

Report No, CE-82-8

Department of Civil Engineering
Rensselaer Polytechnic Insittute
Troy, New York 12181

Sponsored by the Earthquake Hazard Mitigation Program of the National Science Foundation under Grant No. PFR-7905500

July 1982

50272-101

REPORT DOCUMENTATION PAGE	1. REPORT NO. NSF/CEE-82200	2.	3. Recipient's Accession No. PB84 111467

4. Title and Subtitle
Probabilistic Procedures for Determining the Seismic Load Against Retaining Walls That Accounts for Strength Variability

5. Report Date
July 1982

6.

7. Author(s)
D.A. Grivas, S. Slomski

8. Performing Organization Rept. No.
CE-82-8

9. Performing Organization Name and Address
Rensselaer Polytechnic Institute
Department of Civil Engineering
Troy, NY 12181

10. Project/Task/Work Unit No.

11. Contract(C) or Grant(G) No.
(C)
(G) CEE7905500

12. Sponsoring Organization Name and Address
Directorate for Engineering (ENG)
National Science Foundation
1800 G Street, N.W.
Washington, DC 20550

13. Type of Report & Period Covered

14.

15. Supplementary Notes
Submitted by: Communications Program (OPRM)
National Science Foundation
Washington, DC 20550

16. Abstract (Limit: 200 words)

Methods available for the determination of the force system acting on rigid retaining walls under static or seismmic conditions are reviewed. The function of random soil parameters is described statistically. Two techniques capable of providing approximations to the statistical values of functions of random soil properties are investigated. It is determined that the point estimates method is more accurate and easier to implement than the series approximation method. In a similar investigation of procedures available to describe the spatial variability of soil properties, it is concluded that the quasi-stationary autoregressive method provides a better approach than the average mean-crossings distance method or the moving average method. The effect of important material, loading, and model parameters on the force system against rigid retaining walls is considered.

17. Document Analysis a. Descriptors

Soils
Walls
Retaining walls
Loads (structures)
Soil properties
Mathematical models
Earthquakes
Dynamic structural response
Earthquake resistant structures
Computer programs

b. Identifiers/Open-Ended Terms
Ground motion

D.A. Grivas, /PI

c. COSATI Field/Group

18. Availability Statement	19. Security Class (This Report)	21. No. of Pages
NTIS	20. Security Class (This Page)	22. Price

(See ANSI-Z39.18) See Instructions on Reverse

OPTIONAL FORM 272 (4-77)
(Formerly NTIS-35)
Department of Commerce

TABLE OF CONTENTS

TABLE OF CONTENTS
(Continued)

TABLE OF CONTENTS
(Continued)

LIST OF TABLES

LIST OF TABLES
(Continued)

LIST OF FIGURES

LIST OF FIGURES
(Continued)

LIST OF FIGURES
(Continued)

LIST OF SYMBOLS

ENGLISH CHARACTERS

a_h	Horizontal component of maximum ground acceleration
a_v	Vertical component of maximum ground acceleration
d_A	Distance between the base of the wall and the point of application of active earth thrust
d_i	Thickness of the equivalent statistically independent layers
E[ ]	Expected value of the quantity in brackets.
F	Force normal to interface between slices
f( )	Probability density function of the quantity in parenthesis
g	Acceleration of gravity
H	Height of retaining wall
h	Distance between base of retaining wall and point of application of interslice normal force
i	Inclination with the horizontal direction of surface of backfill material
k	Constant
k	Number of data point included in spatial averages
k*	Parameter entering the variance reduction function

ENGLISH CHARACTERS (Continued)

ℓ	Correlation Length
N	Number of data points
n_i	Number of equivalent statistically independent layers
P_A	Active earth thrust (under static conditions)
P_{AE}	Active earth thrust (under seismic conditions)
P_{PE}	Passive earth thrust (under seismic conditions)
P_-, P_o, P_+	Probabilities associated with the point approximation of a random variable
R	Resultant force on failure plane
r	Autocorrelation function
S_u	Undrained shear strength
u	Ratio of material parameter x(z) over depth z
$\bar{u}_k$	Spatial averages of k consecutive points
V	Coefficient of variation
V_i	Shear force along interface between slices
V[ ]	Variance of the quantity in brackets
W	Weight
x	Random variable
y( )	Function of the random variables in parenthesis
z	Depth
Δz_o	Distance between two consecutive uniformly-spaced points along a borehole

GREEK CHARACTERS

α_3	Coefficient of skewness (normalized third central moment)
α_4	Coefficient of kurtosis (normalized fourth central moment)
β	Inclination with the vertical direction of the back face of the retaining wall
β_o, β_1	Parameters used in the quasi-stationary autoregressive method
γ	Unit weight of the backfill material
$\Gamma^2( )$	Variance reduction function
δ	Angle of soil-wall friction
δ_i	Distance between two consecutive mean-crossings of the value of a material parameter
ε	Error term
θ	Inclination of the failure plane with the horizontal direction
θ	Angle of rotation of the direction of maximum acceleration (in Mononobe-Okabe analysis)
μ	Central moment
σ^2	Variance
σ_k^2	Spatial variance for k consecutive points
ρ	Correlation coefficient
ϕ	Angle of internal friction of the backfill material

PREFACE

This is the second in a series of reports on the research project entitled "Reliability of Soil Retaining Structures during Earthquakes". This study is sponsored by the Earthquake Hazard Mitigation Program of the National Science Foundation under Grant No. PFR-7905500, and is directed jointly by Dr. Dimitri A. Grivas, Associate Professor of Civil Engineering, Rensselaer Polytechnic Institute, and Dr. Milton E. Harr, Professor of Civil Engineering, Purdue University. Drs. Ralph B. Peck and Neville C. Donovan serve as advisors to the project of which Dr. Michael Gaus is the Earthquake Hazard Mitigation Program Manager.

The authors are thankful to the National Science Foundation for sponsoring this research. Special thanks are also extended to Mrs. Betty Alix and Mrs. Jo Ann Grega for their typing of this report.

ABSTRACT

A procedure is presented for the determination of the force system acting on rigid retaining walls located in an earthquake environment. This is based on a quasi-static, Coulomb type analysis that satisfies the additional requirement of equilibrium of moments and, at the same time, it accounts for two important uncertainties: the spatial (vertical) variability of the strength of the backfill material and the randomness in the value of the seismic loading. The latter is introduced into the analysis in terms of the maximum ground acceleration expected to occur at the site of the retaining wall during an earthquake.

As a part of this study, an investigation is made of two techniques capable of providing approximations to the statistical values of functions of random soil properties (case of statistically homogeneous soil deposits). It is concluded that the "point estimates method" is more accurate and easier to implement than the "series approximation method". Moreover, in a similar investigation on procedures currently available for the description of the spatial variability of soil properties (case of heterogeneous soil deposits), it is concluded that the "quasi-stationary autoregressive method" provides a better approach than the "average mean-crossings distance method" and the "moving average method". This is particularly true for the commonly encountered situations of limited data available or of soil properties exhibiting a trend (e.g.,

increase) with depth.

The quasi-stationary, autoregressive method is subsequently employed to describe the vertical variability of the strength of cohesionless backfill materials. This results to two distinct but equivalent models for the backfill (a single-layer and a multi-layer representation) both of which are presented and discussed.

The effect of important material, loading and model parameters on the force system against rigid retaining walls is examined in a comprehensive parametric study, the findings of which are presented in a series of figures and tables.

CHAPTER 1

TECHNICAL BACKGROUND

A brief review is presented herein of the methods available for the determination of the force system acting on rigid retaining walls under static or seismic conditions. This is followed by a summary of the knowledge that has been acquired on the subject through tests performed on models of retaining walls under simulated earthquake conditions. Finally, the scope of this study is presented together with an overview of its content.

1.1 Theoretical Methods

1.1.1 The Coulomb Method

The first procedure for the determination of the earth thrust against retaining walls was proposed by Coulomb in 1776. It is based on the notion that failure of a retaining wall is accompanied by a sliding of the soil mass located in the back of the wall and on the following assumptions:

(a) the failure surface has a planar shape;

(b) the shear strength of the soil material is fully mobilized along the failure plane; and

(c) the lateral earth pressure on the wall increases linearly with depth.

The first two assumptions are valid if the wall experiences a sufficient movement during failure. While the third assumption is valid only in the case of smooth, vertical walls with a horizontal backfill (Terzaghi, 1936). Moreover, results obtained with model walls have shown that the third assumption is definitely invalid for walls under dynamic loading conditions (Matsuo and Ohara, 1960; Ichihara, 1965; Nazarian and Hadjian, 1979; etc.).

In Fig. 1.1 is shown schematically the force system acting on a retaining wall and its backfill material in accordance with the Coulomb method. This includes the weight of the backfill, W, the resultant of the shearing forces, R, and the earth thrust against the wall, P. The value of the latter was found by Coulomb to be equal to

$$P_A = \frac{\gamma H^2}{2} \frac{\tan(\theta-\phi)}{\tan\theta} \tag{1.1}$$

in which

γ = the unit weight of the backfill,

H = the height of the retaining wall,

ϕ = the angle of internal friction of the backfill material and

θ = the angle between the failure plane and the horizontal direction ($\theta = 45° + \phi/2$).

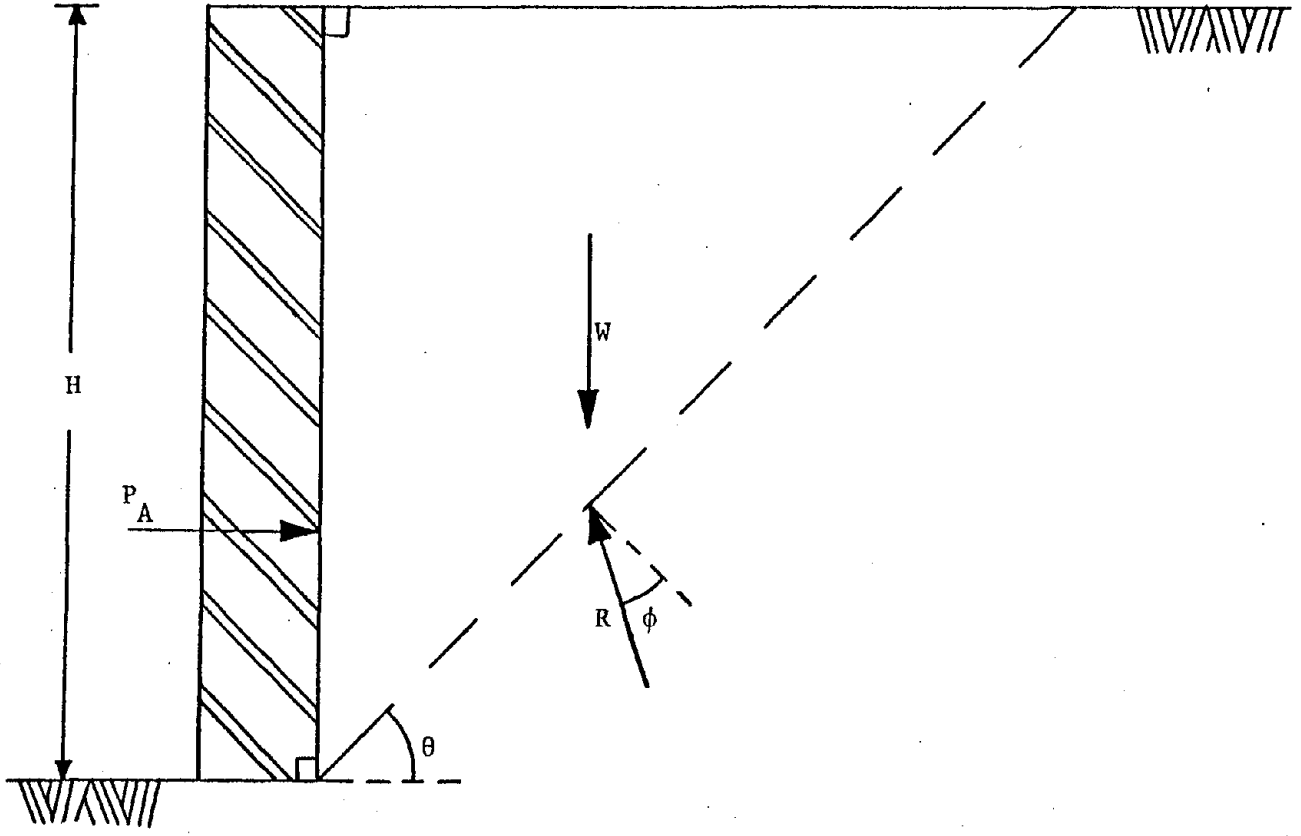

FIGURE 1.1 FORCE SYSTEM ON THE SLIDING SOIL MASS IN ACCORDANCE WITH THE COULOMB METHOD

1.1.2 The Mononobe-Okabe Method

The Coulomb theory was considered to be sufficient for the design of retaining walls for approximately one and a half century. The 1923 earthquake in Kwanto, Japan, however, brought to the attention of the engineering community the effects that earthquakes have on retaining walls which, in turn, generated considerable interest on the subject. Thus, in the late 1920's Okabe (1926) and Mononobe (1929) proposed a method for determining the "dynamic" loads on retaining walls due to earthquakes. This method commonly referred to as "the Mononobe-Okabe Method" is basically a simple extension of Coulomb's theory which includes the seismic force on the backfill material. The additional assumption was made that the acceleration of the backfill is uniform throughout the soil mass. This allowed the seismic forces to be expressed as two additional body forces equal to $a_h W$ and $a_v W$ along the horizontal and vertical direction, respectively. The resulted force system on the sliding edge is shown schematically in Fig. 1.2.

The dynamic active earth thrust P_{AE} against the retaining wall, shown in Fig. 1.2, was given by Mononobe (1929) as

$$P_{AE} = \frac{\gamma H^2}{2} (1+a_v) K_{AE} \tag{1.2}$$

in which

$$K_{AE} = \frac{\cos^2(\phi-\theta-\alpha)}{\cos\theta\cos^2\alpha\cos(\delta+\alpha+\theta)\left[1+\left\{\frac{\sin(\phi+\delta)\sin(\phi-\theta-i)}{\cos(\delta+\alpha+\theta)\cos(i-\alpha)}\right\}^{1/2}\right]^2}$$

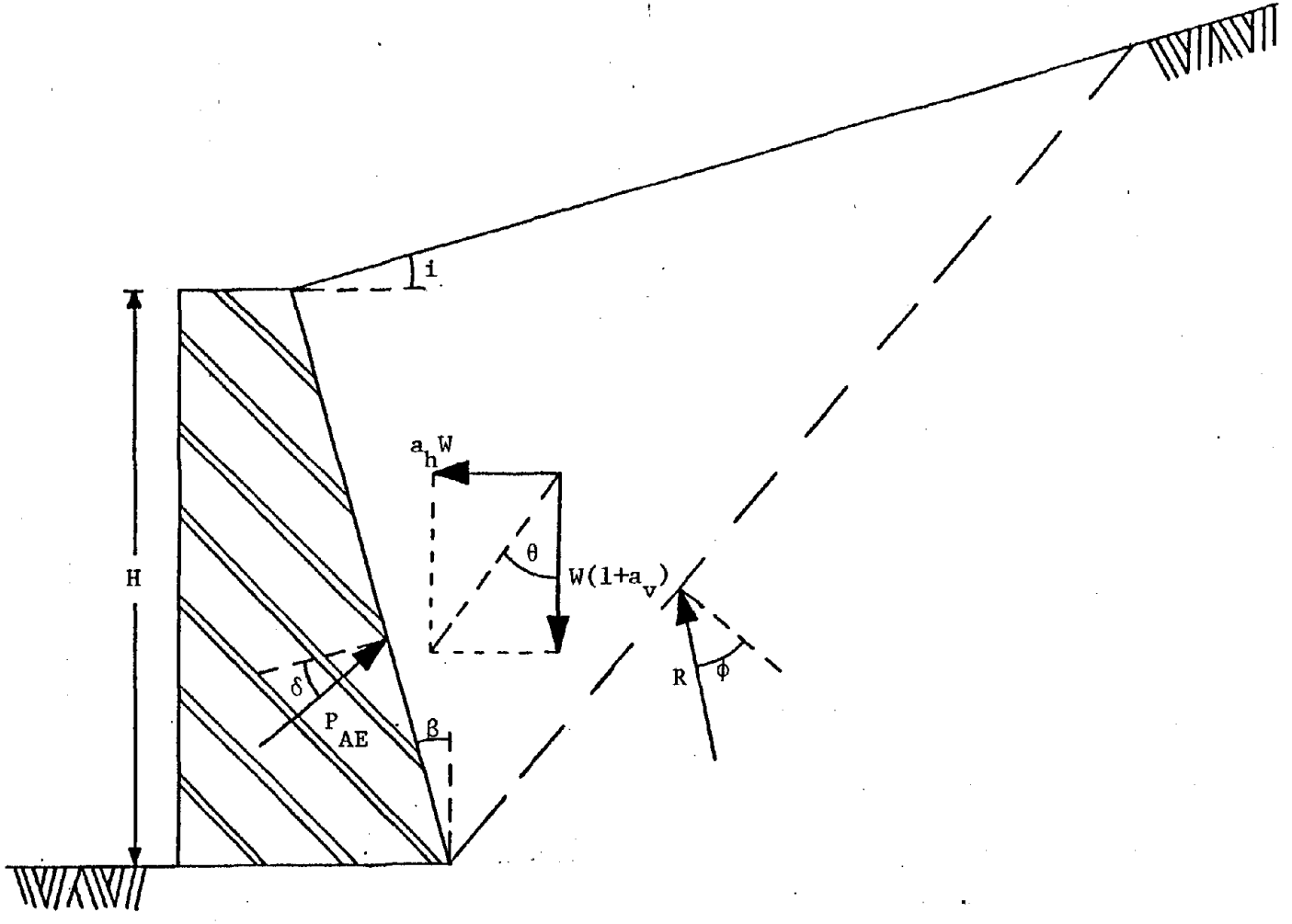

FIGURE 1.2 FORCE SYSTEM ON THE SLIDING SOIL MASS IN ACCORDANCE WITH THE MONONOBE-OKABE METHOD

γ = the unit weight of the backfill material,

H = the height of the retaining wall,

ϕ = the angle of internal friction of the backfill material,

δ = the angle of soil-wall friction,

i = the inclination of the backfill with the horizontal,

α = the inclination of the back face of the wall,

$\theta = \tan^{-1}\left(\frac{a_h}{1+a_v}\right)$,

a_h = the coefficient of the maximum horizontal ground acceleration, in g's, and

a_v = the coefficient of the maximum vertical ground acceleration, in g's.

Finally, it should be noted that the Mononobe-Okabe method provides a dynamic component for the earth thrust that acts at the midpoint of the retaining wall. This has been shown by model tests to be unrealistic (Mononobe and Matsuo, 1929; Prakash and Nandakumaran, 1973; etc.).

1.1.3 The Prakash-Basavanna Method

Prakash and Basavanna (1969) proposed a method of determining the earth thrust against a retaining wall and its point of application by satisfying the additional requirement of equilibrium of moments. This additional condition was used to derive (rather than assume, as was the case for the Coulomb and Mononobe-Okabe methods) the point of application of the earth thrust along the retaining wall.

The following assumptions were made in this method:

(a) the pressure at any point is geostatic, and

(b) the principle of superposition is valid.

In Fig. 1.3 is shown schematically the use of the principle of superposition of forces as employed by Prakash and Basavanna. Fig. 1.3(b) represents the force system on the soil mass for only horizontal body forces and Fig. 1.3(c) that for only vertical forces. From the conditions of equilibrium of moments around point A located at the base of the wall, Fig. 1.3(a), the following expression was obtained for the active earth thrust P_{AE}:

$$P_{AE} = \frac{\gamma H^2 \sin(\beta+i)[\cot(\beta+i)+\cos(\theta-i)]}{2\sin^2\beta\sin(\beta+i-\delta)} \cdot \qquad (1.3)$$

$$\cdot \left[\frac{\{(1+a_v)\sin i+a_h\cos i\}\tan(\beta+i-\delta)}{\tan(\beta+i-\delta)+\tan(\theta-i-\phi)} + \frac{(1+a_v)\cos i+a_h\sin i}{\cot(\beta+i-\delta)+\cot(\theta-i-\phi)}\right]$$

in which θ is the inclination of the failure plane with the horizontal.

The distance d_A between the point of application of P_{AE} and the base of the wall was found using the expressions of the moment M_A of the force system around point A (Fig. 1.3) and of the active thrust P_{AE}, given in Eqn. (1.3).

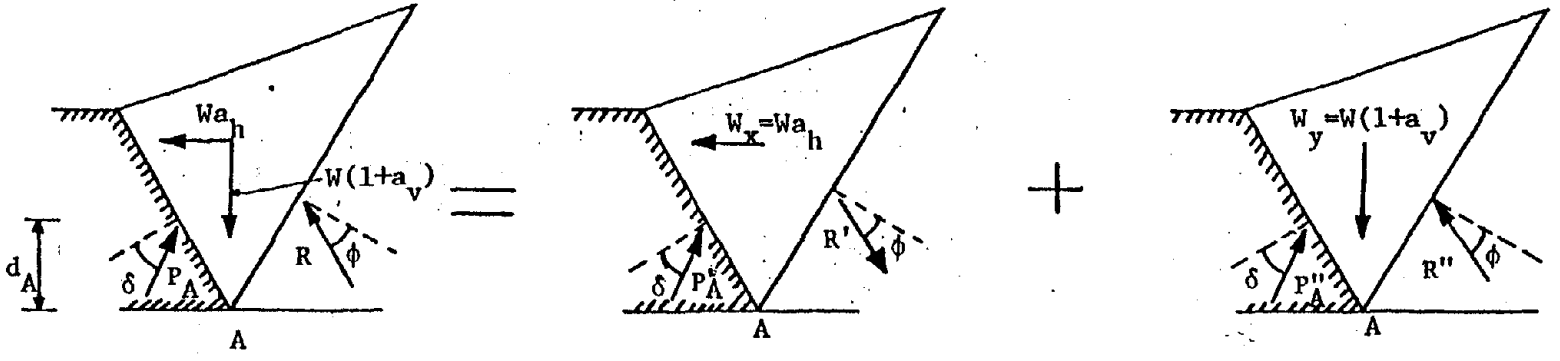

(a) Forces on Sliding Wedge (b) Horizontal Forces (c) Vertical Forces

FIGURE 1.3 SUPERPOSITION OF FORCES ACTING ON THE SLIDING WEDGE (AFTER PRAKASH AND BASAVANNA, 1969)

1.1.4 Other Methods

Other methods of determining the earth thrust against a retaining wall have been presented in the literature. Dubrova (1963) developed a static method including the movement of the wall, while Saran and Prakash (1977) extended Dubrova's theory to include seismic conditions. Finally, Richard and Elms (1979) developed a procedure that is applicable for gravity walls only and includes a maximum limit of acceptable wall movements during earthquakes. A detailed presentation of these methods can be found in Vlavianos (1981).

1.2 Observations During Model Tests

Several investigators have performed tests on models of retaining walls in an attempt to determine the magnitude and distribution of the earth thrust behind the wall.

In general, these model tests were conducted with metal-lined boxes filled with uniform clean sand. The wall was represented by one side of the box which was hinged so movements could occur. The soil pressure against the hinged wall were measured by pressure gauges which were either buried in the fill near the wall or mounted between the wall and a stationary support. The accelerations of the fill were induced by a shaking table or a falling pendulum.

Model test results for earthquake-like loads are summarized in Table 1.1. There is general agreement that the height h_d of the dynamic component of the earth thrust above the base of the wall varies

TABLE 1.1

MODEL TEST RESULTS OF RIGID WALLS UNDER EARTHQUAKE-LIKE LOADS

INVESTIGATORS	TEST CONDITIONS	FINDINGS
Mononobe and Matsuo (1929)	Models of Retaining Walls Apparatus: Metal lined box with a door hinged at base Pressure gauge 4.5 ft. above base Mounted on a shaking table Dimensions: 4 ft high, 9 to 12 ft long Material : Uniform clean dry sand Conditions: Horizontal acceleration, $0.0 \leq a_h \leq 0.4g$	1. Dynamic force at $h_d = H/3$ (h_d measured from wall base) 2. Worst Case: a_h toward wall a_v upward
Matsuo and Ohara (1960)	Models of Quay Walls Apparatus: Metal- or glass-lined box Fixed or hinged at base Pressure cells on wall centerline at 3 heights Mounted on shaking table Dimensions: 0.4m high, 1.0m long Material : Uniform clean sand, dry and saturated Conditions: $0.2g \leq a_h \leq 0.4g$	1. Dynamic force at $h_d \simeq 0.55H$
Ichihara (1965)	Models of Retaining Walls Apparatus: Metal lined wall inside a box 8 pressure cells on wall face Shaking table struck by falling pendulum Dimensions: 1m high, 5m long Material : Uniform clean dry sand Conditions: horizontal shock acceleration $3.3g \leq a_h \leq 4.2g$	1. $0.36H \leq h_d \leq 0.44H$ 2. Dynamic pressure ≈ parabolic 3. Failure plane located at $\theta_{cr} < 45° + \phi/2$, slightly concave

TABLE 1.1

(continued)

INVESTIGATORS	TEST CONDITIONS	FINDINGS
Prakash et al. (1973)	Models of Retaining Walls Apparatus : Metal-lined wall inside a box 8 pressure cells on wall face Shaking table struck by falling pendulum Dimensions: 1 m. high, 5 m. long Material : Uniform clean dry sand Conditions: horizontal shock acceleration $3.3g \leq a_h \leq 4.28$	1. $0.36H \leq h_d \leq 0.444$ 2. Dynamic pressure $\approx$ parabolic 3. Failure plane located at $\theta_{cr} < 45° + \phi/2$, slightly concave
Nazarian et al. (1979)	Reviewed previously done model tests, including those by Nandakumaran and Joshi	1. h_d increases parabolically as δ decreases 2. h_d decreases with β 3. h_d increases with surcharge 4. h_d increases linearly with increasing a_h 5. $0.33H \leq h_d \leq 0.66H$

between 0.35H and 0.65H, where H is the height of the wall.

1.3 Scope of the Present Study

In general, although a large amount of experience has accumulated concerning the design and performance of retaining walls, geotechnical engineers still face considerable uncertainties when analyzing their stability. These reflect the variability of the material parameters, the randomness associated with the applied loading conditions, as well as the uncertainty associated with the employed analytical procedures.

None of the methods presented above considers the uncertainties involved in either the material parameters (including their spatial variability) or the loading conditions. To explicitly account for these uncertainties and to provide a statistical description of the force system on retaining walls during earthquakes is the overall objective of the present study.

A statistical description of the functions of random soil parameters is presented in Chapter 2. In Chapter 3 are given in detail methods available for the determination of the spatial variability of soil properties together with a case study in which these methods are applied and compared. Chapter 4 presents a procedure developed to determine the earth thrust against a retaining wall which accounts for the spatial variability of the strength of the backfill material and the uncertainty around the exact value of the seismic loads. The results

of a parametric study on the effect of important material, loading and modeling parameters on the force system acting on retaining walls are presented in Chapter 5. Finally, Chapter 6 provides a comparison of results obtained from the developed procedure and those measured during previously conducted model tests.

CHAPTER 2

STATISTICAL VALUES OF FUNCTIONS OF RANDOM SOIL PARAMETERS

2.1 Soil as a Statistically Homogeneous Medium

In geotechnical practice, the numerical values of soil parameters are determined on the basis of measurements taken during a few, relatively simple, field or laboratory tests. Because of the inherent variability of the soil material and the errors that are intrinsic to all experimental methods, the numerical value of any measured soil parameter is expected to exhibit some degree of variation. This variation is properly accounted for by introducing soil parameters as random variables, an approach that has been systematically pursued in recent applications of probabilistic methods in geotechnical engineering.

Let x denote a random soil parameter and $f_x(x)$ its probability density function. If the statistical values (e.g., mean, variance, etc.) and the probability density function of x remain constant anywhere within a soil layer, then the latter is said to represent a statistically homogeneous medium. In this case, the statistical characteristics of x may be obtained simply by performing a statistical analysis on the values of x as determined in the field (measured at different points within the same soil layer) or in the laboratory (measured through tests on samples drawn from different locations of same soil layer).

In practice, however, one is often interested in the statistical characteristics of a function of one or more random variables.

An example of such a function is the expression for the earth thrust against a retaining wall, in which the angle of internal friction represents the random variable x; or, the expression for the factor of safety of a slope under drained conditions, in which the soil cohesion and its angle of internal friction are the random variables. A geotechnical engineer's ability to provide a statistical description of such functions is essential for a probabilistic formulation of the problem at hand.

2.2 Exact Statistical Values of Functions of Random Parameters

Let y represent a function of a random variable x, i.e.,

$$y = y(x) \tag{2.1}$$

A probabilistic study of a geotechnical problem usually requires the determination of the first two central moments of y, i.e., its expected value E[y] and variance V[y]. If $f_x(x)$ denotes the probability density function of x, then the general expressions for E[y] and V[y] are given as (Papoulis, 1965)

$$\begin{aligned} E[y] &= \bar{y} = \int_{-\infty}^{\infty} y\, f_x(x)\, dx \\ V[y] &= \int_{-\infty}^{\infty} (y - \bar{y})\, f_x(x)\, dx \end{aligned} \tag{2.2}$$

For relatively simple functions of y and $f_x(x)$, the integrations denoted in Eqns. (2.2) may be easy to perform analytically. If, however, the expressions for y and/or $f_x(x)$ are complicated, then the indicated integrations may be difficult to accomplish. In this

case, one has to perform a numerical integration or use some alternative, approximate method to obtain the statistical values of y.

Statistical theory provides two approximate methods of determining Eqns. (2.2): one, based on a Taylor's series approximation of y, and, another, using a point estimate technique. These two methods are presented below.

2.3 Series Approximation Method (SAM)

When the first and second derivatives of y(x) with respect to x can be determined, then a Taylor's series approximation of y can be employed in order to perform the integration appearing in Eqns. (2.2).

A Taylor's series expansion of function y(x) about the mean value $\bar{x}$ of the variable x has the following expression:

$$y(x) = y(\bar{x}) + y'(\bar{x})(x-\bar{x}) + \frac{y''(\bar{x})}{2!}(x-\bar{x})^2 + \ldots \tag{2.3}$$

in which the number of primes denotes the order of the derivative of y(x) evaluated at the mean value $\bar{x}$. By retaining only terms up to the second order, the first two central moments of y are equal to (Hahn and Shapiro, 1967)

$$E[y] = y(\bar{x}) + \frac{1}{2} y''(\bar{x})\ \sigma_x^2$$

$$V[y] = y'(\bar{x})\ \sigma_x^2 \tag{2.4}$$

in which σ_x is the standard deviation of x and all derivatives are evaluated at $\bar{x}$.

2.4 Point Estimate Method (PEM)

A general procedure for estimating the statistical moments of a function of one or more variables was proposed for the first time by Rosenblueth (1975). It is based on evaluations of the function at two or more discrete points which can be easily determined from the statistical values of the random variables.

Thus, in the case of a function y of only one random variable x, i.e., $y = y(x)$, the method requires that the continuous probability density function of x be replaced by an equivalent discrete distribution $p_x(x_i)$ whose statistical values (e.g., mean, variance, etc.) are identical to those of the continuous variable x. The number and magnitude of the discrete values x_i depend on the statistical values of x and on the desirable level of accuracy.

2.4.1 Two-Point Estimates

The simplest possible representation of x by a discrete variable x_i is one in which x is considered to be concentrated at only two points. These points may be conveniently denoted as x_- and x_+ and correspond to values of x below and above its mean value $\bar{x}$, respectively. There are two weights, P_- and P_+, that are associated with the two point estimates of x and represent the percentage of the density function $f_x(x)$ that is concentrated at x_- and x_+, respectively. In discretizing x, the following conditions must be satisfied:

$$
\begin{aligned}
&P_+ + P_- = 1 \\
&P_+ x_+ + P_- x_- = \bar{x} \\
&P_+(x_+ - \bar{x})^2 + P_-(x_- - \bar{x})^2 = \sigma_x^2 \\
&P_+(x_+ - \bar{x})^3 + P_-(x_- - \bar{x})^3 = \alpha_3 \sigma_x^3
\end{aligned}
\tag{2.5}
$$

in which α_3 is the coefficient of skewness of x defined as

$$\alpha_3 = \frac{\mu_3}{\sigma_x^3}$$

When the statistical values ($\bar{x}$, σ_x, α_3) of x are known, from Eqns. (2.5) one can determine the corresponding values of x_+, x_- and P_+, P_-. These are equal to

$$
\begin{aligned}
&P_+ = \frac{1}{2}\left[1 \pm \left(1 - \frac{1}{1 + \left(\frac{\alpha_3}{2}\right)^2}\right)^{1/2}\right] \\
&P_- = 1 - P_+ \\
&x_+ = \bar{x} + \sigma_x (P_-/P_+)^{1/2} \\
&x_- = \bar{x} - \sigma_x (P_+/P_-)^{1/2}
\end{aligned}
\tag{2.6}
$$

The sign preceding the parenthesis in the first of the equations above is opposite that of α_3 (i.e., positive, when $\alpha_3 < 0$ and negative, when $\alpha_3 > 0$). When $\alpha_3 < 0$, the distribution is skewed to the lower values of x; when $\alpha_3 > 0$, the distribution is skewed to the higher values of x; and when $\alpha_3 = 0$, the distribution is symmetrical.

The estimate of the m-th moment of function y has the following expression:

$$E[y^m] = P_+ \, y(x_+)^m + P_- \, y(x_-)^m \tag{2.7}$$

The expected value E[y] and second moment $E[y^2]$ of y can be found from Eqn. (2.7) by letting m become equal to one and two, respectively. The variance V[y] of y can be determined by subtracting the square of the expected value of y from its second moment. Thus, the expressions for E[y] and V[y] found from Eqn. (2.7) are equal to

$$E[y] = P_+ \, y(x_+) + P_- \, y(x_-)$$

$$V[y] = P_+ \, y(x_+)^2 + P_- \, y(x_-)^2 - E[y]^2 \tag{2.8}$$

2.4.2 Three-Point Estimate

The point estimate method can be easily generalized to include more points in the distribution $p_x(x_i)$ in order to increase the accuracy with which $f_x(x)$ is represented by $p_x(x_i)$. In this case, the determination of the point estimates of x and of the associated weights require a previous knowledge of higher moments of x.

A three point estimate can be made by locating the third point at the mean value of x. In this case, five equations are needed in order to specify the distrete distribution of x, i.e., the values of x_-, x_+ and those of the probabilities P_-, P_o and P_+ at x_-, $\bar{x}$ and x_+, respectively. The first of these equations is obtained as the sum of the probabilities P_-, P_o, P_+, at the discrete values x_-,

$\bar{x}$, x_+, respectively, equal to one. The remaining four equations are provided by specifying the mean value, second, third and fourth central moments of x. Thus,

$$\begin{aligned} &P_+ + P_o + P_- = 1 \\ &P_+ x_+ + P_o \bar{x} + P_- x_- = \bar{x} \\ &P_+(x_+ - \bar{x})^2 + P_- (x_- - \bar{x})^2 = \sigma_x^2 \\ &P_+(x_+ - \bar{x})^3 + P_-(x_- - \bar{x})^3 = \alpha_3 \sigma_x^3 \\ &P_+(x_+ - \bar{x})^4 + P_-(x_- - \bar{x})^4 = \alpha_4 \sigma_x^4 \end{aligned} \tag{2.9}$$

where P_o is the probability associated with $\bar{x}$ and α_4 is the coefficient of kurtosis of x, defined as

$$\alpha_4 = \frac{\mu_4}{\sigma_x^4}$$

The coefficient of kurtosis refers to the degree of peakedness of the distribution of x. The normal distribution, frequently used as a standard of comparison for other distributions, has a value of α_4 equal to three ($\alpha_4 = 3$). Thus, when $\alpha_4 < 3$, the distribution is flatter than the normal distribution, while when $\alpha_4 > 3$, the distribution is more peaked than the normal.

Equations (2.9) represent a system of five algebraic equations with five unknowns: P_-, P_o, P_+, x_- and x_+. Solving Eqns. (2.9), it is found that

$$P_o = 1 - \frac{1}{\alpha_4 - \alpha_3^2}$$

$$P_- = \frac{2}{\alpha_4 - \alpha_3^2}\left\{4 + \frac{\alpha_3^2}{\alpha_4 - \alpha_3^2} \pm \left[\frac{4\alpha_3^2}{\alpha_4 - \alpha_3^2} + \left(\frac{\alpha_3^2}{\alpha_4 - \alpha_3^2}\right)^2\right]^{1/2}\right\}^{-1}$$

$$P_+ = \frac{1}{\alpha_4 - \alpha_3^2} - P_- \qquad (2.10)$$

$$x_+ = \bar{x} + \sigma_x \left[P_+(1 + P_+/P_-)\right]^{-1/2}$$

$$x_- = \bar{x} - \frac{P_+}{P_-}(x_+ - \bar{x})$$

in which the sign preceding the brackets in the expression for P_- is opposite that of α_3 (i.e., positive, when $\alpha_3 < 0$ and negative, when $\alpha_3 > 0$).

In the case of three point estimates, the estimates of the expected value and variance of y are expressed as

$$E[y] = P_+ y(x_+) + P_o y(\bar{x}) + P_- y(x_-)$$

$$V[y] = P_+ y(x_+)^2 + P_o y(\bar{x})^2 + P_- y(x_-)^2 - E[y]^2 \qquad (2.11)$$

The point estimate method has been generalized for functions of several random variables by Harrop-Williams (1980) and Howland (1981).

For the case of a function y of two symetrically distributed random variables, i.e., $y = y(x_1, x_2)$, whose statistical values and correlation coefficient ρ are known, the expression for the m-th moment of y is equal to

$$E[y^m] = P_{++}y(x_{1+},x_{2+})^m + P_{+-}y(x_{1+},x_{2-})^m + P_{-+}y(x_{1-},x_{2+})^m + P_{--}y(x_{1-},x_{2-})^m \tag{2.12}$$

in which

$$P_{++} = P_{--} = \frac{1+\rho}{4}$$

$$P_{+-} = P_{-+} = \frac{1-\rho}{4},$$

and

$$y(x_{1+}, x_{2+}) = y(\bar{x}_1 + \sigma_{x_1}, \bar{x}_2 + \sigma_{x_2})$$

$$y(x_{1+}, x_{2-}) = y(\bar{x}_1 + \sigma_{x_1}, \bar{x}_2 - \sigma_{x_2})$$

$$y(x_{1-}, x_{2+}) = y(\bar{x}_1 - \sigma_{x_1}, \bar{x}_2 + \sigma_{x_2})$$

$$y(x_{1-}, x_{2-}) = y(\bar{x}_1 - \sigma_{x_1}, \bar{x}_2 - \sigma_{x_2}).$$

The general expression for Eqn. (2.12), for the case where y is a function of n symmetrically distributed random variables, may be written as

$$E[y^m] = \sum_{i_n=1}^{2} \cdots \sum_{i_2=1}^{2} \sum_{i_1=1}^{2} [P_{i_1 i_2 \ldots i_n} \, y_{i_1 i_2 \ldots i_n}] \tag{2.13}$$

in which

$$P_{i_1 i_2 \ldots i_n} = \frac{1}{2^n} \{1 + \sum_{k=1}^{n-1} \sum_{\ell=k+1}^{n} [(-1)^{i_k + i_\ell} \rho_{k\ell}]\},$$

and

$$y_{i_1 i_2 \ldots i_n} = y[\bar{x}_1 - (-1)^{i_1} \sigma_{x_1}, \bar{x}_2 - (-1)^{i_2} \sigma_{x_2} \ldots, \bar{x}_n - (-1)^{i_n} \sigma_{x_n}]$$

where $\rho_{k\ell}$ is the correlation coefficient for the k-th and ℓ-th variables.

2.5 Comparison of Approximate and Exact Methods

Three methods of estimating the first two moments of a function of one random variable have been presented in the previous sections. These are the Taylor's series approximation, the two-point estimate and the three-point estimate methods. In this section, a comparison will be made between the statistical values of functions obtained using the exact and the presented approximate methods.

This is achieved using several expressions for function y and frequency distribution $f_x(x)$ of the random variable x. Relatively simple expressions are chosen for y and $f_x(x)$ so that the exact values of the moments of y may be determined by the analytical expressions given in Eqns. (2.2).

The first comparison examines the effects of the type of distribution of x on the estimated statistical moments of y. The models used for $f_x(x)$ are the uniform, normal, exponential, and beta distributions; while the functions employed are y = c(constant), $y = x$, $y = x^2$, and $y = e^{-x}$. The results are presented in Table 2.1.

The expected value of the function is determined from Eqn. (2.2a) and the Taylor's series approximation from Eqn. (2.4). The discrete distribution of x for use in the two-point estimate is found from Eqns. (2.6) and its expected value from Eqn. (2.8a).

From Table 2.1, it can be seen that, for the first three functions examined, the resulting values of E[y] are equal to the exact values, regardless of the type of distribution. In the case

Table 2.1 Comparison of the Exact and Approximate Expected Values of Several Functions

$y = y(x)$	$f_x(x)$	Expected Value		
		Exact	SAM	PEM-2 point
$y = c$	Uniform	C	C	C
	Normal	C	C	C
	Exponential	C	C	C
	Beta	C	C	C
$y = x$	Uniform	0.0	0.0	0.0
	Normal	0.0	0.0	0.0
	Exponential	1.0	1.0	1.0
	Beta	0.5	0.5	0.5
$y = x^2$	Uniform	3.0	3.0	3.0
	Normal	1.0	1.0	1.0
	Exponential	2.0	2.0	2.0
	Beta	0.33	0.33	0.33
$y = e^{-x}$	Uniform	3.33	2.50	2.92
	Normal	1.58	1.50	1.54
	Exponential	0.500	0.572	0.568
	Beta	0.632	0.632	0.632

SAM = Series Approximation Method

PEM-2 = Point Estimate Method Using 2 Points

of $y = e^{-x}$, there is a difference between the exact and the approximate values. Furthermore, it can be seen that the two-point estimate method provides a better approximation than the Taylor's series method.

The effect of the coefficient of skewness α_3 of x on the statistical moments of y is examined by assuming x to follow the general beta distribution. The lower and upper values of the latter are taken to be equal to -2 and +2, respectively (i.e., $-2 \leq x \leq 2$), while the coefficient of kurtosis of x is assumed to be equal to 2.14. Case I involves a distribution skewed to the left with $\alpha_3 = -2.63$; Case II a symmetrical distribution with $\alpha_3 = 0$; and Case III a distribution skewed to the right with $\alpha_3 = 2.63$. The results, obtained for several expressions of function y, are presented in Table 2.2. They were found using Eqns. (2.4a), (2.8a), and (2.11a), for the cases of a Taylor's series approximation, the two-point and three-point estimates, respectively.

From Table 2.2, it is seen that, as in the previous comparison, the estimates for the polynomial functions do not differ from the exact values of the first moment. Also, for the case where y has an exponential form, the approximations obtained through the point estimate method are better than those found using the Taylor's series expansion.

Table 2.2 also shows that the three-point estimate is more accurate than the two-point one. In many cases, the error associated with the use of the two-point estimate method can be quite large. For example, when $y = xe^{-3x}$ and the distribution of x is skewed, the

Table 2.2 Effect of Coefficient of Skewness on the Expected Value of Several Functions

Case I: $f_x(x)$ skewed to the left ($\alpha_3 = -2.63$)

Function y	Expected Value			
	Exact	SAM	PEM-2 point	PEM-3 point
$y = x$	-0.40	-0.40	-0.40	-0.40
$y = x^2$	0.80	0.80	0.80	0.80
$y = e^{-x}$	1.99	1.97	2.08	2.06
$y = e^{-3x}$	23.8	12.9	22.5	33.8
$y = xe^{-3x}$	-0.20	0.72	0.13	-0.08

Case II: $f_x(x)$ symmetric ($\alpha_3 = 0$)

Function y	Expected Value			
	Exact	SAM	PEM-2 point	PEM-3 point
$y = x$	0.00	0.00	0.00	0.00
$y = x^2$	0.80	0.80	0.80	0.80
$y = e^{-x}$	1.46	1.40	1.43	1.46
$y = e^{-3x}$	14.0	4.6	7.40	12.4
$y = xe^{-3x}$	0.00	0.00	0.00	0.00

Case III: $f_x(x)$ skewed to the right ($\alpha_3 = 2.63$)

Function y	Expected Value			
	Exact	SAM	PEM-2 point	PEM-3 point
$y = x$	0.40	0.40	0.40	0.40
$y = x^2$	0.80	0.80	0.80	0.80
$y = e^{-x}$	0.93	0.88	0.87	0.90
$y = e^{-3x}$	4.20	1.17	1.19	2.01
$y = xe^{-3x}$	0.20	-0.72	-0.13	0.08

SAM = Series Approximation Method
PEM-2 = Point Estimate Method Using 2 Points
PEM-3 = Point Estimate Method Using 3 Points

two-point estimate was found to have a sign opposite to that of the exact value.

The final comparison examines the effect of varying the exponent of function y on its statistical values. Function y is assumed to have the form $y = e^{-ax}$, while coefficient a is allowed to vary from zero to five (i.e., $0 \leq a \leq 5$).

Three symmetrical distributions of x are used, all with the same coefficient of kurtosis ($\alpha_4 = 2.14$). The parameters of the distributions are given in Table 2.3.

Tables 2.4 and 2.5 present the obtained results for the expected value and variance, respectively. They were found using Eqns. (2.8) and (2.11), for the two-point and three-point estimates, respectively.

From Tables 2.4 and 2.5, it is seen that, for all cases, the three-point estimate of the first two moments is better than that found using the two-point estimate. However, the three-point estimate is not always in close agreement with the exact value. The error between the two values increase as the value of the coefficient a increases.

Figure 2.1 illustrates the effect of the coefficient in the exponent of y on the expected value of y for the second case. It shows that, as the value of the coefficient a increases, there is an increasing difference between the estimated and the exact expected value of y.

From Tables 2.4 and 2.5, it is seen that the point estimates of the variance diverge more rapidly from the exact values than do the estimates of the expected value.

Table 2.3 Statistical Parameters of Three Symmetrical Distributions

Case	Mean Value $\bar{x}$	Variance σ_x^2	Frequency Distribution $f_x(x)$	Range $a \leq x \leq b$
I	0.00	1.00	$\frac{3}{20\sqrt{5}}(5-x^2)$	$-5 \leq x \leq 5$
II	0.00	0.80	$\frac{3}{32}(4-x^2)$	$-2 \leq x \leq 2$
III	0.50	0.05	$6(x-x^2)$	$0 \leq x \leq 1$

Table 2.4 Effect of the Coefficient a on the Expected Value of Exponential Functions for Symmetric Distributions

Coeff.	Case I			Case II			Case III		
a	Exact	PEM-2	PEM-3	Exact	PEM-2	PEM-3	Exact	PEM-2	PEM-3
0.0	1.00	1.00	1.00	1.00	1.00	1.00	1.00	1.00	1.00
1.0	1.60	1.54	1.60	1.46	1.43	1.46	0.622	0.622	0.622
2.0	5.10	3.76	4.91	3.84	3.08	3.75	0.406	0.405	0.406
3.0	23.2	10.1	19.4	14.0	7.35	12.4	0.278	0.275	0.278
4.0	128.	27.3	82.0	61.1	17.9	44.4	0.198	0.193	0.198
5.0	786.	74.2	353.	297.	43.8	163.	0.146	0.139	0.146

PEM-2 = Point Estimate Method Using 2 Points
PEM-3 = Point Estimate Method Using 3 Points

Table 2.5 Effect of the Coefficient a on the Variance of Exponential Functions for Symmetrical Distributions

Coeff. a	Case I			Case II			Case III		
	Exact	PEM-2	PEM-3	Exact	PEM-2	PEM-3	Exact	PEM-2	PEM-3
0.0	0.0	0.0	0.0	0.0	0.0	0.0	0.0	0.0	0.0
0.5	0.320	0.272	0.318	0.248	0.214	0.243	0.0077	0.0076	0.0077
1.0	2.55	1.38	2.36	1.69	1.04	1.62	0.0193	0.0187	0.0193
1.5	16.0	4.53	12.3	8.98	3.18	7.42	0.0281	0.0261	0.0280
2.0	101.	13.2	57.9	46.4	8.45	30.4	0.0330	0.0289	0.0328
2.5	672.	36.6	260.	247.	21.4	118.	0.0348	0.0284	0.0345
3.0	4640.	100.	1150.	1360.	53.0	449.	0.0346	0.0260	0.0340

PEM-2 = Point Estimate Method Using 2 Points
PEM-3 = Point Estimate Method Using 3 Points

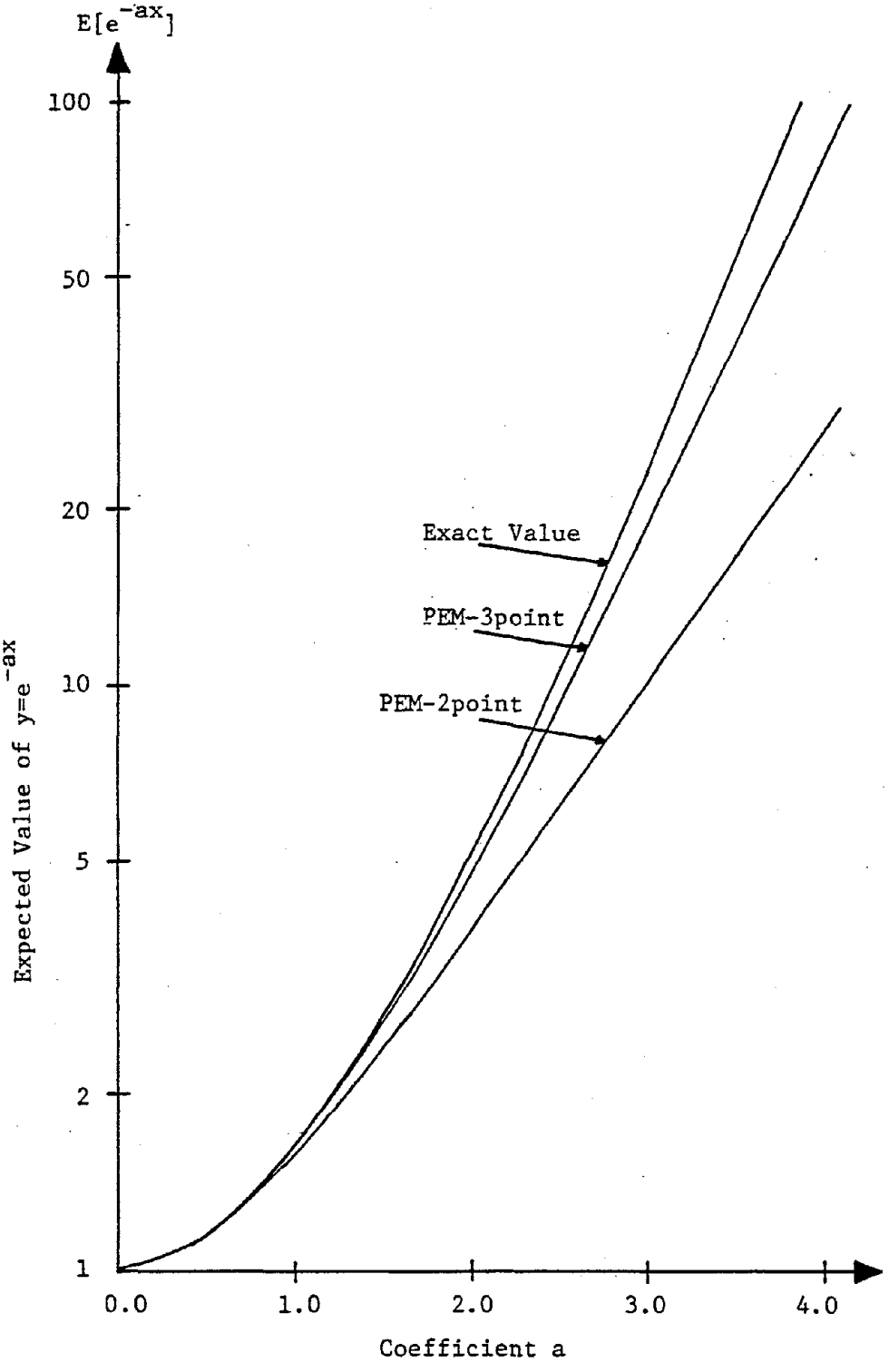

FIGURE 2.1 THE EFFECT OF THE COEFFICIENT IN THE EXPONENT OF $y=e^{-ax}$ ON THE EXPECTED VALUE OF y

CHAPTER 3

VARIABILITY OF SOIL DEPOSITS

3.1 Spatial Variability of Soil Properties

A fundamental task in geotechnical engineering involves the establishment of the soil profile and the determination of the values of soil properties within the various soil layers. This is commonly achieved through a geological examination of the area, a subsurface exploration, and a testing program consisting of in situ and/or laboratory tests. The latter provide continuous or discrete with depth records of the numerical values of soil properties which are used to subdivide the soil deposit into layers.

It is well known, however, that even within the same layer there is an inherent variability in the values of soil properties. In the case of natural deposits, this variability is due mainly to the randomness associated with the geological processes that are involved in the formation of the deposits. A similar variability also exists within layers of man-made soil structures (e.g., random fluctuations of water content or relative density within fills, embankments, etc.).

Moreover, if a soil mass is composed of approximately horizontal layers, properties within such a mass exhibit two distinct characteristics, namely: (a) their variability along a horizontal direction is considerably smaller than that along the vertical direction, and (b) their numerical values follow a distinct trend with depth.

This is illustrated schematically in Fig. 3.1 for the case where the soil property is the undrained strength S_u of a normally consolidated clay deposit. It can be seen that the trend followed by S_u is that of increasing values with depth.

In order to express the spatial (vertical) variability of a soil parameter, one needs to determine the variation of its mean value and standard deviation with depth as well as its autocorrelation function (i.e., the function that describes the correlation between values of the parameter at different locations).

3.2 Soil Properties as Random Functions of Depth

Let $x = x(z)$ denote a depth dependent soil property and A and A' two points within the soil mass at depths z and z', respectively. This is shown schematically in Fig. 3.2. If μ and σ^2 are the mean value and variance, respectively, of soil property x and $r_x = r_x(|z - z'|)$ is its autocorrelation function evaluated at points A and A', then one has

$$\begin{aligned} E[x(z)] &= \mu \\ E[\{x(z) - \mu\}^2] &= \sigma^2 \\ E[\{x(z) - \mu\}\{x(z') - \mu\}] &= \sigma^2 r_x \end{aligned} \tag{3.1}$$

in which E[ ] denotes the expected value of the quantity in brackets and $r_x = r_x(|z - z'|) \leq 1$.

A function, such as a soil property $x = x(z)$ which for any value of depth z is a random variable, is called a random function

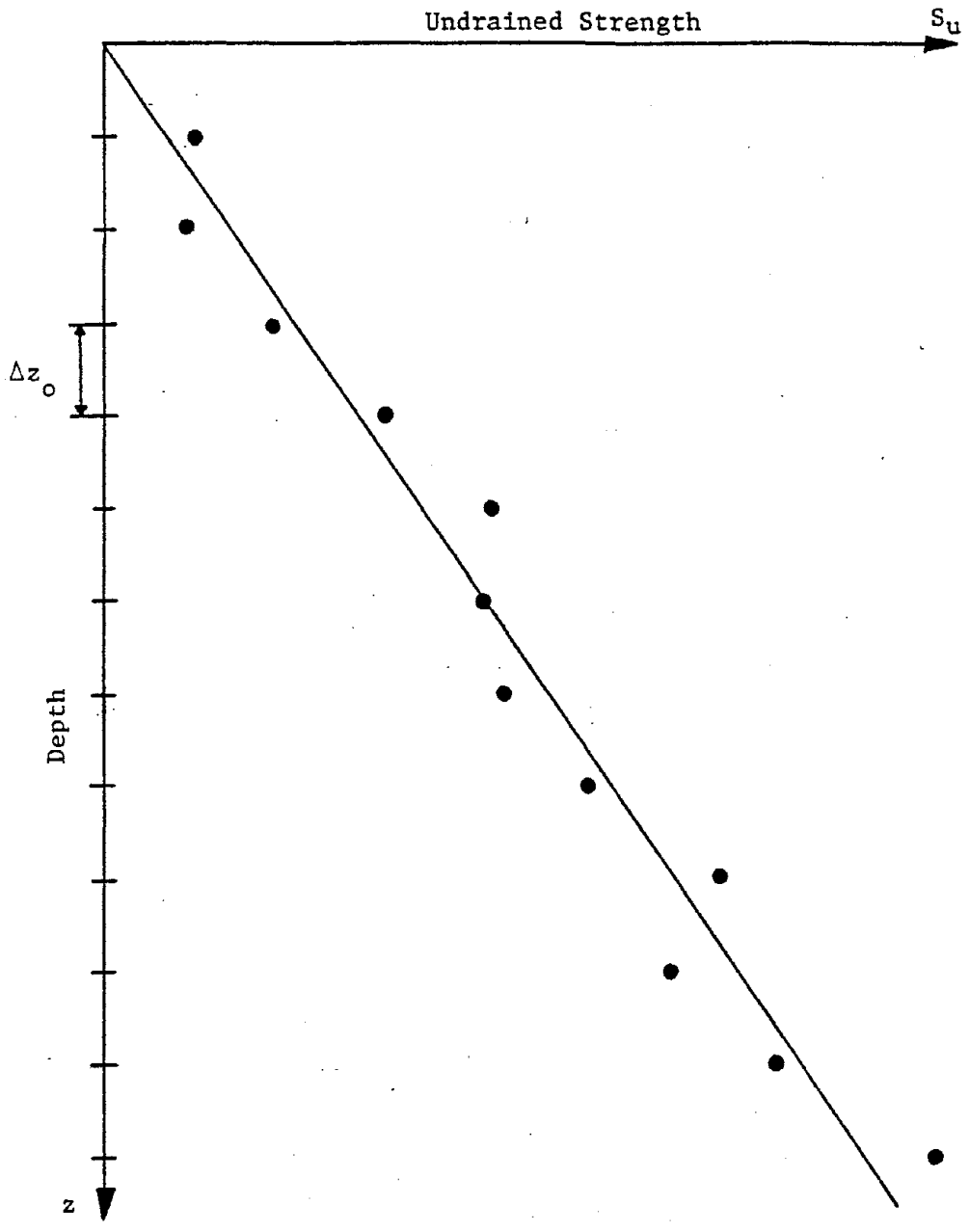

FIGURE 3.1 SCHEMATIC REPRESENTATION OF THE VERTICAL VARIABILITY OF UNDRAINED SHEAR STRENGTH S_u FOR NORMALLY CONSOLIDATED CLAYS

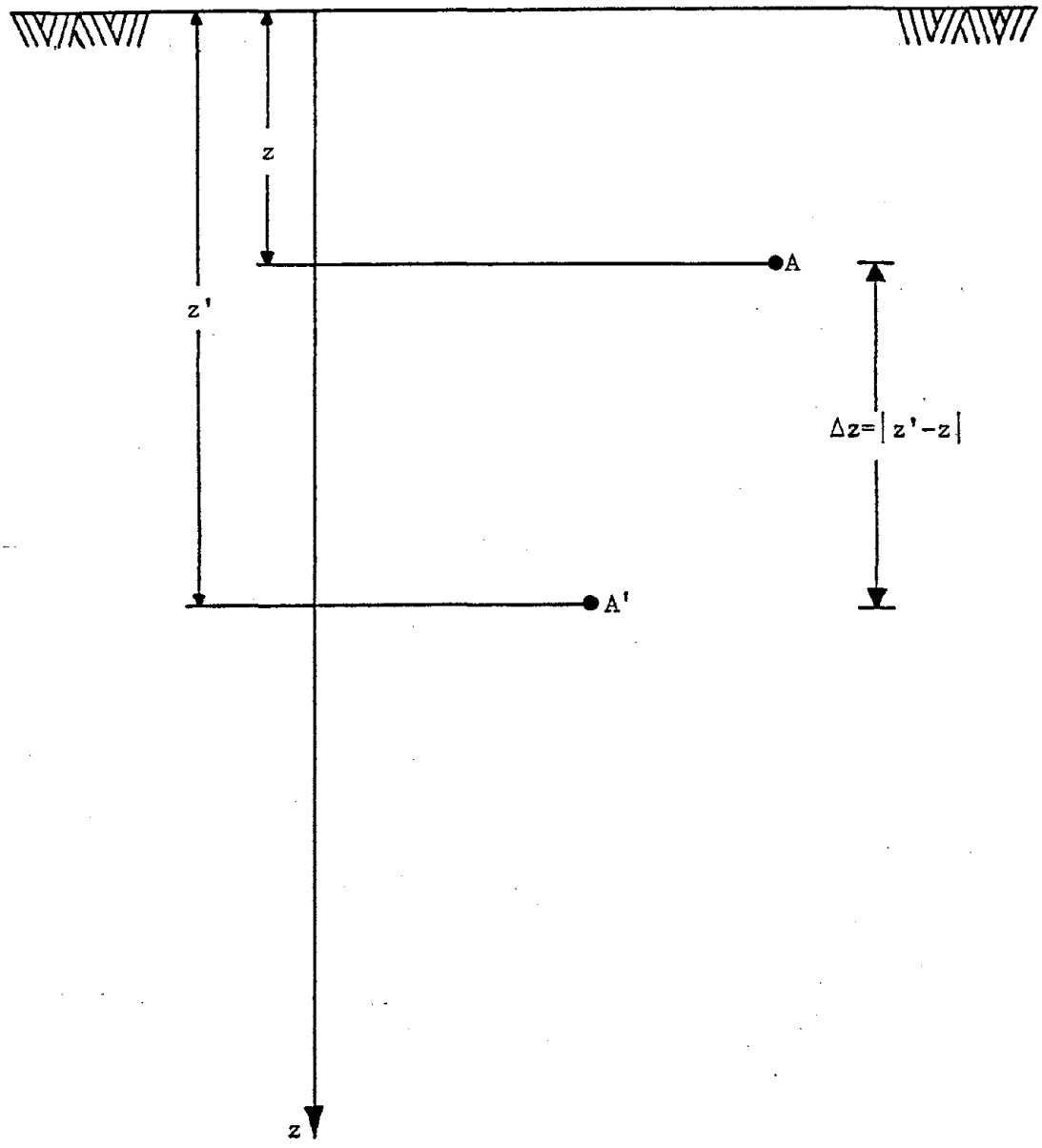

FIGURE 3.2 VERTICAL DISTANCE BETWEEN TWO POINTS APPEARING IN THE AUTOCORRELATION FUNCTION

or stochastic process. When such a function is independent of the origin ($z = 0$) and its statistical values depend only on the relative position between two points, such as A and A' (Fig. 3.2), it is called a stationary function or stationary process. Moreover, if all statistical moments of x are constant anywhere along the z direction, then $x(z)$ is said to be stationary in the strict sense. If only the first two moments of x are constant with z, then $x = x(z)$ is said to be a stationary process in the wide sense. Thus, random function $x(z)$, defined by Eqns. (3.1), represents a stationary process in the wide sense. Its autocorrelation function depends on the vertical distance between two points (Fig. 3.2) at depths z and z' with $r_x(z - z') = r_x(z' - z)$ and $r_x(|z - z'|) \leq 1$.

When the expression for the autocorrelation function $r_x(z - z')$ is known for a given soil deposit and point averages equal spatial averages (e.g., $\mu = \frac{1}{V}\int_V x dV$, where V denotes the volume of a soil deposit), then the quantity

$$n_i = H^2 / \int_0^H \int_0^H r_x(|z - z'|)\, dz\, dz' \tag{3.2}$$

provides the number of equivalent independent layers a soil deposit may be considered to consist of (Asaoka and A-Grivas, 1981a).

3.3 The Autocorrelation Function

The autocorrelation function r_x of a soil property x may be conveniently expressed as an exponential decay function of the form

$$r_x = r_x(|z - z'|) = \exp\left(-\frac{|z - z'|}{a\,\ell}\right) \tag{3.3}$$

in which ℓ is called the correlation length and a is a modeling constant. This form of the autocorrelation function r_x decreases monotonically from unity at $z = z'$ to zero as the distance $|z - z'|$ approaches infinity.

The correlation length ℓ, entering the expression r_x, is the distance between two points within which the soil property shows relatively strong correlation (e.g., at two points which lie within the distance ℓ, the corresponding values of x are likely to be either both above or both below the mean μ), and thus it provides an approximate measure of the distance between two independent observations.

Substituting Eqn. (3.3) into Eqn. (3.2) and performing the indicated integration, on has

$$n_i = H^2/2a\,\ell\{H + a\,\ell[\exp(-H/a\,\ell) - 1] \tag{3.4}$$

From Eqn. (3.4), it is found that the thickness of the statistically independent layers in a soil deposit of depth H is equal to

$$d_i = H/n_i \tag{3.5}$$

3.4 Modeling the Soil Profile Using the Autocorrelation Function

Several methods of modeling a soil profile have been previously reported in the literature (e.g., Alonso, 1976; Matsuo and Asaoka, 1977; Vanmarcke, 1977, etc.). The difference between these

methods as well as the new approach that is introduced later in this section is due to the assumption made about the stationarity of the process and the manner whereby the correlation length is determined.

Figure 3.3 illustrates schematically the various assumptions made concerning the vertical variability of a soil property. In Fig. 3.3a is shown a stationary process in the wide sense with a constant mean value and standard deviation, while Fig. 3.3b represents a non-stationary process with a linearly increasing mean and standard deviation.

Once the process describing the variation of a soil property with depth has been assumed, the correlation length is determined using the test data and boring log found from the testing program. The test data is used to determine the numerical value of the correlation length, while the boring log is used to indicate different soil types in the soil mass. It is important that each soil type is analyzed separately, since combining data from different soils will give erroneous results.

Three methods are currently available for the determination of the correlation length of a given property within a soil deposit, namely: (a) the average mean-crossings distance method, (b) the moving average method, and (c) the quasi-stationary autoregressive method. A description of each of these methods and a review of their applicability and limitations is given below.

3.4.1 The Average Mean-Crossings Distance Method (AMCDM)

This method may be used to determine the correlation length

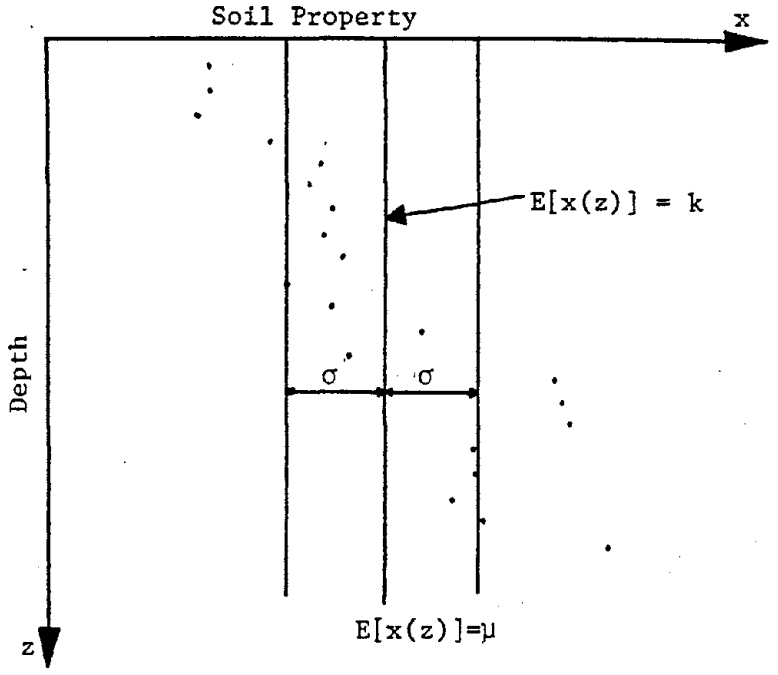

(a) Stationary Process

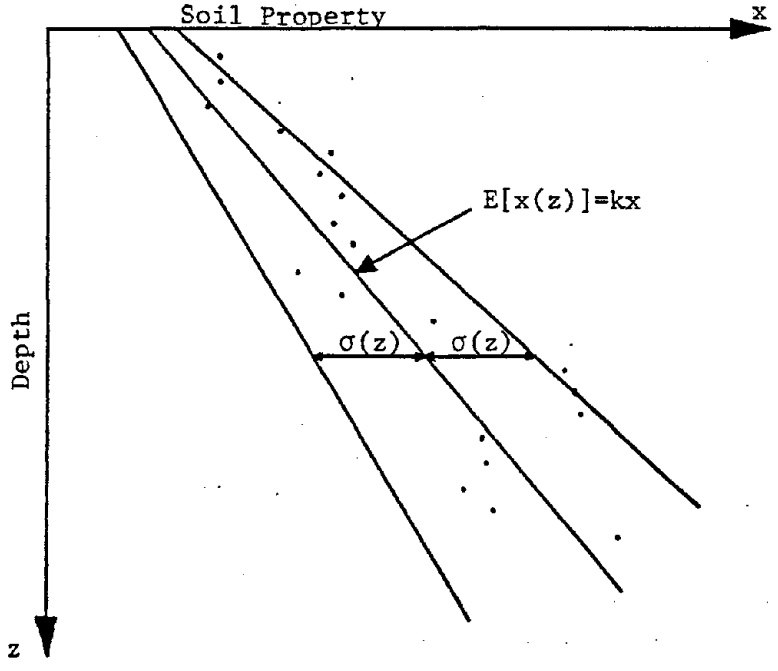

(b) Non-Stationary Process

FIGURE 3.3 TWO EXAMPLES OF VERTICAL VARIABILITY OF A SOIL PROPERTY x

ℓ of soil properties that represent a stationary process. It is illustrated in Fig. 3.4 in which x_i, i = 1,2...,N, denotes the value of the soil property measured at a depth z_i within the deposit. The mean value $\bar{x}$ and variance σ_x^2 of the N measured values of x_i are equal to

$$\bar{x} = \frac{1}{N} \sum_{i=1}^{N} x_i$$

$$\sigma_x^2 = \frac{1}{N-1} \sum_{i=1}^{N} (x_i - \bar{x})^2 \tag{3.6}$$

The correlation length ℓ is defined as the average distance between the points of intersection of the trace of the measured values x = x(z) and the mean value $\bar{x}$ (Fig. 3.4). That is,

$$\ell = \frac{1}{m} \sum_{i=1}^{m} \delta_i \tag{3.7}$$

in which δ_i is the length of the interval between intersections i and i+1 of x(z) and $\bar{x}$, and m is the total number of such intervals.

The autocorrelation function r_x in accordance with this method is expressed as a squared exponential decay function of the form (Rice, 1944)

$$r_x(\Delta z) = \exp\left[-\frac{\pi^2}{2}\left(\frac{\Delta z}{\ell}\right)^2\right] \tag{3.8}$$

in which $\Delta z = z - z'$.

A summary of the average mean-crossings distance method is given in Table 3.1.

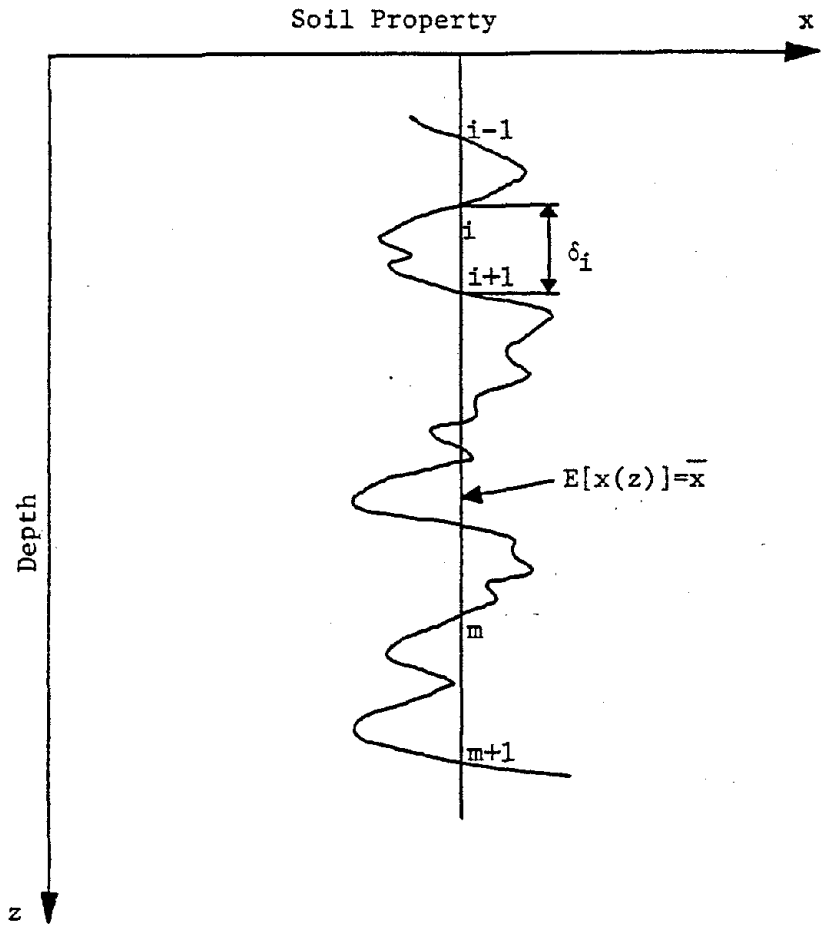

FIGURE 3.4 SOIL PROFILE FOR THE AVERAGE MEAN-CROSSINGS DISTANCE MODEL

Table 3.1 Procedure for Estimating the Correlation Length ℓ of a Soil Property Using the Average Mean-Crossings Method

Data	Values of soil property x at various depths z along a borehole; i.e., $x_i = x(z_i)$, z_i, $i = 1,2,...N$.
Step 1	Find the mean value of $\bar{x}$ of x_i $$\bar{x} = \frac{1}{N} \sum_{i=1}^{N} x_i$$
Step 2	Find the depths C_i at which the linear extrapolation of x(z) between two consecutive points equals $\bar{x}$, where $i = 1,2,...m+1$.
Step 3	Find the length of the intervals between intersections of x(z) and $\bar{x}$ $$\delta_i = C_{i+1} - C_i, \; i = 1,2,...m.$$
Step 4	Find the correlation length ℓ given by Eqn. (3.7) $$\ell = \frac{1}{m} \sum_{i=1}^{m} \delta_i$$

3.4.2 The Moving Average Method (MAM)

The moving average method has been applied in geotechnical engineering for the first time by Vanmarcke (1977) to model the spatial variability of a soil property x. The latter is assumed to follow a stationary process (Fig. 3.3a) and, therefore, its mean value and variance are constant with depth and $r_x(\Delta z) = r_x(-\Delta z)$.

In accordance with this procedure, the autocorrelation function is found by obtaining the variance of average values along a series of space intervals. This variance is then expressed as a decreasing function of the number of the interval, called the variance reduction function, and is used to determine the correlation length.

In Fig. 3.5 are shown schematically the values of a soil property x measured at equal distances Δz_o (i.e., the vertical distance between two adjacent samples). The vertical line represents the mean value $\bar{x}$ of x determined on the basis of all data points x_i, i = 1,2 ...,N, where N is the total number of data. To obtain the correlation length ℓ, one must first find the spatial averages $\bar{u}_k$ and the spatial variances σ_k^2 from the test results, where k is the number of adjacent observations of x that are used in the averaging scheme.

The k-th spatial average is formed by first determining the averages of sets of k consecutive observations of x (e.g., if k = 2; $\frac{x_1+x_2}{2}$, $\frac{x_2+x_3}{2}$, ... $\frac{x_{N-1}+x_N}{2}$) and then averaging these values. The spatial variation is found in a similar manner. For N data points the values of $\bar{u}_k$ and σ_k^2 are equal to

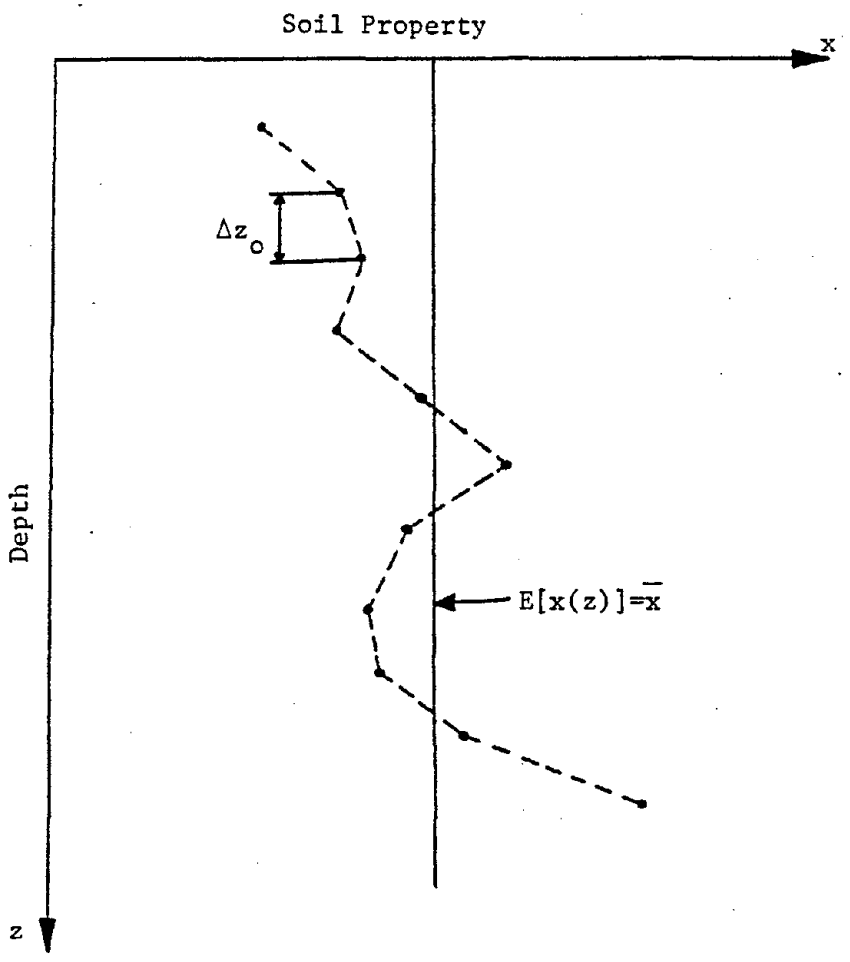

FIGURE 3.5 SOIL PROFILE FOR THE MOVING AVERAGE METHOD

$$\bar{u}_k = \frac{1}{N-k+1} \sum_{i=1}^{N-k+1} \left[\frac{1}{k} \sum_{j=i}^{i+k-1} x_j\right]$$

$$\sigma_k^2 = \frac{1}{N-k} \sum_{i=1}^{N-k+1} \left[\left(\frac{1}{k} \sum_{j=i}^{i+k-1} x_j\right) - \bar{u}_k\right]^2 \tag{3.9}$$

where x_j is the value of property x at depth $z_j = j\Delta z_o$ and $k = 2,3,\ldots N-1$.

The spatial variance may be normalized by forming the ratio of σ_k^2 over σ_x^2, i.e.,

$$\Gamma^2(k) = \frac{\sigma_k^2}{\sigma_x^2} \tag{3.10}$$

in which $\Gamma^2(k)$ is the variance reduction function. The variance reduction function is plotted against the spatial distances k, as shown schematically in Fig. 3.6 by the dashed line. A best fit of the results shown in Fig. 3.6 can be made to provide a relationship between $\Gamma^2(k)$ and k of the form

$$\Gamma^2(k) = \begin{cases} 1 \ , \ k \leq k^* \\ \\ \dfrac{k^*}{k} \ , \ k > k^* \end{cases} \tag{3.11}$$

in which k^* is determined by a least squared error analysis (i.e., $k^* = \text{Min} \left[\frac{1}{N-2} \sum_{k=1}^{N-1} \left(\frac{\sigma_k^2}{\sigma_x^2} - \Gamma^2(k)\right)^2\right]$ where $\Gamma^2(k)$ is given by Eqn. (3.11)). Equation (3.11) is plotted as a solid line in Fig. 3.6.

The correlation length ℓ is then equal to (Vanmarcke, 1977)

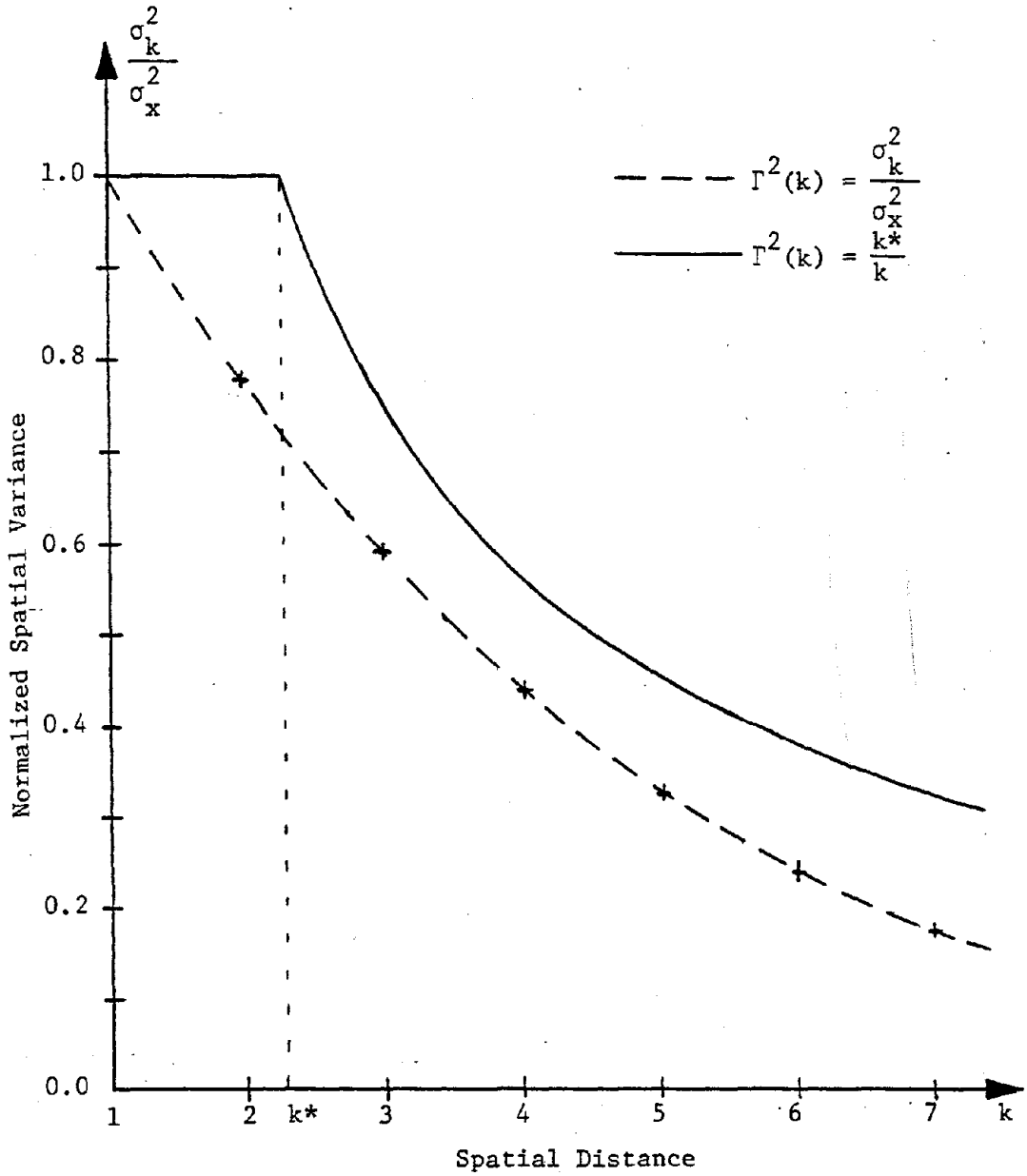

FIGURE 3.6 VARIANCE REDUCTION FUNCTION OF THE SPATIAL VARIANCES OF SOIL PROPERTY x

$$\ell = 2\Delta z_o \{\ell n[(k^*+1)/(k^*-1)]\}^{-1} \qquad (3.12)$$

The autocorrelation function r_x for the moving average method, the number of equivalent independent layers n_i, and the thickness of such a layer are determined by substituting Eqn. (3.12) into Eqns. (3.3), (3.4), and (3.5), respectively, with the modeling constant equal to one-half (i.e., a = 1/2).

The moving average method is summarized in Table (3.2).

3.4.3 The Quasi-Stationary Autoregressive Method (QSARM)

The two methods of determining the correlation length of a soil property x discussed above are based on the assumption that x follows a stationary process. If, however, x exhibits a trend with depth, then x represents a non-stationary process, therefore, the above methods cannot be applied.

An alternative procedure is presented herein that is applicable for the commonly encountered situations in which the mean value $\bar{x} = \bar{x}(z)$ and standard deviation $\sigma_x = \sigma_x(z)$ of x increase linearly with depth z. It is based on the observation that x(z) can be reduced to a stationary process by forming the ratio of x(z) over z (hence the term quasi-stationary process). Furthermore, it is observed that the value of x at a point z_i depends on the value taken by x at z_{i-1}, where i = 1,2,...N, an attribute of autoregressive processes.

Let $x(z_i)$ denote the value of a soil property x at depth z_i, where i = 1,2,...N, and let u_i be the ratio of $x(z_i)$ over z_i, i.e.,

Table 3.2 Procedure for Estimating the Correlation Length ℓ of a Soil Property Using the Moving Average Method

Data	Values of soil property x at constant sampling intervals Δz_o along a borehole; i.e., $x_o = x(i \cdot \Delta z_o)$, i = 1,2,...N.
Step 1	Find the spatial averages $\bar{u}_k$ and spatial variance σ_k^2 of x_i, where k = 1,2,...N-1 $$\bar{u}_k = \frac{1}{N-k+1} \sum_{i=1}^{N-k+1} [\frac{1}{k} \sum_{j=1}^{i+k-1} x_j]$$ $$\sigma_k^2 = \frac{1}{N-k} \sum_{i=1}^{N-k+1} [(\frac{1}{k} \sum_{j=i}^{i+k-1} x_j) - \bar{u}_k]^2$$
Step 2	Find k^* by using a least squared error method given by $$k^* = \text{Min } [\frac{1}{N-2} \sum_{k=1}^{N-1} (\frac{\sigma_k^2}{\sigma_x^2} - \frac{k^*}{k})^2]$$
Step 3	Find the correlation length ℓ given by Eqn. (3.12) $$\ell = 2\Delta z_o \{\ell n[(k^*+1)/(k^*-1)]\}^{-1}$$

$$u_i = \frac{x(z_i)}{z_i} \tag{3.13}$$

Quantity u_i represents a quasi-stationary process as (a) the mean value $\bar{x}(z)$ of x is a linearly increasing function of depth, (b) the coefficient of variation of x is constant, and (c) the autocorrelation functions of x and u are identical. These conditions are expressed analytically in the following form:

$$\begin{aligned} E[x(z)] &= \bar{x}(z) = kz \\ V_x &= \frac{\sigma_x(z)}{\bar{x}(z)} = \text{constant} \\ r_x(\Delta z) &= r_u(\Delta z) \text{ with } a = 1 \end{aligned} \tag{3.14}$$

Furthermore, successive values of u_{i-1} and u_i, evaluated at constant intervals Δz_o, are related in the following manner (the autoregressive character of u):

$$u_i = \beta_o + \beta_1 u_{i-1} + \varepsilon_i \tag{3.15}$$

in which β_o and β_1 are parameters to be determined from available data and ε_i is an error term the mean value and variance of which are constant for all i's and equal to zero and σ_ε^2, respectively. Furthermore, the errors ε_i are assumed to be independent of each other, i.e.,

$$E[\varepsilon_i \times \varepsilon_j] = \delta_{ij} \sigma_\varepsilon^2$$

in which δ_{ij} is Kronecker's Delta (i.e., $\delta_{ij} = 1$, $i = j$; $\delta_{ij} = 0$, $i \neq j$).

The expected value $E[u_i]$, variance $V[u_i]$, and autocorrelation

function r_u of u_i can be expressed as (Cox and Miller, 1965)

$$E[u_i] = \frac{\beta_o}{1-\beta_1}$$

$$V[u_i] = \frac{\sigma^2}{1-\beta_1^2} \tag{3.16}$$

$$r_u(k\text{-}\Delta z_o) = \beta_1^k$$

in which $\sigma^2 = \frac{1}{N-2} \sum_{i=1}^{N-1} [u_i - \beta_o - \beta_1 u_{i-1}]^2$, N denotes the number of samples, and k is the number of sampling intervals Δz_o between two points z_i and z_{i+k} within the soil deposit (i.e., $k = \frac{|z_i - z_{i+k}|}{\Delta z_o}$).

Substituting in the above expression u_i by x(z), found from Eqn. (3.13), one has that the mean value, variance, and autocorrelation function of x are equal to

$$E[x(z)] = \bar{x}(z) = \frac{\beta_o}{1-\beta_1} z$$

$$V[x(z)] = \sigma_x^2(z) = \frac{\sigma^2}{1-\beta_1^2} z^2 \tag{3.17}$$

$$r_x(k \cdot \Delta z_o) = \beta_1^k$$

Moreover, substituting the last of Eqns. (3.17) into Eqn. (3.3), it is seen that the correlation length ℓ for the quasi-stationary autoregressive method is

$$\ell = - \frac{\Delta z_o}{\ell n |\beta_1|} \tag{3.18}$$

The number of equivalent independent layers n_i and their thickness d_i can be determined by substituting Eqn. (3.18) into Eqns. (3.4) and (3.5), respectively, in which a = 1.

In Fig. 3.7 is shown schematically the values of soil property x measured at equal distances Δz_o. The mean value $\bar{x}(z)$ and standard deviation $\sigma_x(z)$ of x as determined by the quasi-stationary autoregressive method (Eqns. (3.17)) are represented by the lower and upper lines, respectively.

Finally, the quasi-stationary autoregressive method is summarized in Table 3.3.

3.5 Case Study

The three procedures in the preceding section are applied to evaluate the spatial variability of the undrained shear strength S_u of a soft clay deposit. Two sites, denoted as A and B, are selected for this purpose from the general area investigated in connection with the West Side Highway in New York City. Values of S_u along two boreholes are used to describe each site. Tables 3.4 and 3.5 list the values of S_u from Boreholes A-1 and A-2; while Tables 3.6 and 3.7 list the values of S_u from Boreholes B-1 and B-2. The sampling distance Δz_o is equal to 3.3 feet for all boreholes.

The numerical values of k^*, β_1, and β_o were found for both boreholes at each site using the procedures outlined in Tables 3.2 and 3.3. The results are listed in Table 3.8 along with the thickness of the clay deposit and the number of samples taken in each borehole.

The correlation length ℓ provided by the average mean-

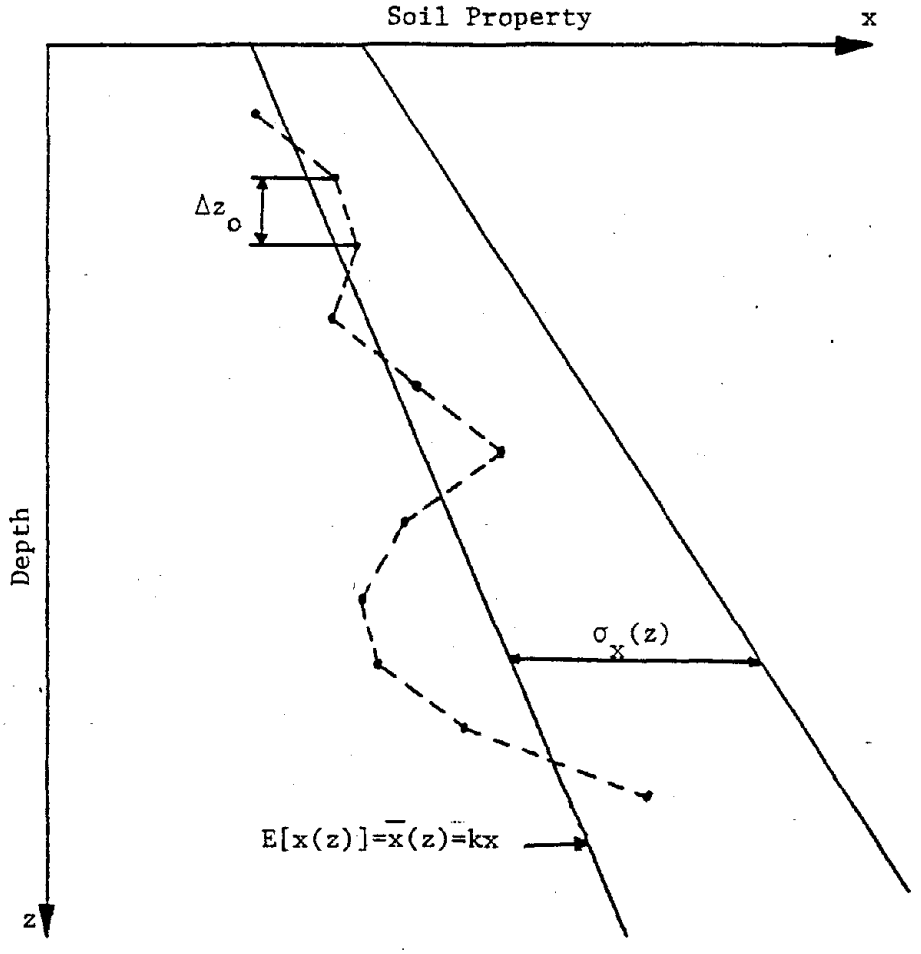

FIGURE 3.7 THE ASSUMED SOIL PROFILE FOR THE QUASI-STATIONARY AUTOREGRESSIVE METHOD

Table 3.3 Procedure for Estimating the Correlation Length ℓ of a Soil Property Using the Quasi-Stationary Autoregressive Method

Data	Values of soil property x at constant sampling intervals Δz_o along a borehole; i.e., $x_i = x(z_i)$, $z_i = i\Delta z_o$, $i = 1,2,...N$.
Step 1	Find the ratio of $x(z_i)$ over z_i, denoted by u_i $$u_i = \frac{x(z_i)}{z_i}, \quad i = 1,2,...N$$
Step 2	Find the parameters β_o and β_1 using a least square fitting technique of u_{i-1} and u_i, i.e., $$\beta_o = \frac{\Sigma u_{i-1}^2 \, \Sigma u_i - \Sigma u_{i-1} \, u_i \, \Sigma u_{i-1}}{N \, \Sigma u_{i-1}^2 - (\Sigma u_{i-1})^2}, \quad i = 2,3,...N.$$ $$\beta_1 = \frac{N \, \Sigma u_{i-1} \, u_i - \Sigma u_{i-1} \, \Sigma u_i}{N \, \Sigma u_{i-1}^2 - [\Sigma u_{i-1})^2}$$
Step 3	Find the correlation length ℓ given by Eqn. (3.18) $$\ell = -\frac{\Delta z_o}{\ell n \lvert \beta_1 \rvert}$$

Table 3.4 Values of S_u at Various Depths along A-1 Borehole

DEPTH BELOW GROUND SURFACE ft	UNDRAINED SHEAR STRENGTH ksf
47.9	0.42
51.2	0.42
54.5	0.39
57.8	0.58
60.5	0.71
63.7	0.68
67.0	0.74
70.3	0.72
73.6	0.77
76.9	0.62
80.3	0.74
83.5	0.98
86.8	0.79
90.1	1.33
93.4	1.35
96.7	1.37
100.0	1.11
103.3	1.12
106.7	1.06
110.0	1.14
113.3	1.47

Table 3.5 Values of S_u at Various Depths along A-2 Borehole

DEPTH BELOW GROUND SURFACE ft	UNDRAINED SHEAR STRENGTH ksf
52.3	0.57
55.3	0.79
58.8	0.72
62.1	0.75
65.4	0.72
68.6	0.63
73.1	0.61
76.8	0.82
81.6	0.78
84.9	0.85
88.2	0.92
91.5	0.96
94.7	0.99

Table 3.6 Values of S_u at Various Depths along B-1 Borehole

DEPTH BELOW GROUND SURFACE ft	UNDRAINED SHEAR STRENGTH ksf
29.0	0.05
32.2	0.09
35.5	0.11
38.8	0.13
41.6	0.15
44.8	0.22
48.1	0.23
51.4	0.23

Table 3.7 Values of S_u at Various Depths along B-2 Borehole

DEPTH BELOW GROUND SURFACE ft	UNDRAINED SHEAR STRENGTH ksf
29.4	0.06
32.7	0.09
36.0	0.09
39.3	0.12
43.4	0.11
46.6	0.24
49.9	0.24
53.2	0.33
56.4	0.30

TABLE 3.8

NUMERICAL VALUES OF PARAMETERS FOR THE FOUR BOREHOLES IN THE CASE STUDY

PARAMETER	SITE A		SITE B	
	A-1	A-2	B-1	B-2
SAMPLE SIZE	21	13	8	9
DEPOSIT THICKNESS	65.4 ft.	42.7 ft.	22.4 ft.	27.0 ft.
K*	3.0	1.3	1.9	2.0
β_1	0.490	0.484	0.651	0.624
β_o	5.62×10^{-3}	5.52×10^{-3}	1.60×10^{-3}	2.82×10^{-3}

crossings distance method, the moving average method, and the quasi-stationary autoregressive method are obtained using Tables 3.1, 3.2, and 3.3., respectively. The number of equivalent independent layers n_i and their thickness d_i obtained by Eqns. (3.4) and (3.5), respectively, are found for the moving average method in which $a = \frac{1}{2}$ and for the quasi-stationary autoregressive method in which $a = 1$. The results are listed in Table 3.9.

TABLE 3.9

VALUES OF THE CORRELATION LENGTH, NUMBER AND THICKNESS OF INDEPENDENT LAYERS FOR THE CASE STUDY

PARAMETER	METHOD	SITE A		SITE B	
		A-1	A-2	B-1	B-2
Correlation length, ℓ, feet	QSARM	4.6	4.5	7.7	7.1
	MAM	9.5	3.2	5.6	6.0
	AMCDM	2.7	7.8	-	4.3
Number of independent layers n_i	QSARM	7.6	5.2	2.2	2.3
	MAM	7.4	13.7	4.5	5.1
Thickness of independent layer d_i, feet	QSARM	8.6	8.2	10.4	10.1
	MAM	8.8	3.1	4.9	5.3

QSARM-Quasi-Stationary Autoregressive Method
MAM -Moving Average Method
AMCDM-Average Mean-Crossings Distance Method

CHAPTER 4

SEISMIC EARTH THRUST AGAINST RETAINING WALLS

4.1 Vertical Variability of the Frictional Component of Backfill Strength

The vertical variability of a soil property was examined in the preceding chapter and three methods were presented for its description. The present chapter will apply the quasi-stationary autoregressive method to analyze the vertical variability of the ϕ parameter of strength of granular materials located behind retaining walls. The results of this analysis will be incorporated into an available procedure to determine the earth thrust against a retaining wall during an earthquake.

Let μ, σ^2, and $r_\phi(\Delta z)$ denote the expected value, variance, and autocorrelation function, respectively, of the ϕ parameter of strength. From Eqns. (3.1), one has

$$\begin{aligned} E[\phi(z)] &= \mu \\ E[\{\phi(z)-\mu\}^2] &= \sigma^2 \\ E[\{\phi(z)-\mu\}\{\phi(z')-\mu\}] &= r_\phi(\Delta z)\ \sigma^2 \end{aligned} \tag{4.1}$$

Under the assumption that $\phi(z)$ represents a stationary process, one has that μ and σ^2 are constant with depth, $r_\phi(\Delta z) = r_\phi(-\Delta z)$, and $|r(\Delta z)| \leq 1$. Furthermore, if H denotes the thickness of the backfill material, Eqn. (4.1) may be written in the form

$$E[\frac{1}{H}\int_0^H \phi(z)\ dz] = \mu$$
$$V[\frac{1}{H}\int_0^H \phi(z)\ dz] = \sigma^2/n \tag{4.2}$$

in which n is given in Eqn. (3.4) as

$$n = \frac{H}{2\ell\{H + \ell[\exp(-\frac{H}{\ell}) - 1]\}} \tag{4.3}$$

Quantity n represents the number of statistically independent layers the backfill material is composed of. Numerically, n is an integer the value of which is obtained when the right-hand side of Eqn. (4.3) is rounded to the nearest integer other than zero (i.e., $n \geq 1$). This is illustrated schematically in Fig. 4.1. Figure 4.1a shows the equivalent statistically independent layers of the backfill (n = 5). Within each of these layers, the ϕ parameter of strength is a random variable having mean value and variance equal to μ and σ^2, respectively. This is denoted as ϕ: (μ, σ^2) and is shown in Fig. 4.1a.

An alternative representation of the soil medium behind a retaining wall is shown in Fig. 4.1b. Here, the backfill is considered to consist of a single layer, the ϕ parameter of which has a mean value equal to μ and variance equal to σ^2/n, where n = 5. The distribution of ϕ for this representation of the backfill is denoted as ϕ: $(\mu, \sigma^2/5)$ and is shown in Fig. 4.1b.

The two models for the backfill material that are illustrated in Figs. 4.1, i.e., the statistically independent layered

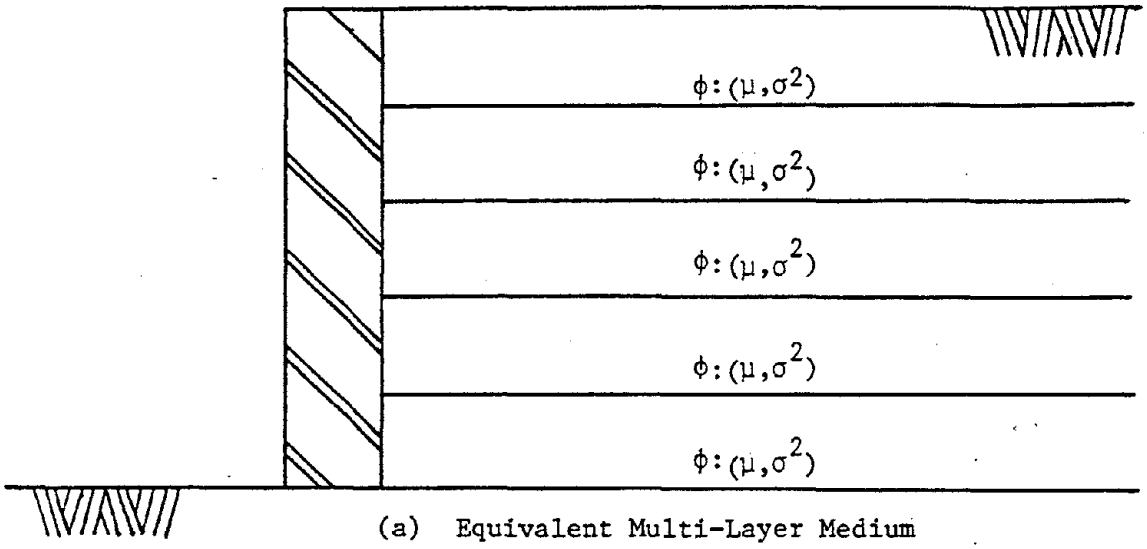

(a) Equivalent Multi-Layer Medium

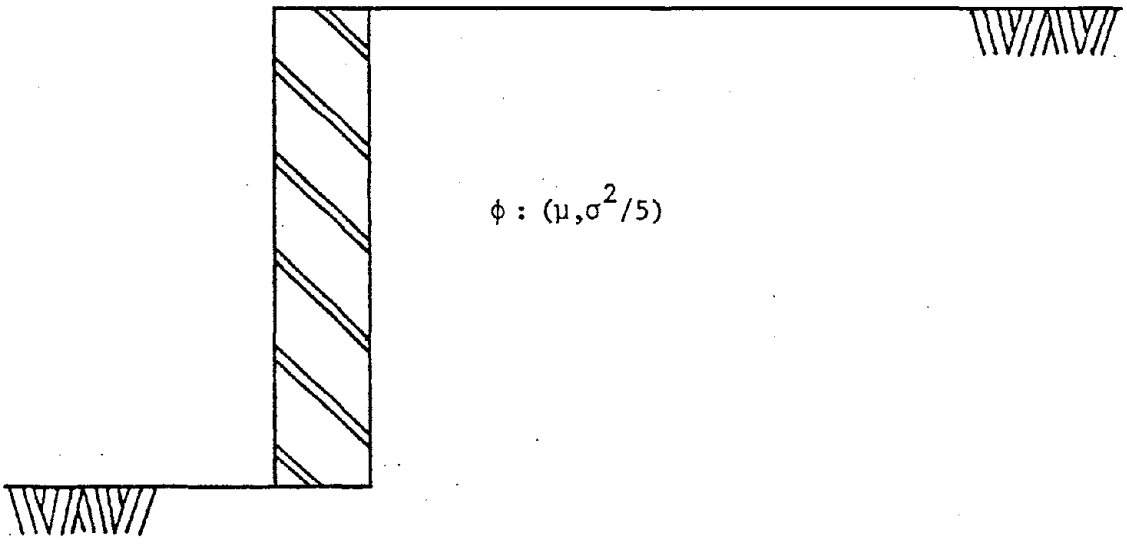

(b) Equivalent Single-Layer Medium

FIGURE 4.1 THE TWO REPRESENTATIONS OF THE BACKFILL MEDIUM AS OBTAINED FROM THE AUTOCORRELATION FUNCTION

model (Fig. 4.1a) and the single layer model (Fig. 4.1b), represent two procedures capable of providing the vertical variation of the ϕ parameter of strength. The difference between the two is in the number of random variables that are employed in their representation of the backfill. Thus, the statistically independent layered model requires n independent variables, one for each layer, with mean value μ and variance σ^2 (i.e., ϕ_1: (μ, σ^2), ϕ_2: (μ, σ^2), ...ϕ_n: (μ, σ^2). While the single layer model requires only one variable ϕ with mean value μ and reduced variance σ^2/n (i.e., ϕ: $(\mu, \sigma^2/n)$).

4.2 Determining the Seismic Earth Thrust Considering Moment Equilibrium and Vertical Variability

The earth thrust against a retaining wall is determined from Coulomb's theory by considering only equilibrium of the forces that act on the sliding soil mass. Equilibrium of moments is satisfied only in the special case of a smooth vertical retaining wall with horizontal backfill. An important feature of the present procedure is that it satisfies all three equations of equilibrium: the sum of the forces along the horizontal and vertical directions and that of the moments around any point on the cross-section of the retaining wall and backfill are equal to zero. Moreover, it includes the effect of an earthquake expressed in terms of equivalent seismic forces as well as the vertical variability of the internal friction of the backfill material.

The two models presented in the preceding section for the

description of the backfill material, i.e., the statistically independent layered model and the single layered model, produce different force systems on the backfill and, therefore, require different assumptions for the seismic earth thrust against the wall.

Common to both models are the following assumptions:

(1) the backfill material is cohesionless;

(2) failure occurs along a planar surface;

(3) shear strength is fully mobilized along the failure plane;

(4) the shear strength is a frictional force proportional to the vertical pressure at a point; and

(5) the backfill behaves as a rigid body (i.e., acceleration is uniform throughout the medium).

Figure 4.2 shows schematically the geometry of a retaining wall and its backfill material. The values of the angles and forces, as shown in the figure, are considered to be positive. In accordance with the fourth assumption above, the resultant force (denoted by R) acts at one third the distance from the base of the retaining wall along the failure plane.

4.2.1 Single Layer Representation of the Backfill

The single layer model of a retaining wall and its backfill are shown schematically in Fig. 4.2. The three unknown quantities to be determined from the three equations of equilibrium are the seismic earth thrust P_{AE}, the point of application of seismic earth thrust d_A, and the resisting force along the failure surface R.

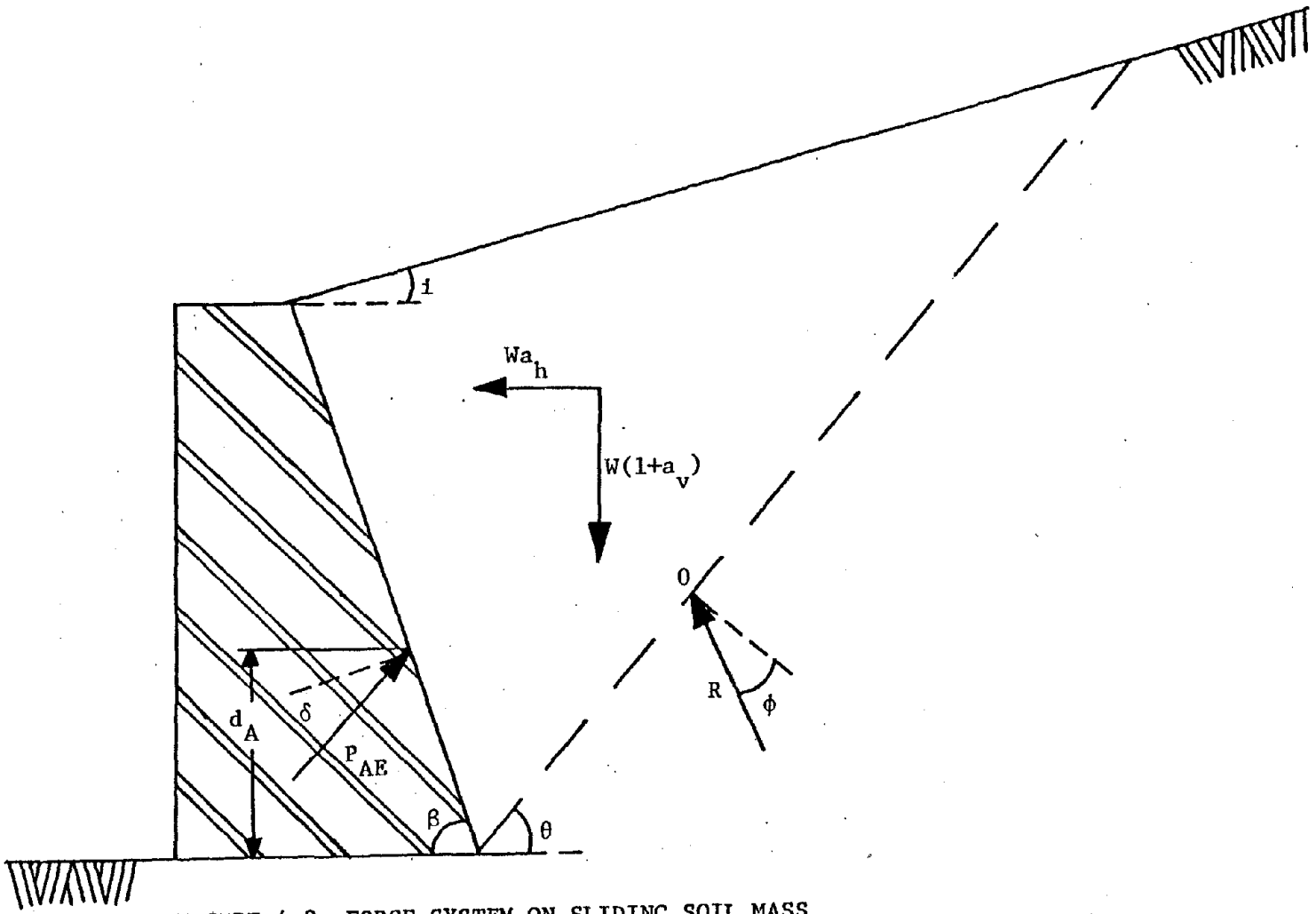

FIGURE 4.2 FORCE SYSTEM ON SLIDING SOIL MASS

For the active case, the equations of equilibrium of forces along the horizontal and vertical directions are expressed as

$$-W(1 + a_v) + R\cos(\theta-\phi) + P_{AE}\cos(\beta-\delta) = 0$$

$$-W\,a_h - R\sin(\theta-\phi) + P_{AE}\sin(\beta-\delta) = 0 \qquad (4.4)$$

in which W = the weight of the soil wedge which is equal to

$$W = \frac{\gamma H^2}{2}\left[1 + \frac{\tan i(\tan\theta + \tan\beta)}{\tan\beta(\tan\theta - \tan i)}\right]\left[\frac{\tan\theta + \tan\beta}{\tan\theta\tan\beta}\right]$$

and H = the height of the retaining wall;

γ = the unit weight of the backfill material;

ϕ = the angle of internal friction of the backfill material;

δ = the angle of soil wall friction;

i = the inclination of the backfill with the horizontal;

β = the angle of inclination of the back of the retaining wall;

a_h = coefficient of the maximum horizontal ground acceleration, in g's;

a_v = coefficient of the maximum vertical ground acceleration, in g's; and

θ = the angle of inclination of the failure plane ($\theta = 45° + \phi/2$).

Solving the first of Eqns. (4.4) with respect to force R and introducing the resulting expression into the second of Eqns. (4.4), the active force P_{AE} against the retaining wall is found to be

$$P_{AE} = \frac{W}{\sin(\beta-\delta)} \left[\frac{a_h + (1 + a_v) \tan(\theta-\phi)}{1 + \frac{\tan(\theta-\phi)}{\tan(\beta-\delta)}}\right] \tag{4.5}$$

while the resisting force R is

$$R = \frac{W}{\sin(\theta-\phi)} \left[\frac{-a_h + (1 + a_v) \tan(\beta-\delta)}{1 - \frac{\tan(\beta-\delta)}{\tan(\theta-\phi)}}\right] \tag{4.6}$$

Taking moments about point 0, Fig. 4.2, and substituting Eqns. (4.5) and (4.6) for P_{AE} and R, respectively, the distance d_A from the base of the wall to the point of application of P_{AE} is found to be equal to

$$d_A = \frac{H}{3}\left\{\frac{W\, a_h}{P_{AE} \sin(\beta-\delta)}\left[1 + \frac{\tan\theta}{\tan\beta}\right] + \left[1 - \cot\theta \cot(\beta-\delta)\right] \cdot \right. \tag{4.7}$$

$$\left. \cdot \left[1 - \frac{\tan\theta}{\tan\beta} + \frac{\tan i(\tan\theta + \tan\beta)}{\tan\beta(\tan\theta - \tan i)}\right]\right\} \left[1 + \cot\beta \cot(\beta-\delta)\right]^{-1}$$

For the passive case, the expressions for the thrust against the wall P_{PE} and its location d_p may be found in a manner similar to the one described above. Thus, one has

$$P_{PE} = \frac{W}{\sin(\beta+\delta)} \left[\frac{-a_h + (1 + a_v) \tan(\theta+\phi)}{1 - \frac{\tan(\theta+\phi)}{\tan(\beta+\delta)}}\right] \tag{4.8}$$

$$d_p = \frac{H}{3}\left\{\frac{W\, a_h}{P_{PE}\sin(\beta+\delta)}\left[1 + \frac{\tan\theta}{\tan\beta}\right] + \left[1 + \cot\theta\,\cot(\beta+\delta)\right]\right.$$

$$\left. \cdot \left[1 - \frac{\tan\theta}{\tan\beta} + \frac{\tan i(\tan\theta + \tan\beta)}{\tan\beta(\tan\theta - \tan i)}\right]\right\}\left[1 - \cot\beta\,\cot(\beta+\delta)\right]^{-1} \qquad (4.9)$$

in which $\theta = 45° - \phi/2$.

In the case of a smooth, vertical wall with a horizontal backfill under static conditions (i.e., $\delta = i = a_h = a_v = 0$ and $\beta = 90°$), Eqns. (4.5) and (4.6) are reduced to the expressions provided by Coulomb's theory; i.e.,

$$P_{AE/PE} = \frac{H^2}{2}\,\frac{\tan(\theta \mp \phi)}{\tan\theta}$$

$$d_{A/P} = \frac{H}{3} \qquad (4.10)$$

in which the upper and lower signs correspond to the active and passive cases, respectively.

4.2.2 Multi-Layered Representation of the Backfill

The statistically independent layered model of the backfill considers the latter to be divided into a series of n horizontal layers each with a thickness equal to H/n. This is shown schematically in Fig. 4.3. The value taken by the angle of internal friction for each layer is independent of the values taken by any other layer. However, each layer has the same distribution of the angle of internal friction.

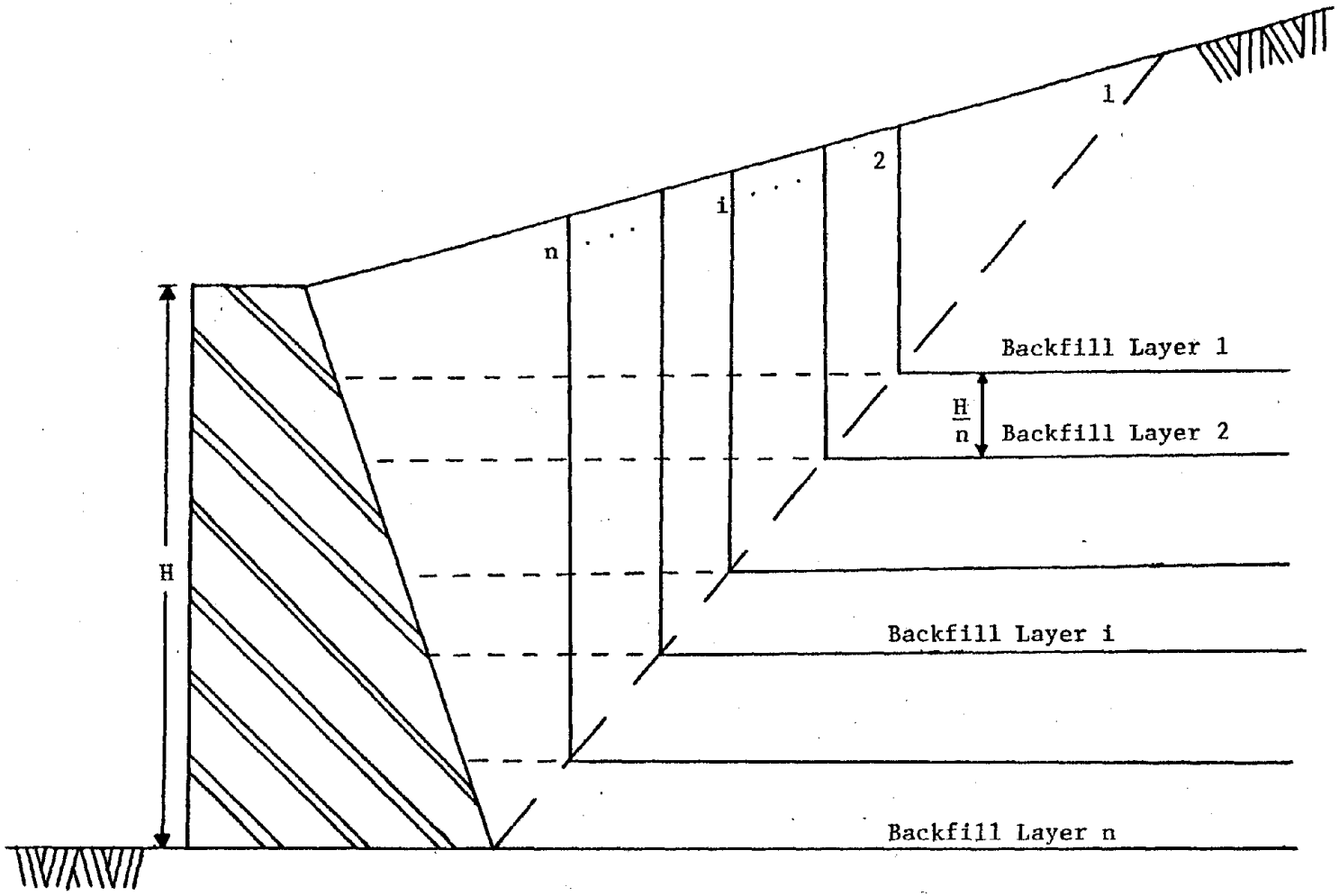

FIGURE 4.3 LOCATION OF BACKFILL SLICES FOR THE MULTI-LAYER BACKFILL MODEL

A procedure similar to the method of slices, often used in slope stability analysis, is employed to determine the forces in this case. This is illustrated in Fig. 4.3.

The forces acting on the i-th slice are shown in Fig. 4.4. An examination of the forces and their points of application on the i-th slice reveals that there are four unknowns (i.e., F_i, V_i, h_i, and R_i, defined in Fig. 4.4). The magnitude of the interslice forces F_{i-1} and V_{i-1} and their point of application h_{i-1}, on the right-hand side of the i-th slice are known from the analysis of slice i-1. The location d_{R_i} of the resultant force R_i is known as it is considered to act at the center of gravity of the slice. Therefore, there are 4n unknown quantities and 3n equations (i.e., three equations of equilibrium for each slice).

Hence, for the force system to become statically determinate, n additional equations are required. If the interslice shear forces V_i are assumed to be equal to zero (i.e., $V_i = 0$), n-1 equations are introduced (the n-th shear force is not equal to zero since it acts on the retaining wall). In addition, the direction of the resultant of the forces on the left-hand side of the n-th slice is known to be equal to the angle of the soil wall friction δ. This provides the last additional equation required.

Thus, the unknown quantities in the equivalent statistically independent layered model are: h_i, F_i, and R_i, for

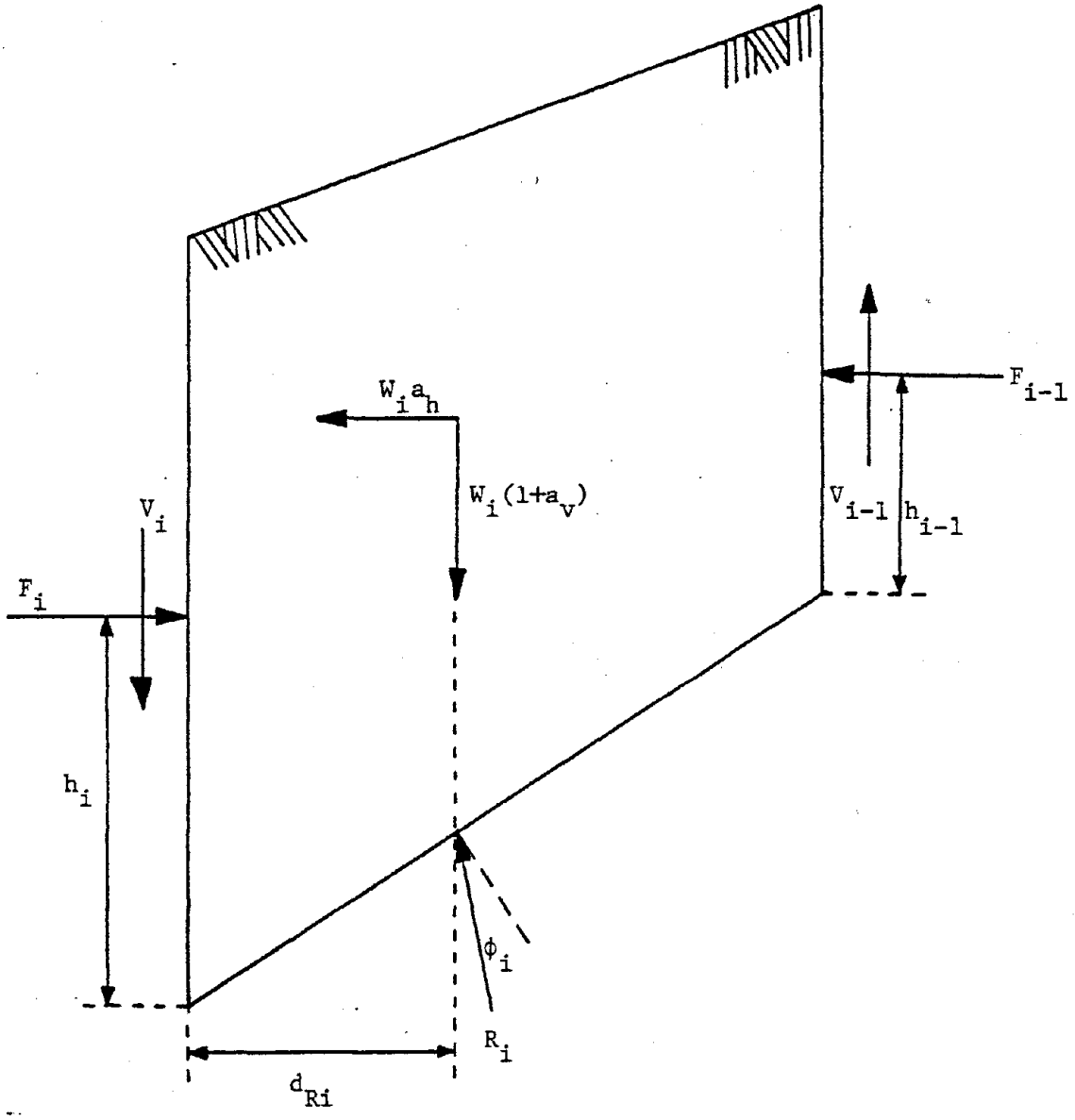

FIGURE 4.4 FORCES ON THE i-th SLICE OF THE BACKFILL MEDIUM

$i = 1,2,\ldots n-1$, and R_n, P_{AE}, and d_A. These are shown in Fig. 4.5.

The numerical values of these quantities are found by considering that, for the general i-th slice, the three equations of equilibrium may be expressed as

$$F_i = F_{i-1} + [(2n-2i+1)W_2+W_3+(2i-1)W_4][a_h+(1+a_v)\tan(\theta-\phi_i)]$$

$$R_i = \frac{(1+a_v)[(2n-2i+1)W_2+W_3+(2i-1)W_4]}{\cos(\theta-\phi_i)} \qquad (4.11)$$

$$d_i F_i = F_{i-1}[\frac{H}{n} + d_{i-1}] + R_i \sin(\theta-\phi_i) d_{R_i} + a_h H\{(2n-2i+1) W_2 \cdot$$

$$\cdot [\frac{i}{n} + \frac{\tan i}{\tan \beta} + \frac{n^2 - 2ni+i^2-i-1/3}{2n^2 - 2n\, i + n} \frac{\tan i}{\tan \theta}]$$

$$+ W_3 [\frac{i}{n} + \frac{\tan i}{2\tan \beta}] + W_4 [\frac{3i^2 - 1}{3n}]\}$$

in which

$$d_{R_i} = \frac{(1+a_v)\, H[(6n - 6i + 4) W_2+3W_3+(6i-4) W_4]}{R_i \cos(\theta - \phi_i)}$$

and the element weights (i.e., W_1, W_2, ... W_6) are defined in Fig. 4.6.

For the n-th slice, the equations of equilibrium yield

$$P_{AE} = \frac{[a_h+(1+a_v)\tan(\theta-\phi_n)]\ \{W_1+ \sum_{i=1}^{n} [(2n-2i+1)W_2+W_3+(2i-1)W_4]+W_5+W_6\}}{\sin(\beta-\delta)\ [1 + \frac{\tan(\theta-\phi_n)}{\tan(\beta-\delta)}]}$$

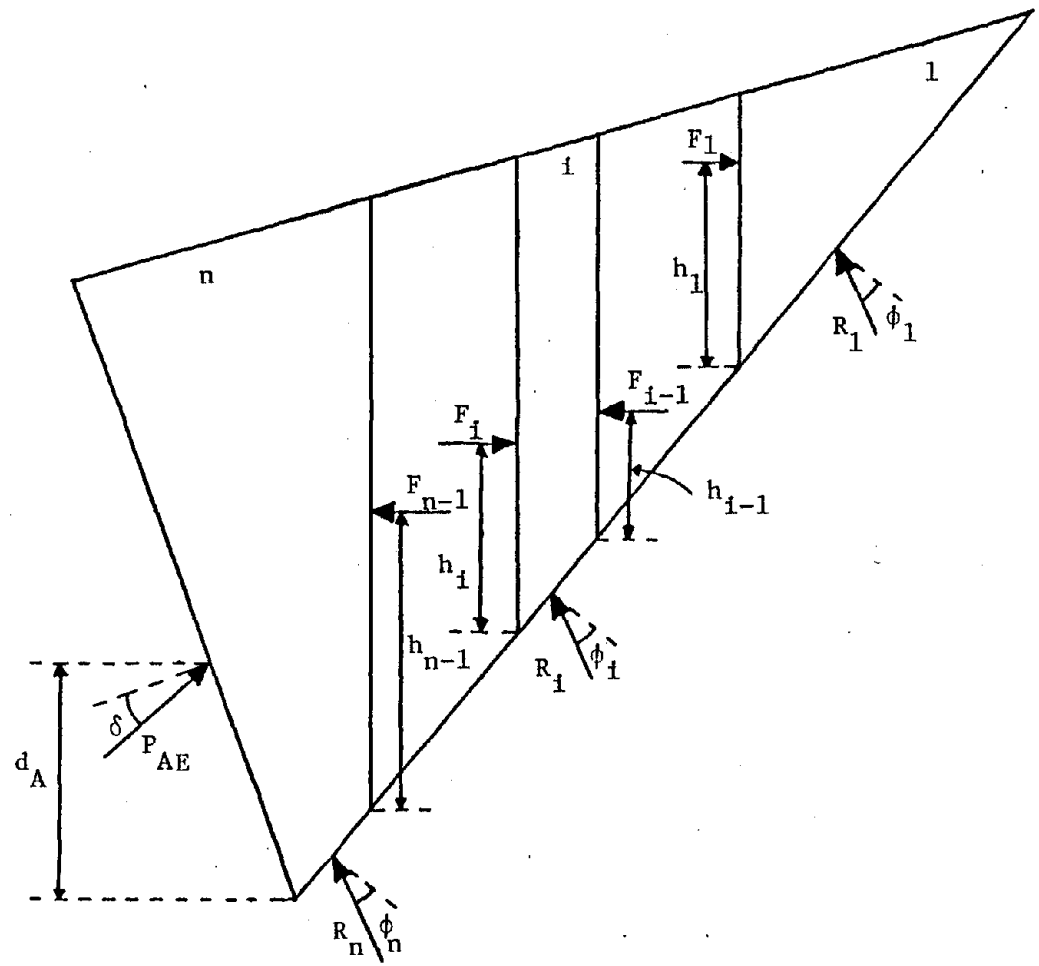

FIGURE 4.5 THE UNKNOWN FORCES ON THE BACKFILL FOR THE MULTI-LAYER MODEL

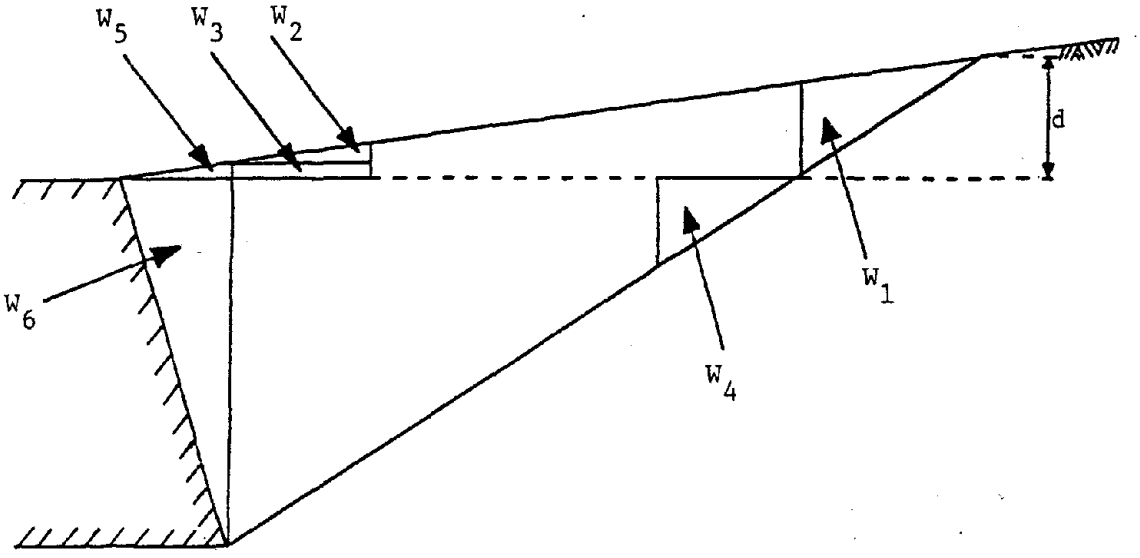

$$W_1 = \frac{\gamma H d}{2} \frac{\tan i}{\tan\theta} \left(\frac{\tan\theta+\tan\beta}{\tan\theta\tan\beta}\right)$$

$$W_2 = \frac{\gamma H^2}{2n^2} \frac{\tan i}{\tan^2\theta}$$

$$W_3 = \frac{\gamma H^2}{n} \frac{\tan^2 i}{\tan\theta\tan\beta}$$

$$W_4 = \frac{\gamma H^2}{2n^2} \frac{1}{\tan\theta}$$

$$W_5 = \frac{\gamma H^2}{2} \frac{1}{\tan\beta}$$

$$d = H\left[\frac{\tan i(\tan\theta+\tan\beta)}{\tan\ (\tan\theta-\tan i)}\right]$$

FIGURE 4.6 DEFINITION OF ELEMENTAL WEIGHTS APPEARING IN EQUATIONS (4.11) AND (4.12)

$$R_n = \frac{(1+a_v)[W_2+W_3+(2n-1)W_4+W_5+W_6]-P_{AE}\cos(\beta-\delta)}{\cos(\theta-\phi_n)} \tag{4.12}$$

$$d_A = H\{F_{n-1}[\frac{d_{n-1}}{H} + \frac{1}{n}] + R_n \cos(\theta-\phi_n)[\tan(\theta-\phi_n) + \cot\phi]\frac{d_R}{H}$$

$$+ W_2[a_h(1 + \frac{\tan i}{\tan\beta} + \frac{\tan i}{3n\tan\theta}) - (1 + a_v)\frac{2}{3n\tan\theta}]$$

$$+ W_3[a_h(1 + \frac{\tan i}{2\tan\beta}) - (1 + a_v)\frac{1}{2n\tan\theta}]$$

$$+ W_4[a_h(\frac{3n^2-1}{3n}) - (1 + a_v)\frac{3n-2}{3n\tan\theta}]$$

$$+ W_5[a_h(1 + \frac{\tan i}{\tan\beta}) + (1 + a_v)\frac{1}{3\tan\beta}]$$

$$+ W_6[a_h\frac{2}{3} + (1 + a_v)\frac{1}{3\tan\beta}]\}/P_{AE}\cos(\beta-\delta)[\tan(\beta-\delta) + \cot\beta]$$

in which

$$d_R = \frac{(1 + a_v)H}{R_n\cos(\theta-\phi_n)}[\frac{2W_2}{3n} + \frac{W_3}{2n} + \frac{(2n-2)W_4}{3n} - \frac{\tan\beta(W_5+W_6)}{3\tan\beta}]$$

and F_{n-1} and d_{n-1} are obtained from Eqns. (4.11).

CHAPTER 5

PARAMETRIC STUDY

5.1 Parameters and Conditions Considered

This chapter examines the effect of material and model parameters on the magnitude and point of application of the active earth thrust against a retaining wall. The specific parameters that are investigated are the following:

(1) the single- and multi-layer representation of the backfill material;

(2) the angle of internal friction of the backfill material;

(3) the maximum ground acceleration;

(4) the angle of soil-wall friction;

(5) the inclination of the back face of the wall; and

(6) the inclination of the backfill with respect to the horizontal direction.

The retaining wall under examination is shown schematically in Fig. 5.1. For the purposes of this study, the following conditions are assumed:

1) the backfill material, when considered as a multi-layer system, consists of four equivalent statistically independent layers (i.e., $n = 4$);

2) the angle of internal friction is a random variable with mean value $\bar{\phi}$ and coefficient of variation V_ϕ equal to

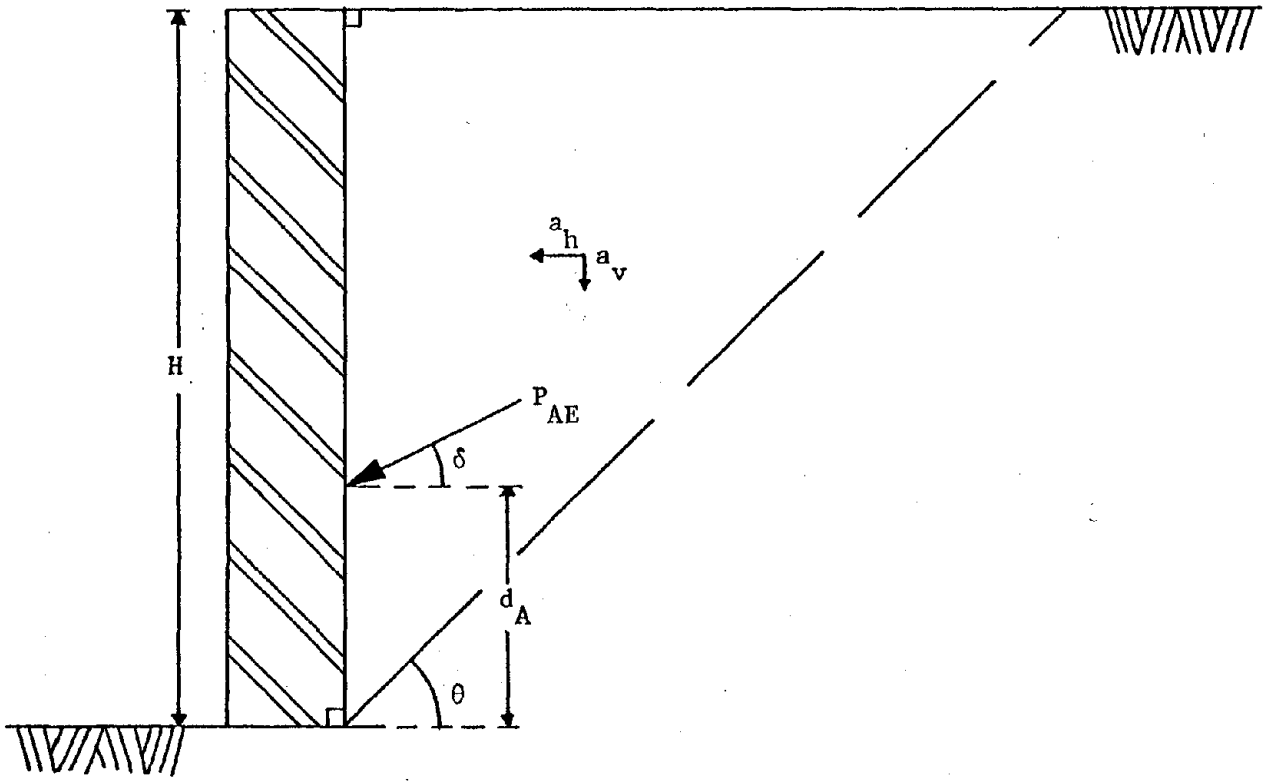

FIGURE 5.1 GEOMETRY AND MATERIAL PARAMETERS OF THE RETAINING WALL USED IN THE PARAMETRIC STUDY

35 degrees and 20 percent, respectively (i.e., $\bar{\phi} = 35°$ and $V_\phi = 20\%$);

3) the maximum ground acceleration is considered to be a random variable with its coefficient of variation equal to 10 percent (i.e., $V_a = 10\%$);

4) the ratio of the vertical to the horizontal components of the maximum ground acceleration, a_v and a_h, respectively, is equal to two-thirds and is directed downward (i.e., $a_v = \frac{2}{3} a_h$);

5) the angle of soil-wall friction δ is equal to one-half the angle of internal friction (i.e., $\delta = \frac{1}{2} \bar{\phi}$);

6) the back face of the wall is vertical (i.e., $\beta = 90°$);

7) the backfill is horizontal (i.e., $i = 0°$); and

8) the angle of internal friction is considered to be independent of the maximum ground acceleration.

The expected value $E[P_{AE}]$ and variance $V[P_{AE}]$ of the active earth thrust and the expected value of its point of application $E[d_A]$ are estimated using the two-point estimate method for independent symmetrically distributed random variables given by Eqn. (2.13). Estimates of $E[P_{AE}]$, $V[P_{AE}]$, and $E[d_A]$ are made for both the single- and multi-layer model of the backfill.

For the single-layer model, the mean value $\bar{\phi}$ and coefficient of variation V_ϕ of the angle of internal friction ϕ are found to be equal to (Eqns. (4.2)) 35° and 10%, respectively. The expressions for the active earth thrust P_{AE} and its point of application d_A are

given in Eqns. (4.5) and (4.7), respectively. In Table 5.1 are presented the values of the point estimates of ϕ and a_h used in this study for the single-layer model.

The mean value $\bar{\phi}$ and coefficient of variation V_ϕ of the angle of internal friction ϕ for each of the four layers of the multi-layer model are equal to 35° and 20%, respectively. The point estimates of ϕ_i and a_h, where i = 1,2,3,4, are presented in Table 5.2. The active earth thrust P_{AE} and its point of application d_A are found from Eqns. (4.12) for the multi-layer model of the backfill.

The expected values of P_{AE} and d_A found in this study are made dimensionless by forming the ratios of $E[P_{AE}]$ over γH^2 and $E[d_A]$ over H (i.e., $E[P_{AE}]/\gamma H^2$ and $E[d_A]/H$), in which γ denotes the unit weight of the backfill material and H denotes the height of the retaining wall.

5.2 Expected Value of the Active Earth Thrust

The expected value of the active earth thrust $E[P_{AE}]$ is presented in Figs. 5.2 through 5.6 for values of the mean maximum horizontal ground acceleration varying from 0.0g to 0.5g.

5.2.1 Effect of the Backfill Model

From Figs. 5.2 through 5.6, it is seen that the expected value of active earth thrust $E[P_{AE}]$ is not affected by the model assumed to represent the backfill. For all conditions examined, it was found that the value of $E[P_{AE}]$ for the single-and multi-layer models were equal.

TABLE 5.1

POINT ESTIMATES OF THE ANGLE OF INTERNAL FRICTION AND THE GROUND ACCELERATION FOR THE SINGLE-LAYER MODEL OF BACKFILL

PARAMETER	POINT ESTIMATES		
Angle of Internal Friction	ϕ_+	$\bar{\phi}+\sigma_\phi$	38.5°
	ϕ_+	$\bar{\phi}-\sigma_\phi$	31.5°
Horizontal Acceleration	a_{h+}	$\bar{a}_h+\sigma_a$	$1.1\bar{a}_h$
	a_{h-}	$\bar{a}_h-\sigma_a$	$0.9\bar{a}_h$
Vertical Acceleration	a_{v+}	-	$2/3a_{h+}$
	a_{v-}	-	$2/3a_{h-}$

Note: $\sigma_\phi = V_\phi \bar{\phi}/\sqrt{n} = 0.2 \times 35°/\sqrt{4} = 3.5°$

$\sigma_a = V_a \bar{a}_h = 0.1 \bar{a}_h$

TABLE 5.2

POINT ESTIMATES OF THE ANGLE OF INTERNAL FRICTION AND THE GROUND ACCELERATION FOR THE MULTI-LAYER MODEL OF BACKFILL

PARAMETER	POINT ESTIMATES		
Angle of Internal Friction Layer 1	ϕ_{1+}	$\bar{\phi} + \sigma_\phi$	42°
	ϕ_{1-}	$\bar{\phi} - \sigma_\phi$	28°
Angle of Internal Friction Layer 2	ϕ_{2+}	$\bar{\phi} + \sigma_\phi$	42°
	ϕ_{2-}	$\bar{\phi} - \sigma_\phi$	28°
Angle of Internal Friction Layer 3	ϕ_{3+}	$\bar{\phi} + \sigma_\phi$	42°
	ϕ_{3-}	$\bar{\phi} - \sigma_\phi$	28°
Angle of Internal Friction Layer 4	ϕ_{4+}	$\bar{\phi} + \sigma_\phi$	42°
	ϕ_{4-}	$\bar{\phi} - \sigma_\phi$	28°
Horizontal Acceleration	a_{h+}	$\bar{a}_h + \sigma_a$	$1.1\bar{a}_h$
	a_{h-}	$\bar{a}_h - \sigma_a$	$0.9\bar{a}_h$
Vertical Acceleration	a_{v+}	-	$2/3a_{h+}$
	a_{v-}	-	$2/3a_{h-}$

Note: $\sigma_\phi = V_\phi \bar{\phi} = 0.2 \times 35° = 7.0°$

$\sigma_a = V_a \bar{a}_h = 0.1 \bar{a}_h$

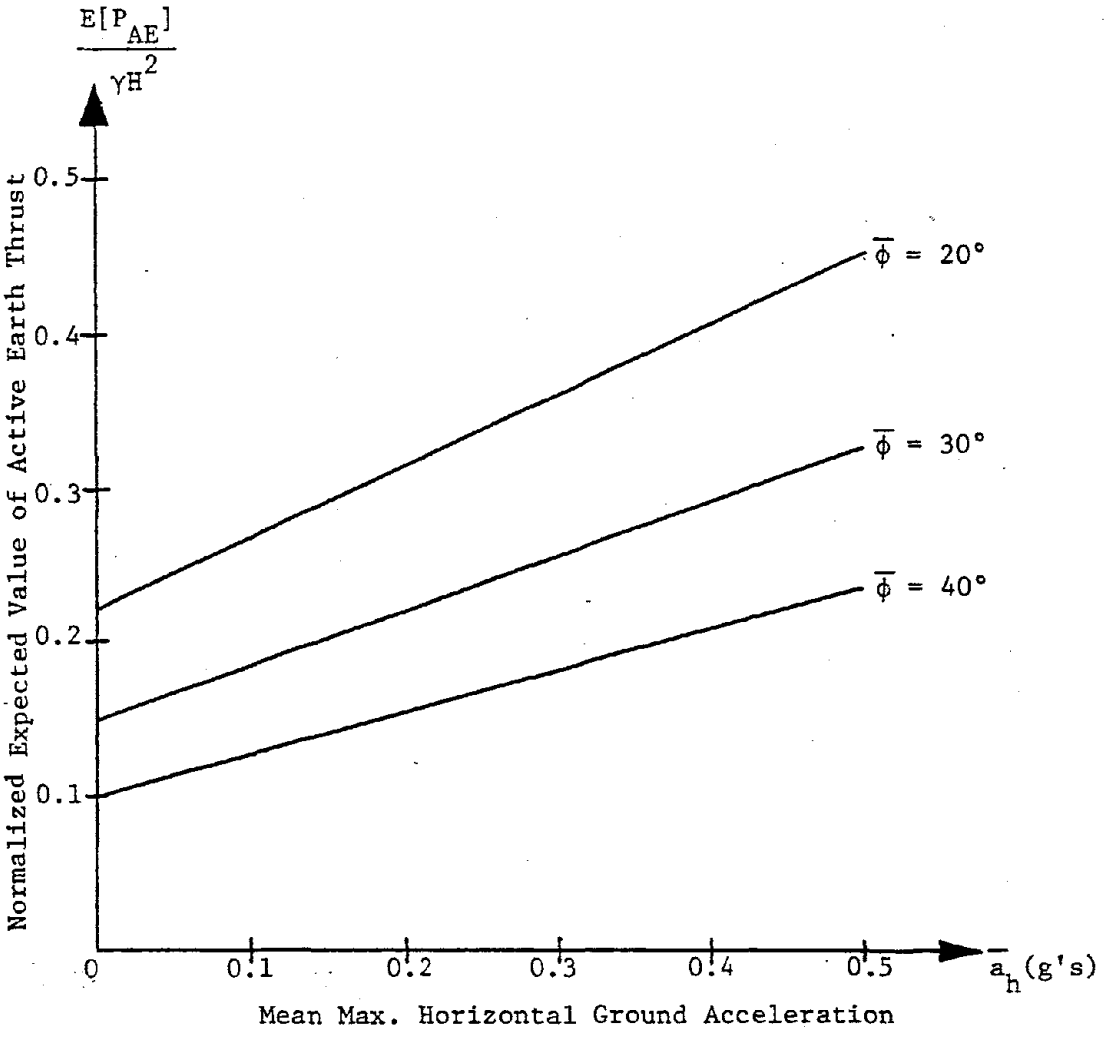

FIGURE 5.2 EFFECT OF MEAN VALUE OF THE ANGLE OF INTERNAL FRICTION ON EXPECTED VALUE OF ACTIVE EARTH THRUST

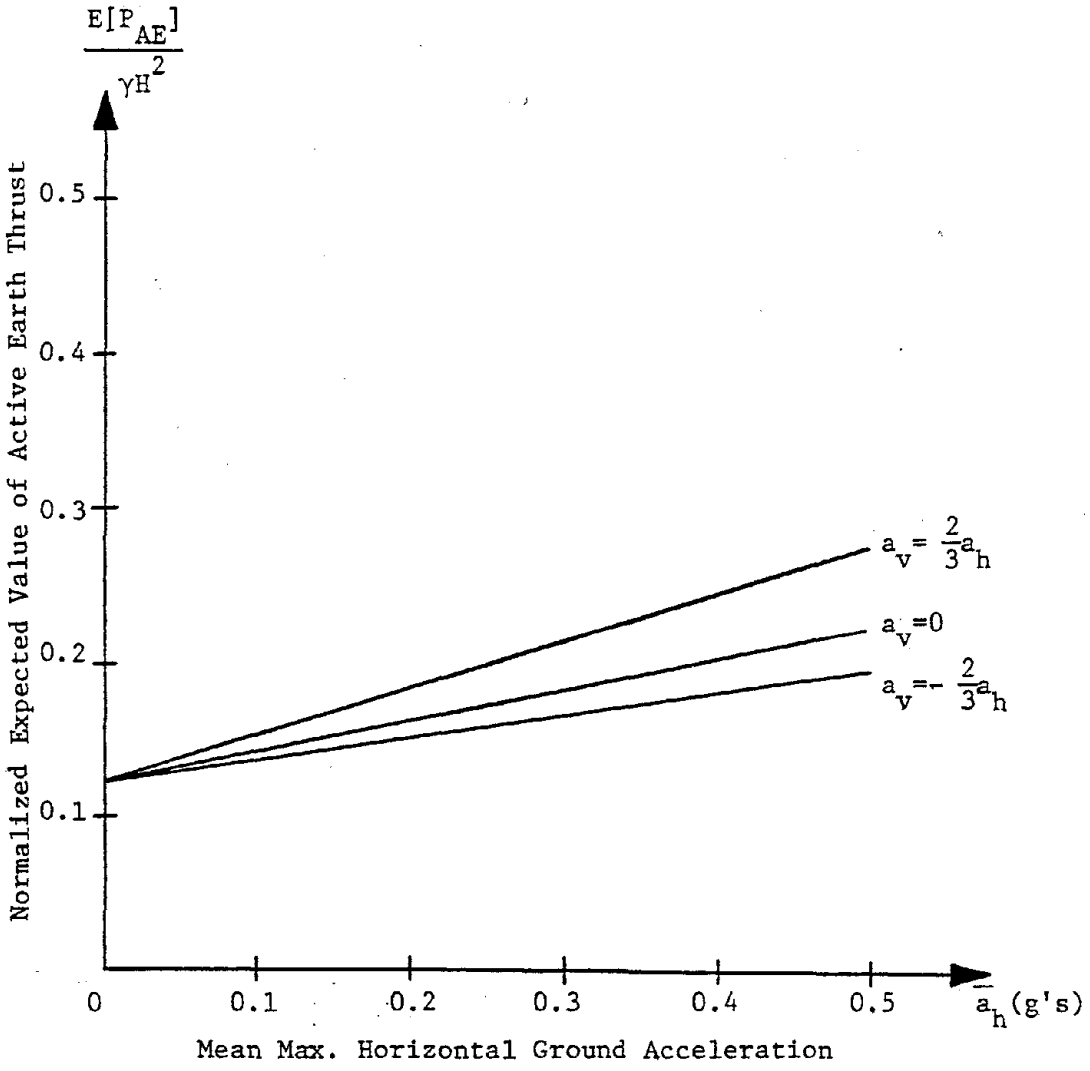

FIGURE 5.3 EFFECT OF DIRECTION OF THE MAX. VERTICAL GROUND ACCELERATION ON EXPECTED VALUE OF ACTIVE EARTH THRUST

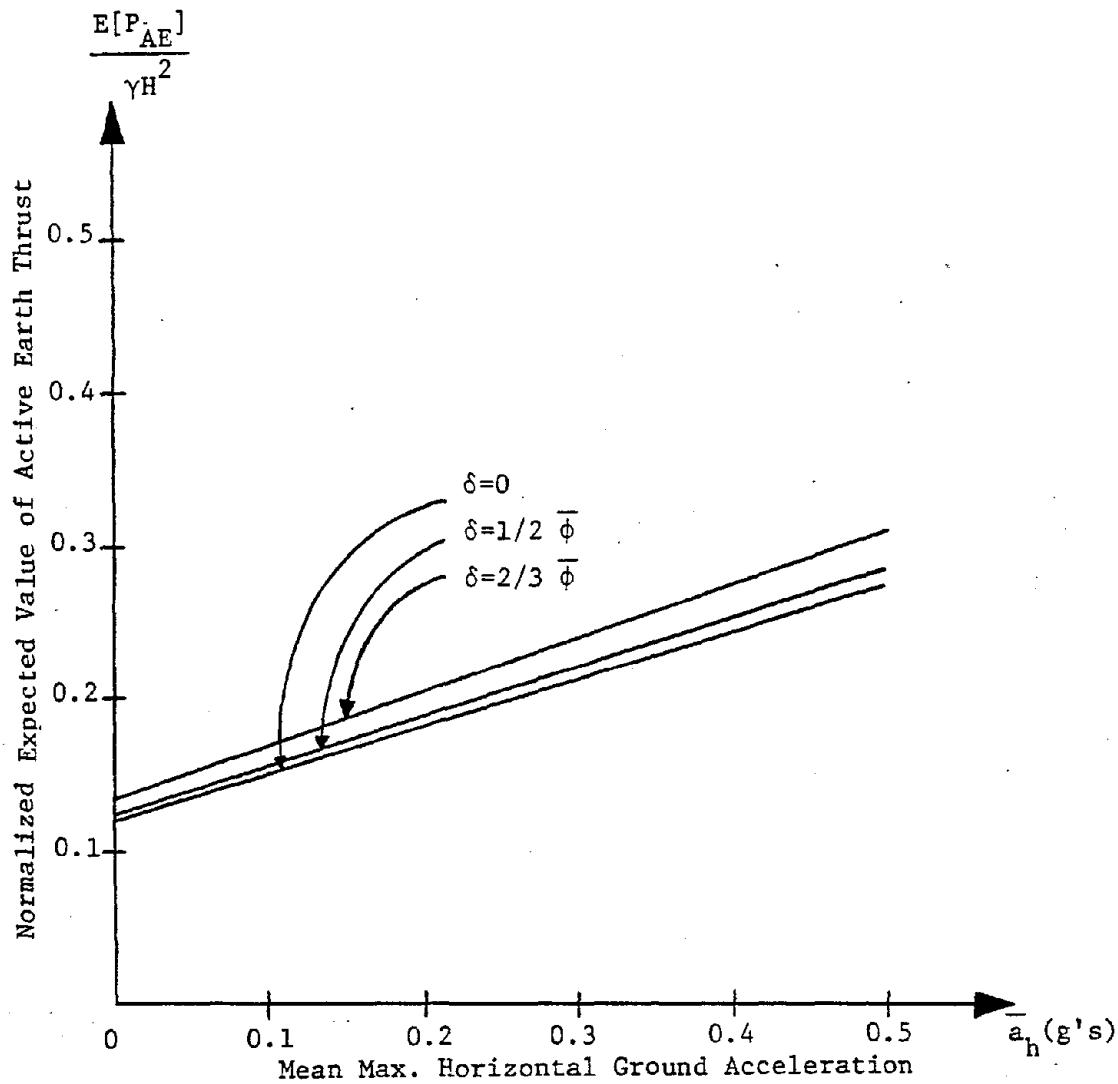

FIGURE 5.4 EFFECT OF ANGLE OF SOIL-WALL FRICTION ON EXPECTED VALUE OF ACTIVE EARTH THRUST

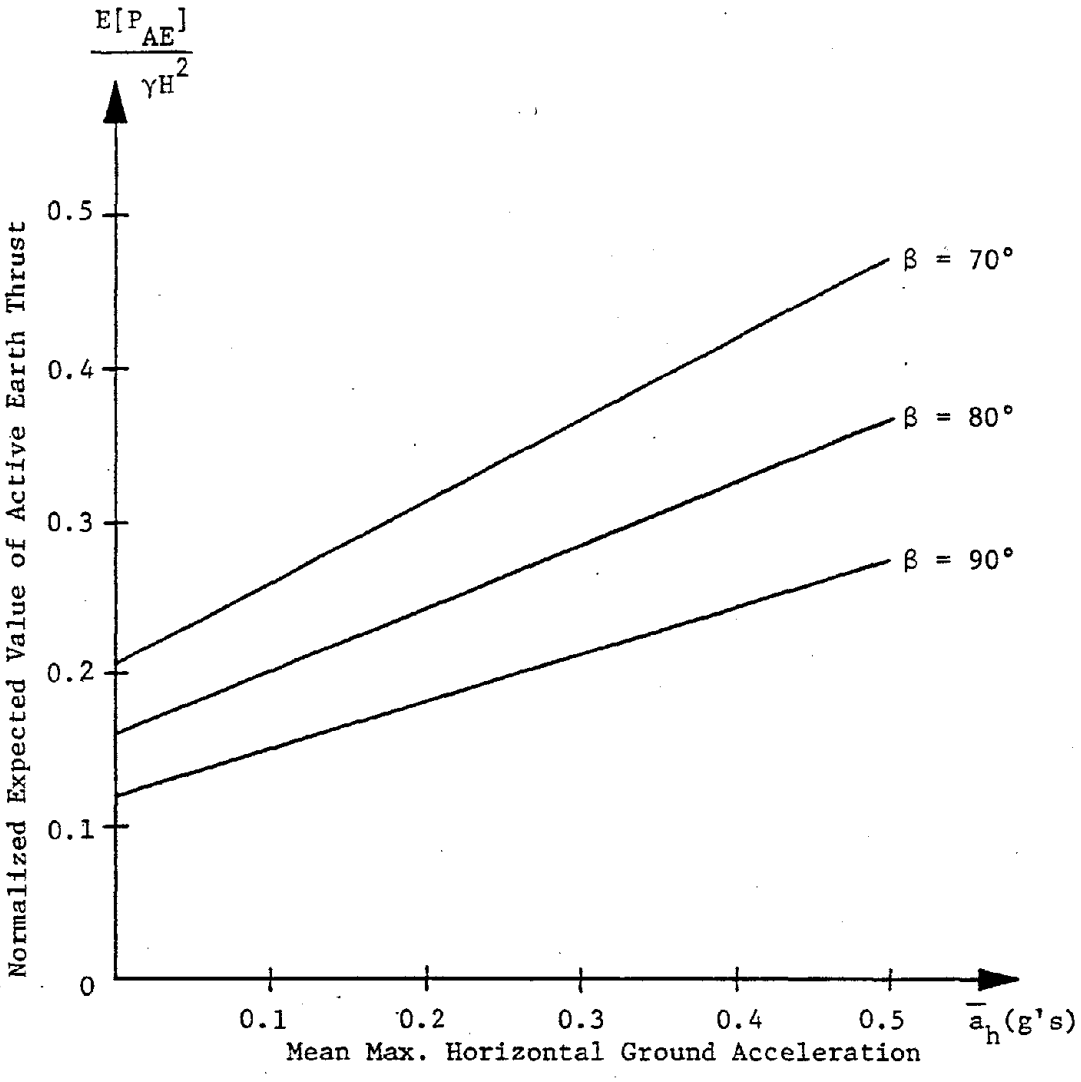

FIGURE 5.5 EFFECT OF INCLINATION OF THE BACK FACE OF WALL ON EXPECTED VALUE OF ACTIVE EARTH THRUST

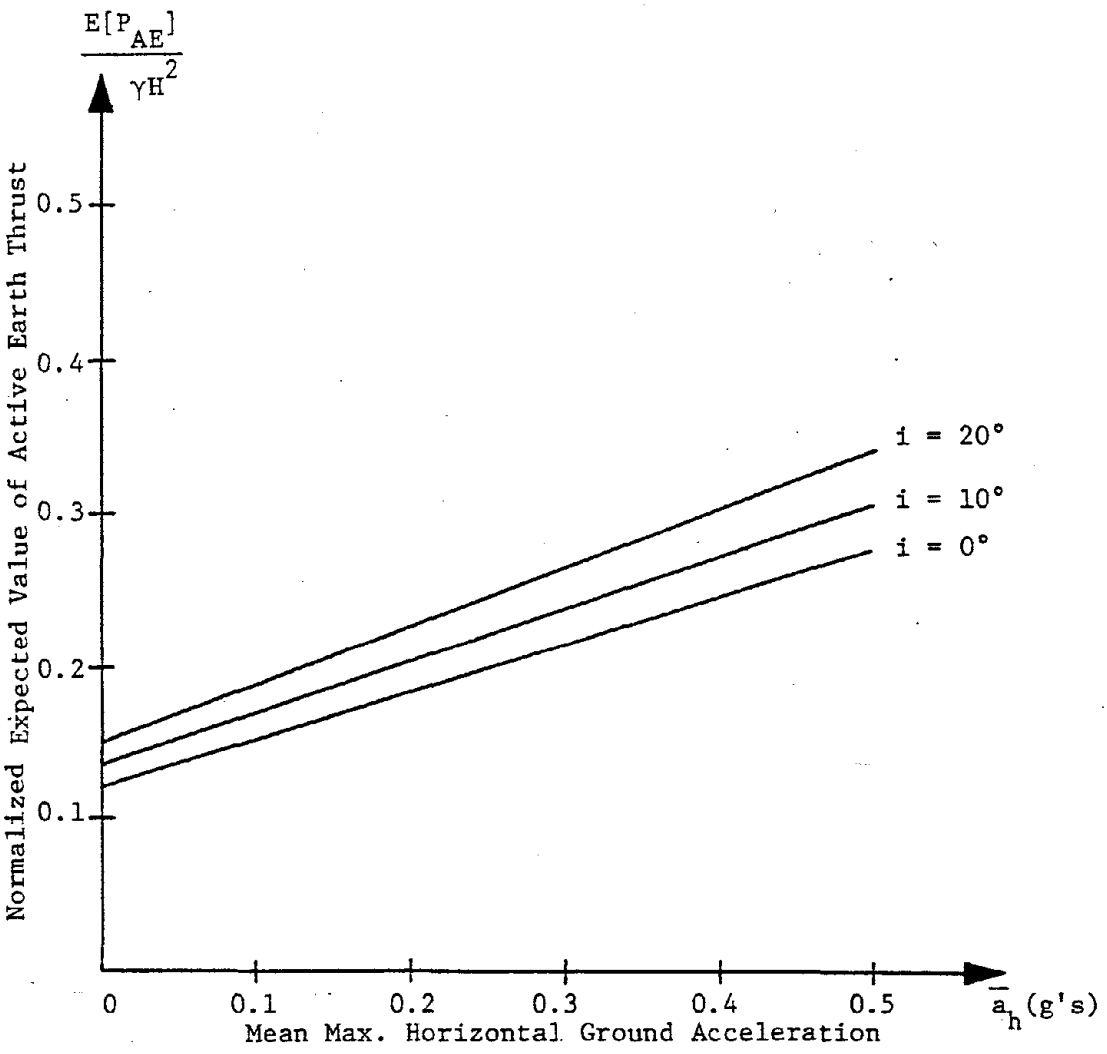

FIGURE 5.6 EFFECT OF INCLINATION OF BACKFILL ON EXPECTED VALUE OF ACTIVE EARTH THRUST

5.2.2 Effect of the Angle of Internal Friction

In Fig. 5.2 is shown the effect of the mean value of the angle of internal friction $\bar{\phi}$ on the expected value of P_{AE}. It can be seen that the magnitude of $E[P_{AE}]$ decreases considerably for increasing values of $\bar{\phi}$.

5.2.3 Effect of the Maximum Ground Acceleration

The effect of the mean value $\bar{a}_h$ of the maximum horizontal ground acceleration on the expected value of P_{AE} is shown in Figs. 5.2 through 5.6. $E[P_{AE}]$ is seen to be linearly dependent on $\bar{a}_h$ for all cases examined.

Figure 5.3 shows the dependence of $E[P_{AE}]$ on the direction of the maximum vertical ground acceleration a_v. The most critical case is seen to be when a_v is directed downward (i.e., $a_v > 0$) and the least critical case is when a_v is directed upward (i.e., $a_v < 0$).

5.2.4 Effect of the Angle of Soil-Wall Friction

In Fig. 5.4 is shown the effect of the soil-wall friction angle δ on the expected value of P_{AE}. The value of $E[P_{AE}]$ increases slightly as δ increases.

5.2.5 Effect of the Inclination of the Retaining Wall

Figure 5.5 shows the dependence of the expected value of P_{AE} on the angle of inclination of the back face of the wall β. It can be seen that $E[P_{AE}]$ increases considerably as β decreases.

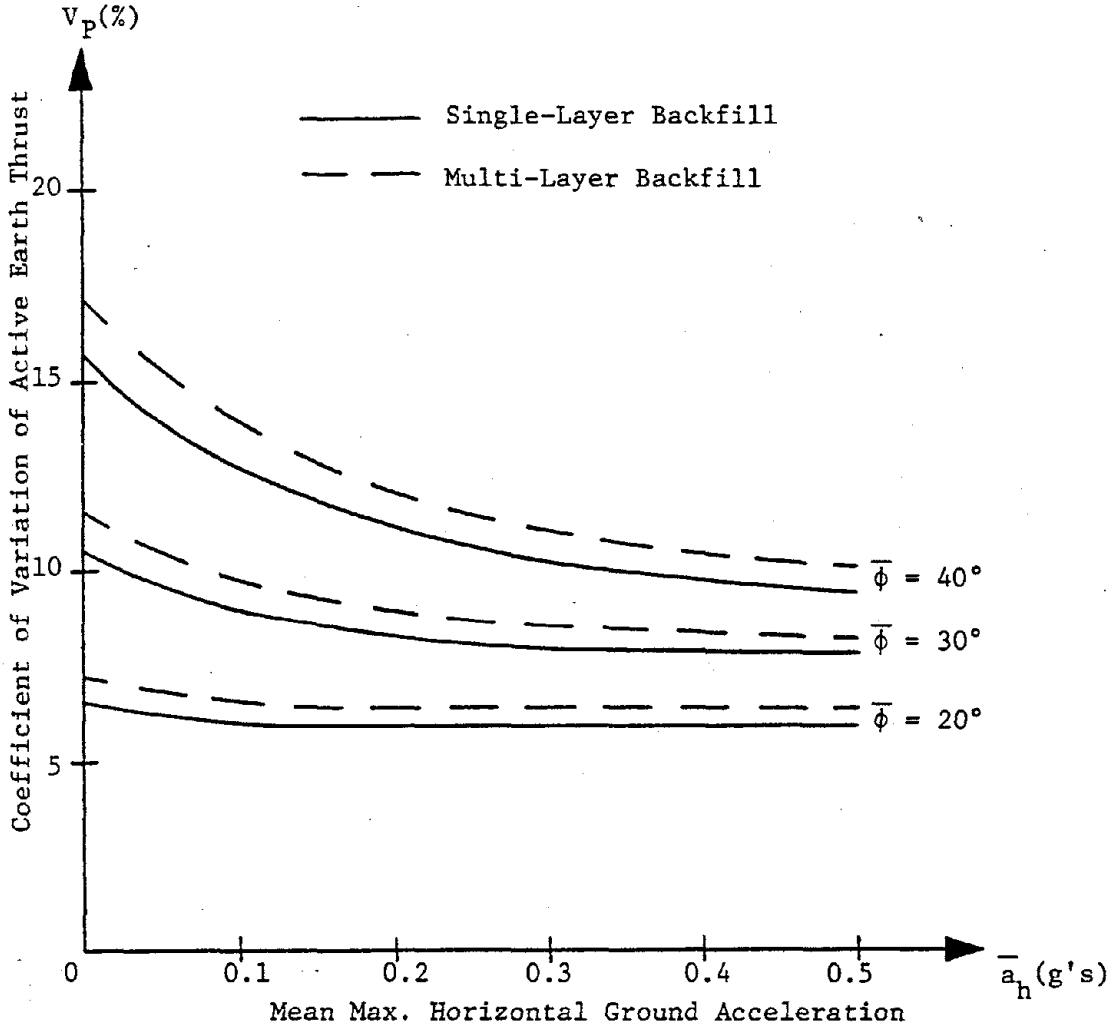

FIGURE 5.7 DEPENDENCE OF COEFFICIENT OF VARIATION OF ACTIVE EARTH THRUST ON MEAN VALUE OF THE ANGLE OF INTERNAL FRICTION

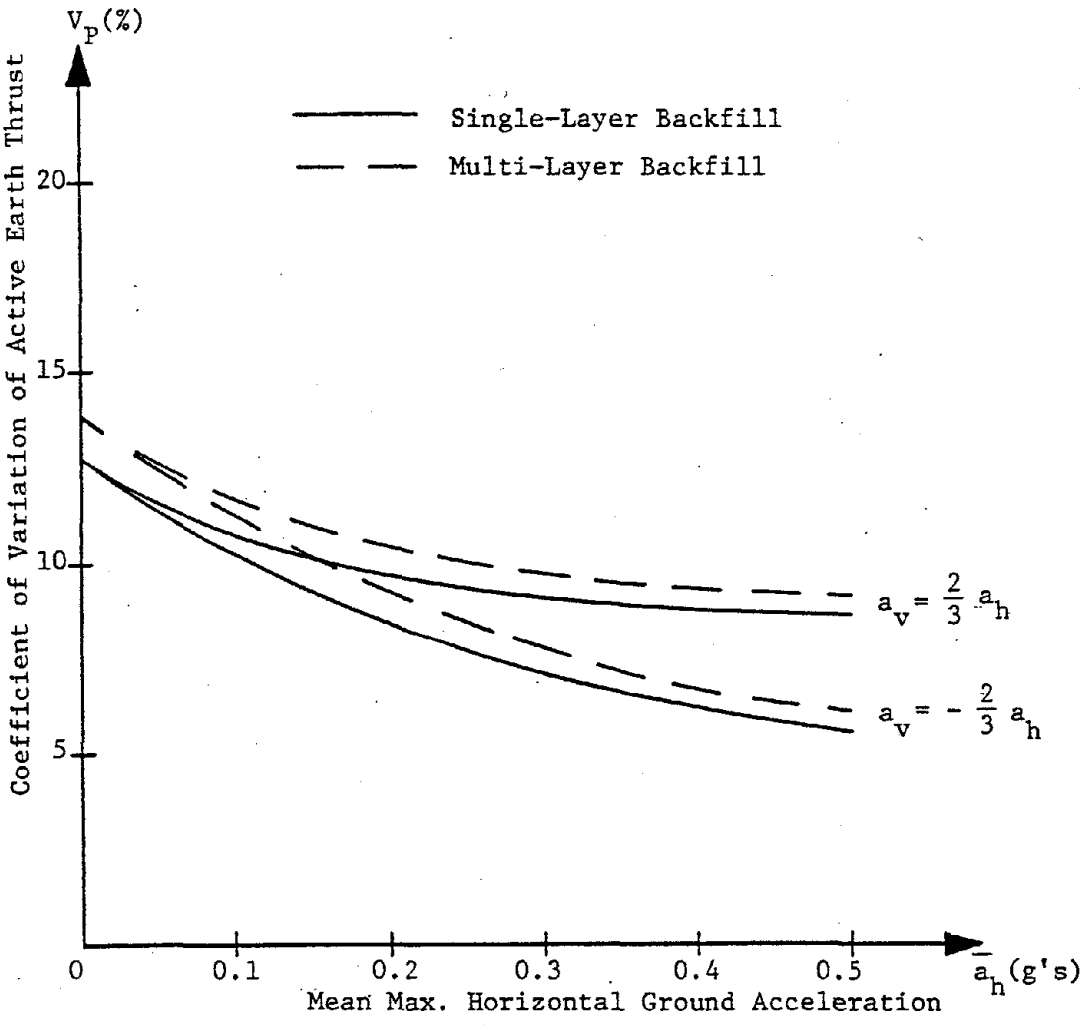

FIGURE 5.8 DEPENDENCE OF COEFFICIENT OF VARIATION OF ACTIVE EARTH THRUST ON DIRECTION OF MAX. VERTICAL GROUND ACCELERATION

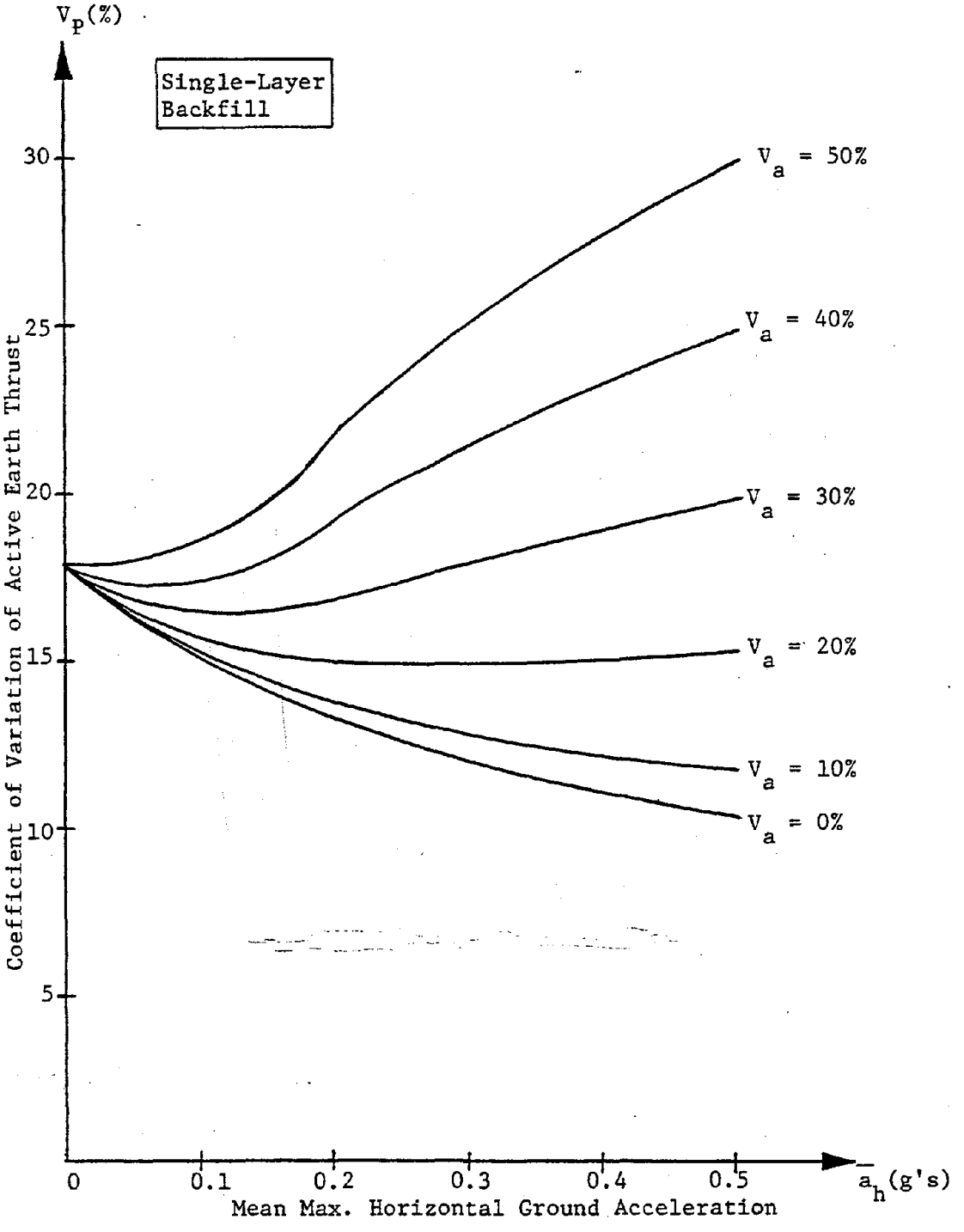

FIGURE 5.9 DEPENDENCE OF COEFFICIENT OF VARIATION OF ACTIVE EARTH THRUST ON COEFFICIENT OF VARIATION OF MAX. GROUND ACCELERATION

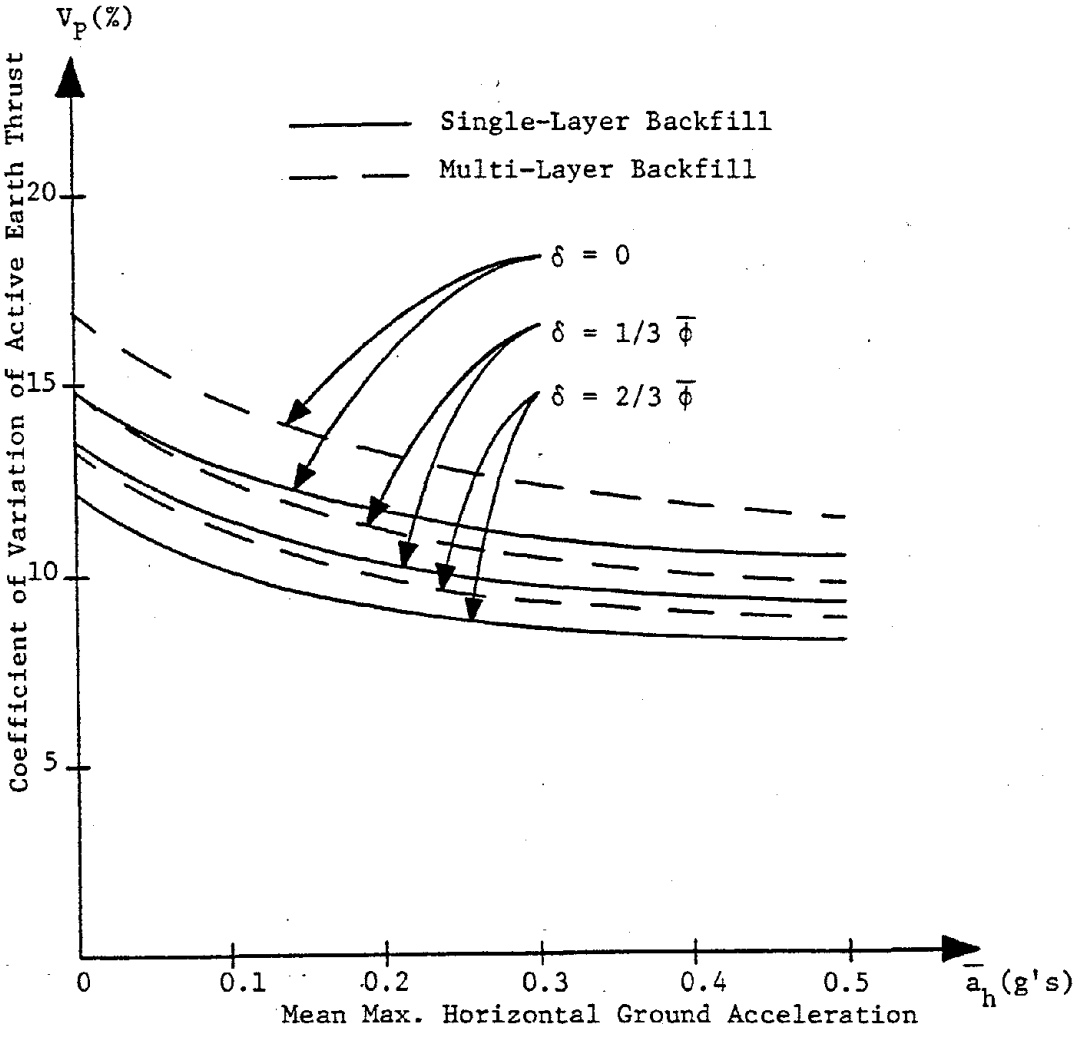

FIGURE 5.10 DEPENDENCE OF COEFFICIENT OF VARIATION OF ACTIVE EARTH THRUST ON ANGLE OF SOIL-WALL FRICTION

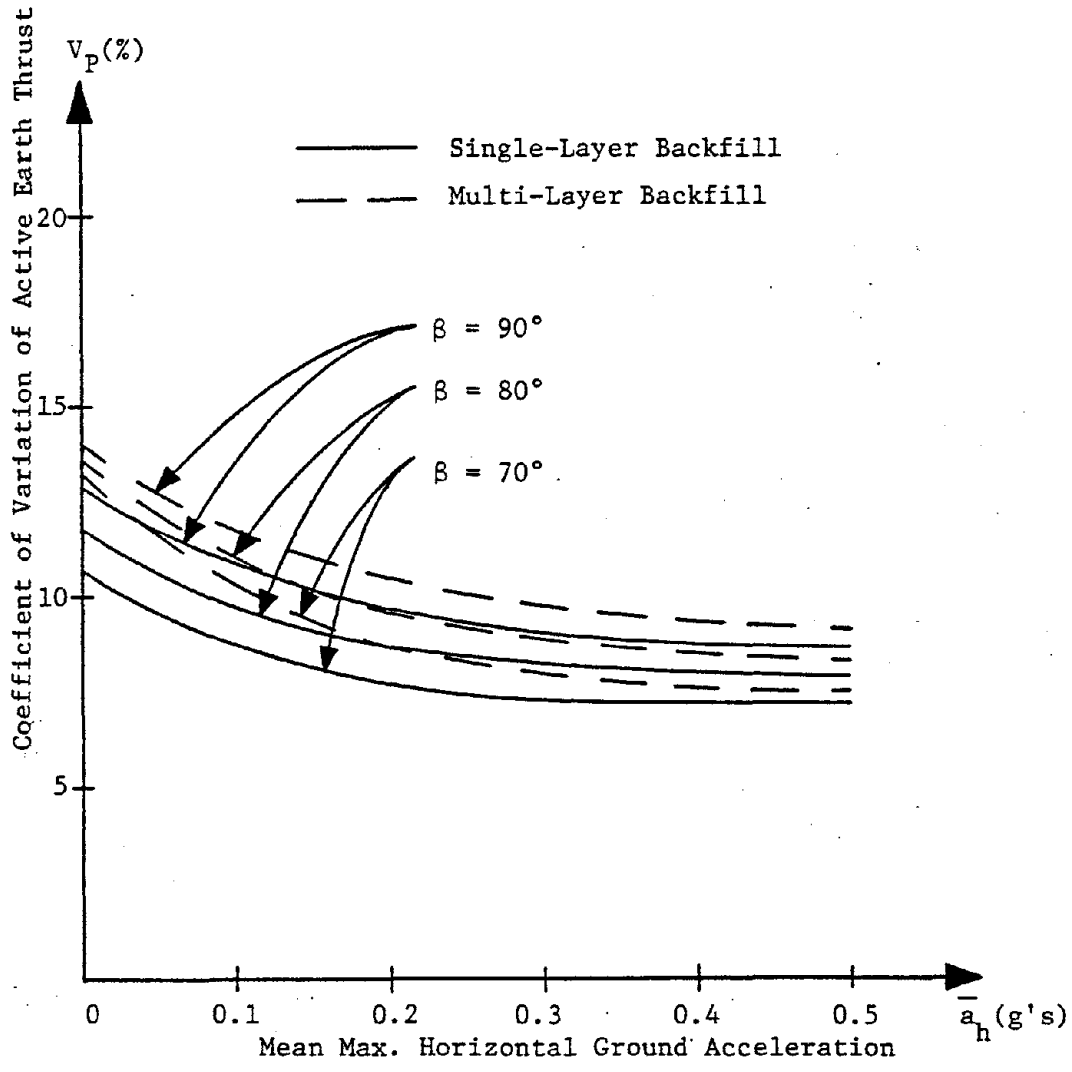

FIGURE 5.11 DEPENDENCE OF COEFFICIENT OF VARIATION OF ACTIVE EARTH THRUST ON INCLINATION OF THE BACK FACE OF WALL

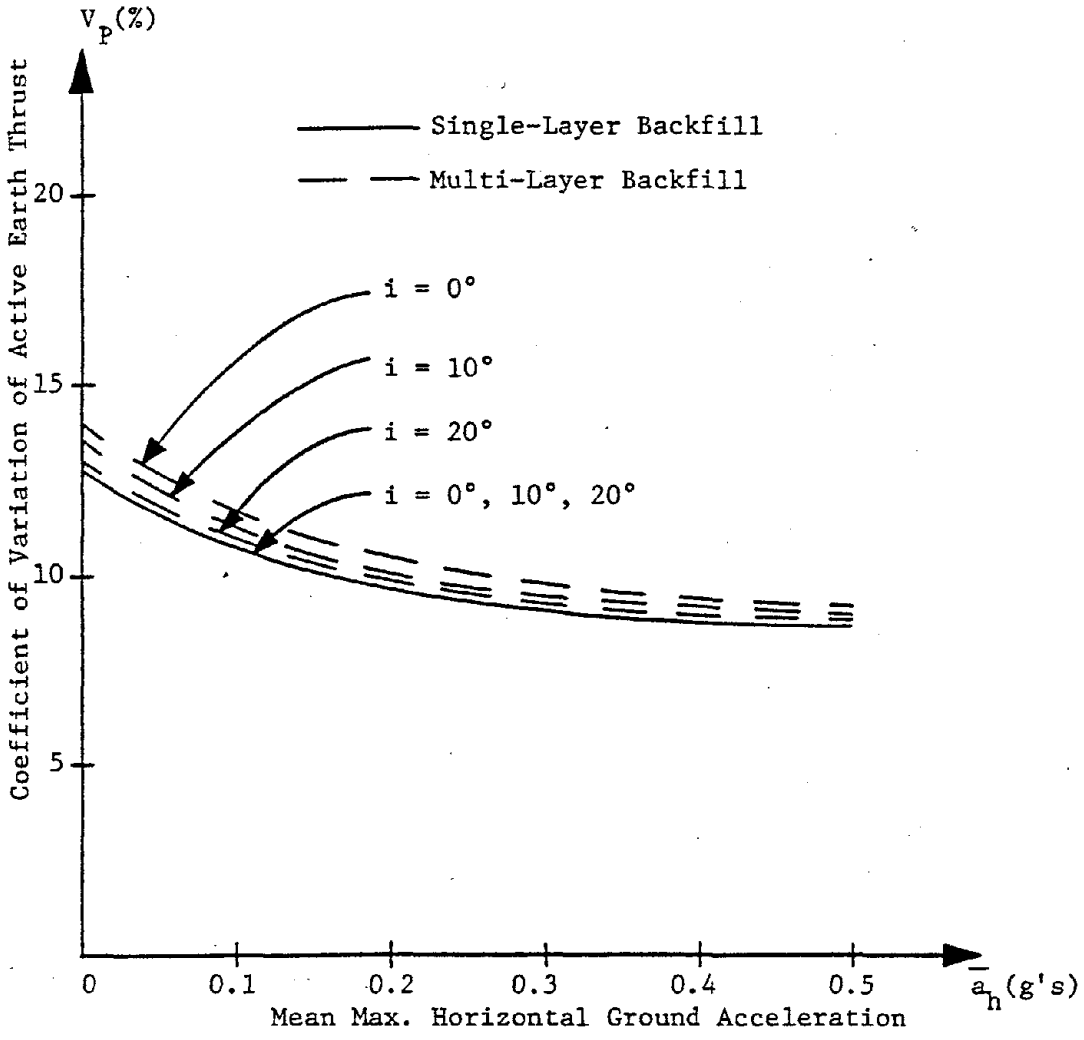

FIGURE 5.12 DEPENDENCE OF COEFFICIENT OF VARIATION OF ACTIVE EARTH THRUST ON INCLINATION OF BACKFILL

5.2.6 Effect of the Inclination of the Backfill

The effect of the angle of the backfill i with respect to the horizontal direction on the expected value of P_{AE} is shown in Fig. 5.6. $E[P_{AE}]$ increases moderately as i increases.

5.3 Coefficient of Variation of the Active Earth Thrust

Values of the coefficient of variation of the active earth thrust V_p for this study are presented in Figs. 5.7 through 5.12.

5.3.1 Effect of the Backfill Model

From Figs. 5.7, 5.8, and 5.10 to 5.12, it is seen that the value of the coefficient of variation of P_{AE} is greater for the multi-layer model of the backfill than for the single-layer model. This occurs because the latter has a reduced variance of the ϕ strength parameter, i.e., σ_ϕ is equal to $V_\phi \bar{\phi}/\sqrt{n}$ (i.e., V_ϕ = 10% for the single layer model).

5.3.2 Effect of the Angle of Internal Friction

In Fig. 5.7 is shown the effect on the coefficient of variation of P_{AE} of the mean value $\bar{\phi}$ of the angle of internal friction of the backfill material. The value of V_p can be seen to increase considerably as $\bar{\phi}$ increases.

5.3.3 Effect of the Maximum Ground Acceleration

The effect of the maximum vertical ground acceleration a_v on the coefficient of variation of P_{AE} is shown in Fig. 5.8. The value of V_p is greater for a downward acceleration ($a_v > 0$) than for

an upward acceleration ($a_v < 0$).

The effect of the coefficient of variation of the maximum ground acceleration V_a on the value of the coefficient of variation of P_{AE} is shown in Fig. 5.9. For values of V_a less than 15 percent, the value of V_p decreases over the entire range of $\bar{a}_h$ examined; while, for values of V_a greater than 15 percent, the value of V_p initially decreases and then increases at $\bar{a}_h = 0.1g$ to $\bar{a}_h = 0.3g$.

5.3.4 Effect of the Angle of Soil-Wall Friction

Figure 5.10 shows the dependence of the coefficient of variation of P_{AE} on the angle of soil-wall friction δ. The value of V_p can be seen to decrease as δ increases from zero to $\frac{2}{3}\bar{\phi}$.

5.3.5 Effect of the Inclination of the Retaining Wall

In Fig. 5.11 is shown the effect of the angle of inclination of the back face of the wall β on the coefficient of variation of P_{AE}. It can be seen that the value of V_p decreases as β decreases.

5.3.6 Effect of the Inclination of the Backfill

Figure 5.12 shows the effect of the angle of the backfill i, with respect to the horizontal direction, on the coefficient of variation of P_{AE}. The value of V_p can be seen to be independent of i for the single-layer model of the backfill; while for the multi-layer model, V_p decreases as i increases.

5.4 Expected Value of the Point of Application of the Active Earth Thrust

The expected values of the point of application of the active earth thrust $E[d_A]$ for the parameteric study are given in Figs. 5.13 through 5.17.

5.4.1 Effect of the Backfill Model

From Figs. 5.13 through 5.17, it can be seen that the expected value of d_A determined for the single-layer model of the backfill is greater than that determined for the multi-layer model. The values of $E[d_A]$ for the two models do not seem to converge at any point, but tend to remain parallel for the range of $\bar{a}_h$ examined.

5.4.2 Effect of the Angle of Internal Friction

Figure 5.13 shows the dependence of the expected value of d_A on the mean value $\bar{\phi}$ of the angle of internal friction of the backfill material. $E[d_A]$ can be seen to be not affected by the value of $\bar{\phi}$ for the range of $\bar{\phi}$ studied.

5.4.3 Effect of the Maximum Ground Acceleration

The effect of the mean value $\bar{a}_h$ of the maximum horizontal ground acceleration on the expected value of d_A is shown in Figs. 5.13 to 5.17. The value of $E[d_A]$ can be seen to increase with $\bar{a}_h$.

In Fig. 5.14 is shown the affect on the expected value of d_A of the direction of the vertical component a_v of the ground acceleration. It can be seen that for $a_v > 0$ (i.e., a_v directed down), the point of application of P_{AE} is lower than when $a_v < 0$ (i.e., when

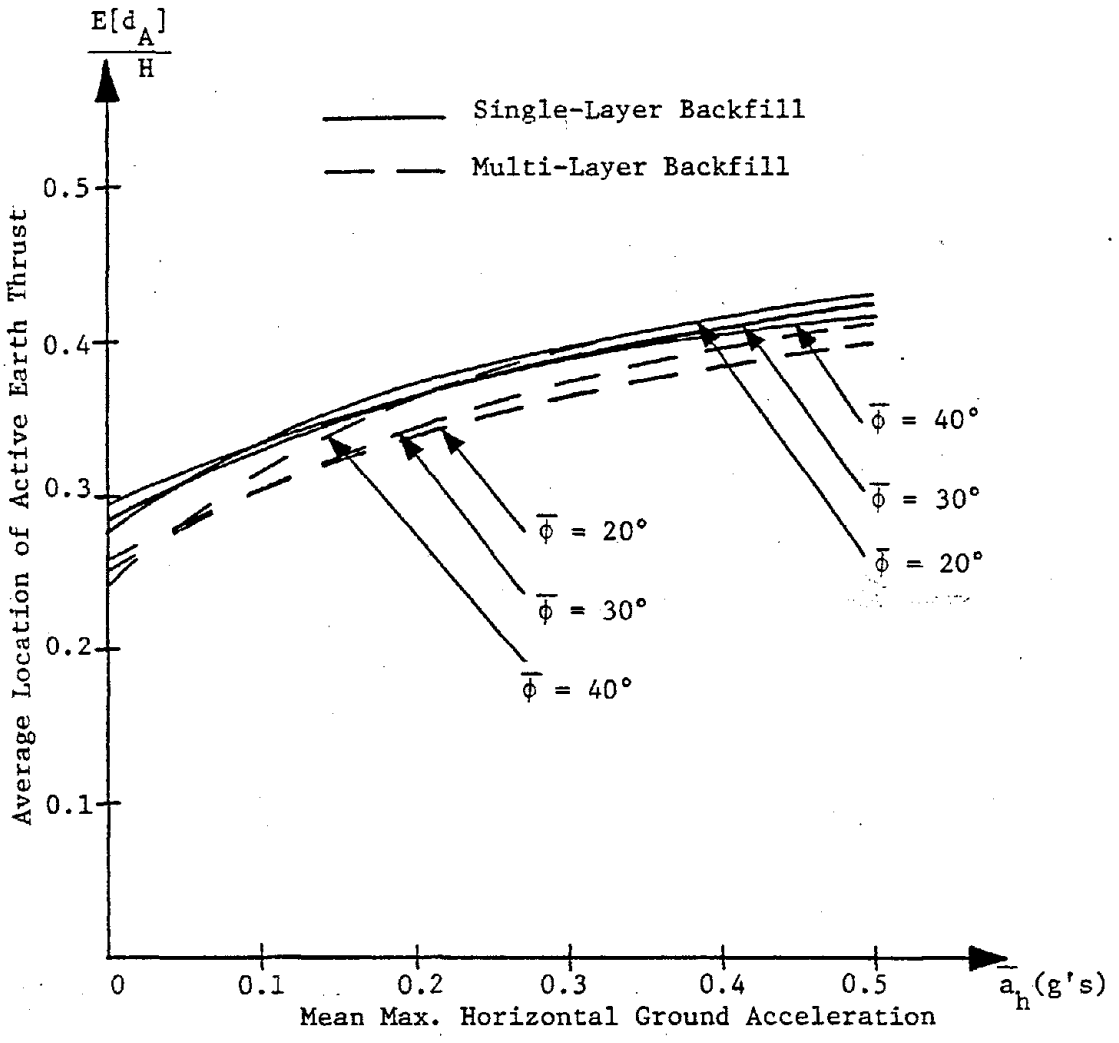

FIGURE 5.13 EFFECT OF MEAN VALUE OF ANGLE OF INTERNAL FRICTION ON THE EXPECTED LOCATION OF ACTIVE EARTH THRUST

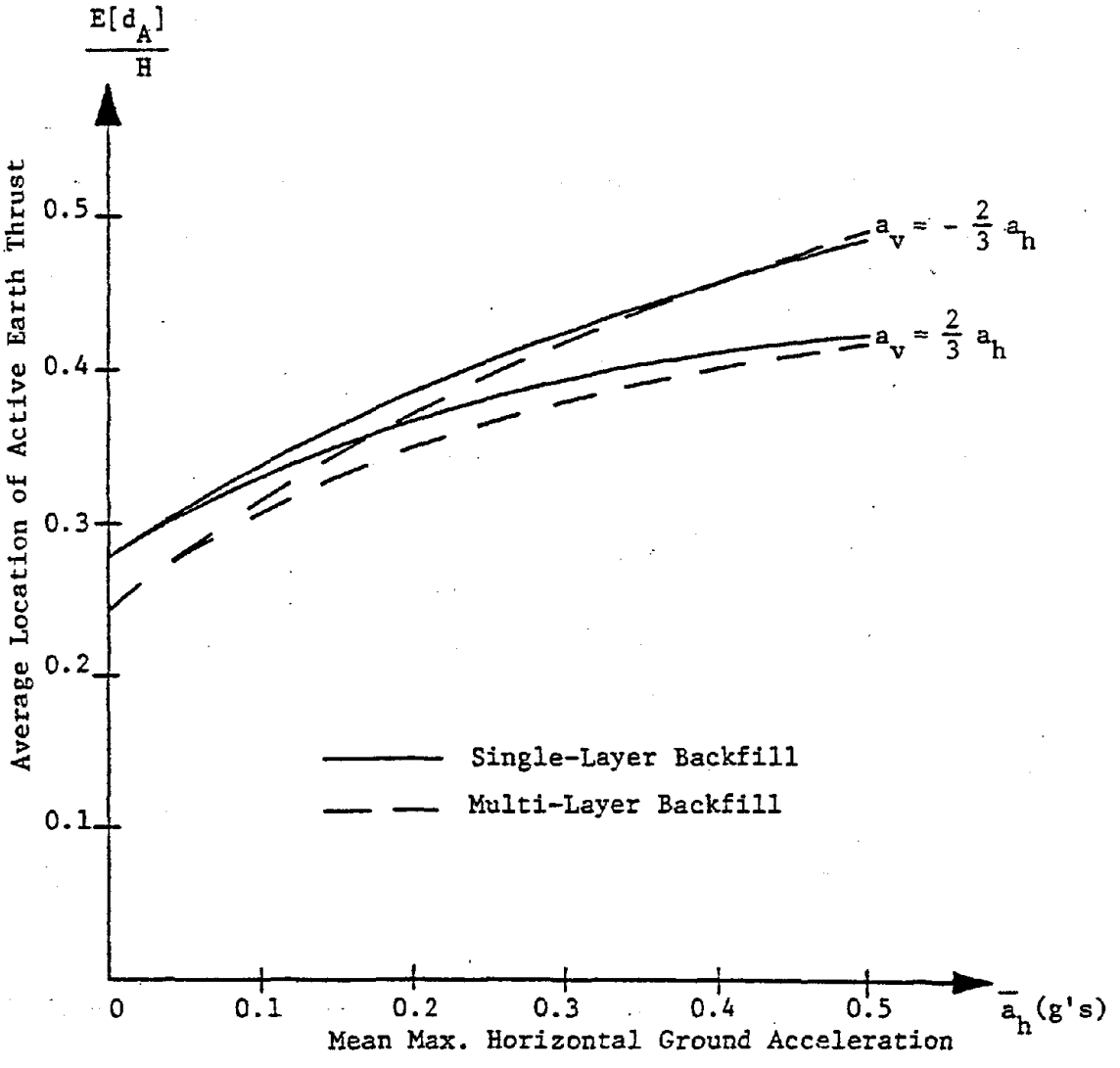

FIGURE 5.14 EFFECT OF DIRECTION OF MAX. VERTICAL ACCELERATION ON THE EXPECTED LOCATION OF ACTIVE EARTH THRUST

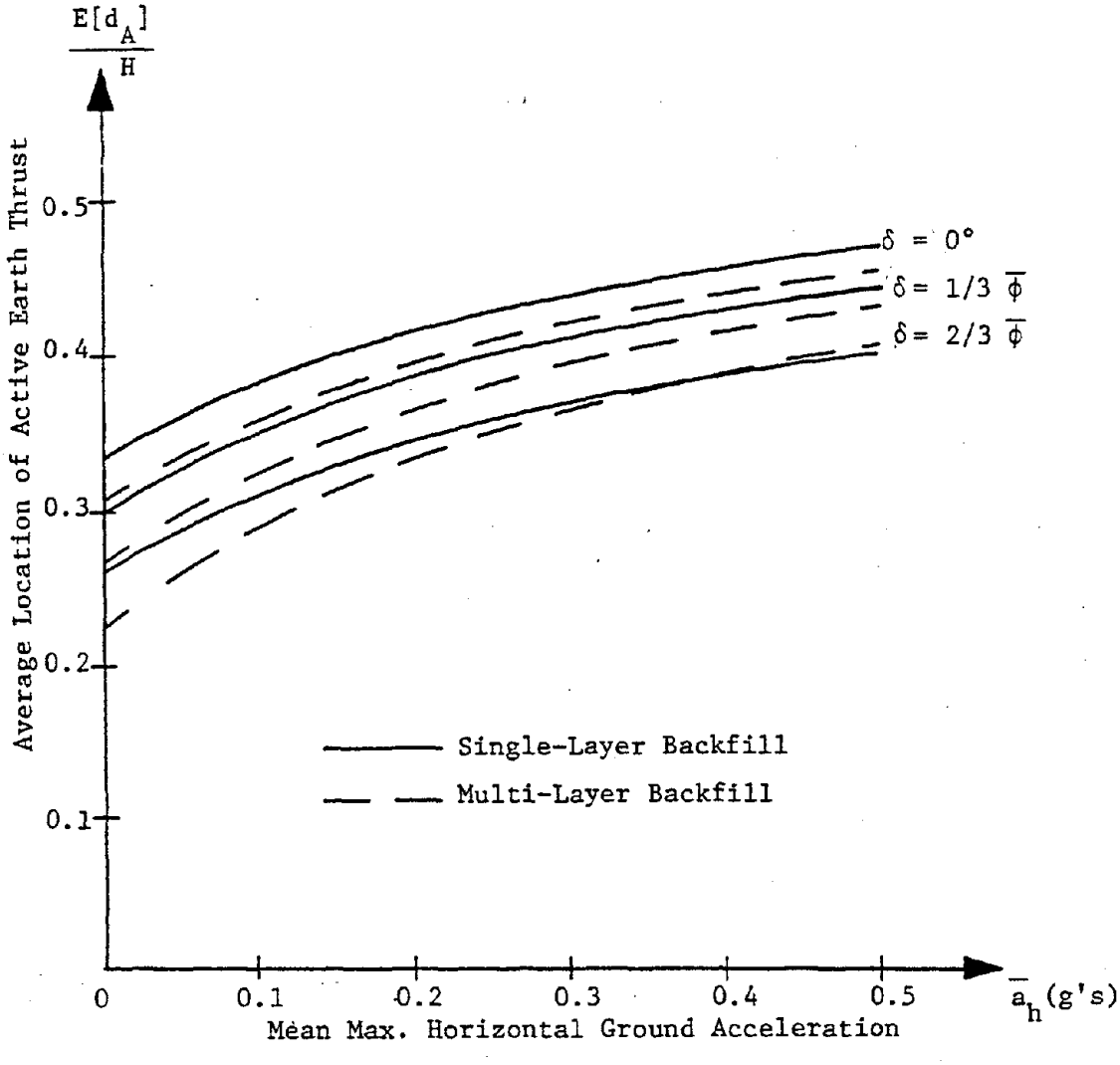

FIGURE 5.15 EFFECT OF ANGLE OF SOIL-WALL FRICTION ON THE EXPECTED LOCATION OF ACTIVE EARTH THRUST

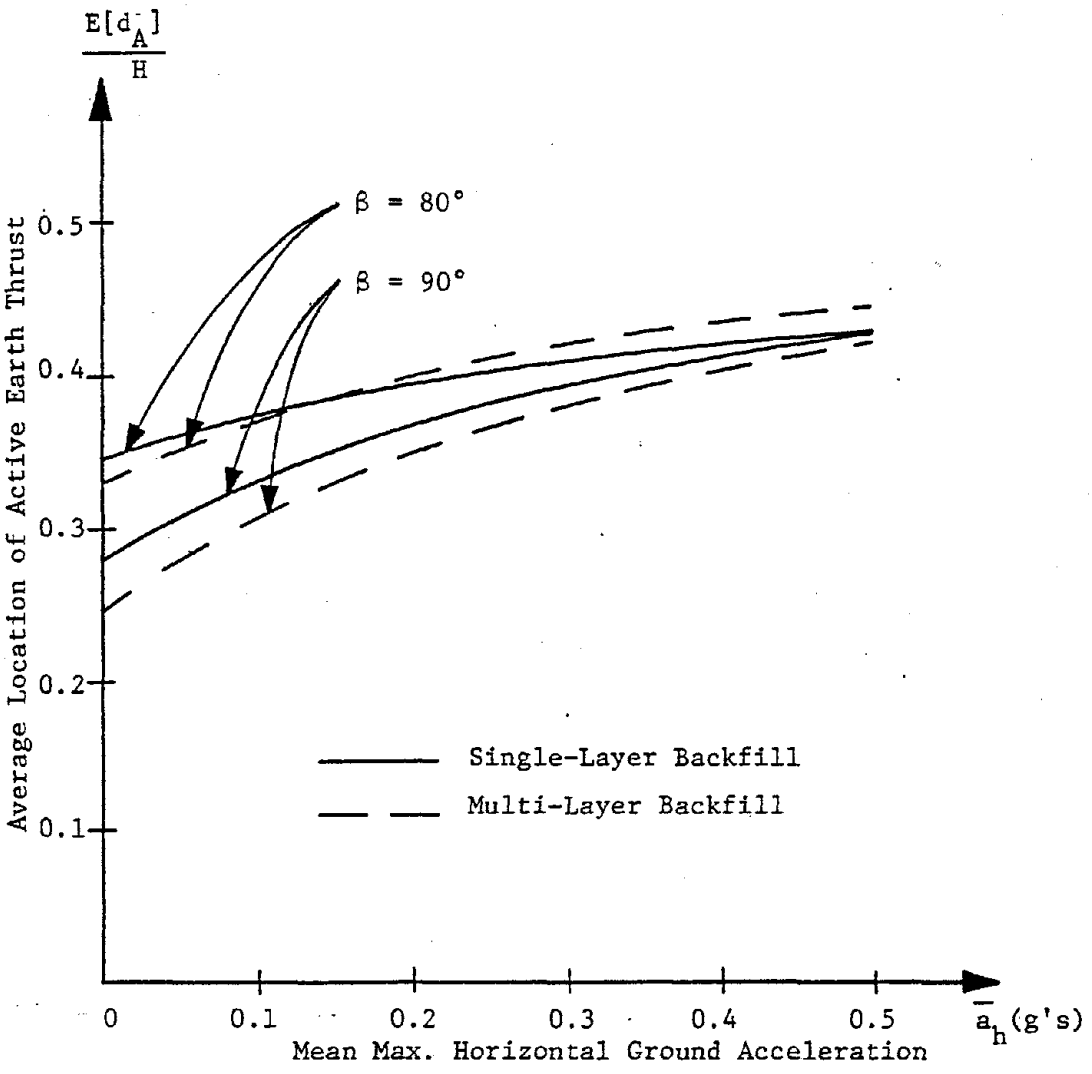

FIGURE 5.16 EFFECT OF INCLINATION OF BACK FACE OF THE WALL ON THE EXPECTED LOCATION OF ACTIVE EARTH THRUST

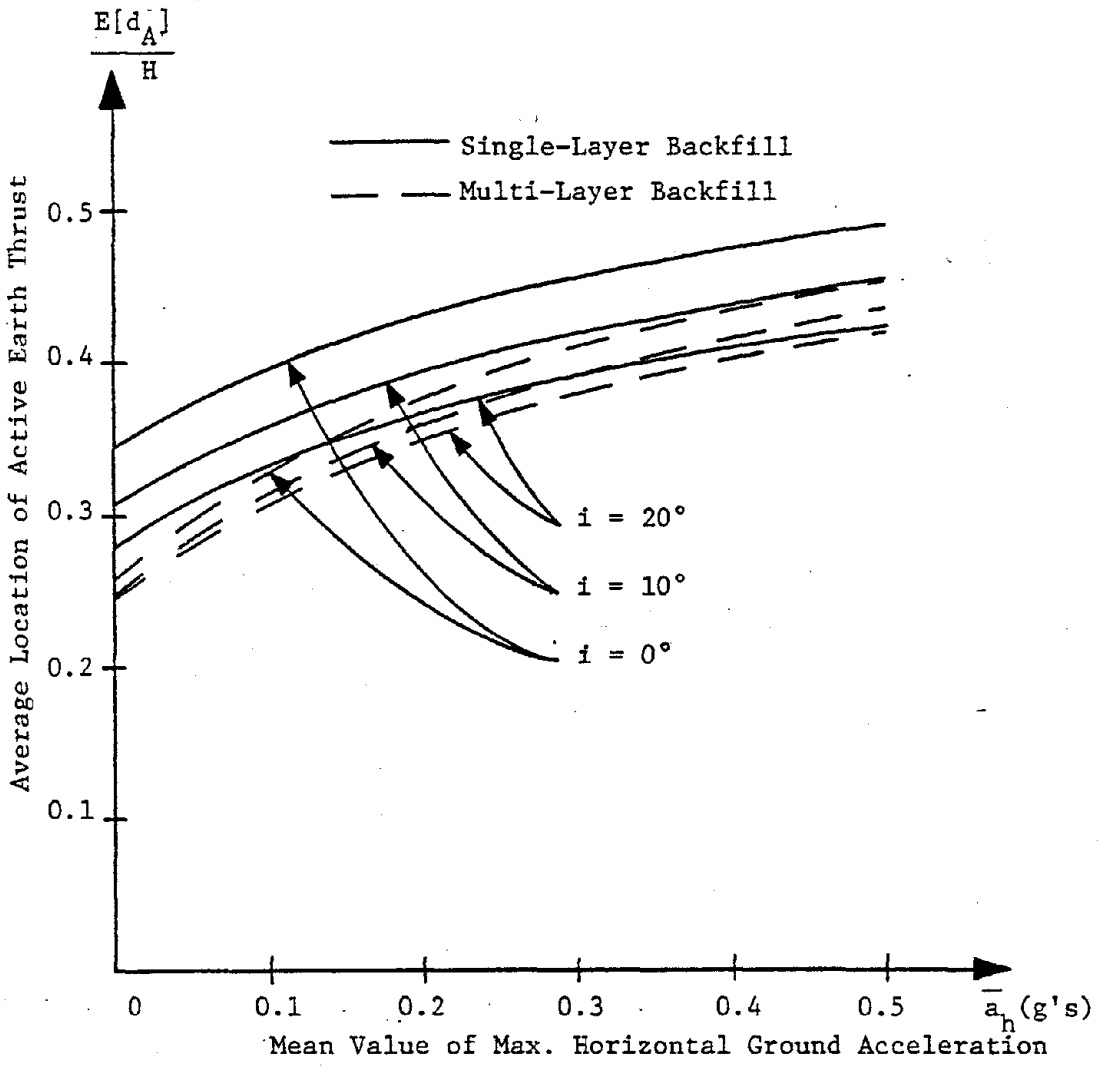

FIGURE 5.17 EFFECT OF INCLINATION OF BACKFILL ON THE EXPECTED LOCATION OF ACTIVE EARTH THRUST

a_v is directed upward).

5.4.4 Effect of the Angle of Soil-Wall Friction

Figure 5.15 shows the dependence of the expected value of d_A on the angle of soil-wall friction δ. It can be seen that $E[d_A]$ increases considerably as δ increases.

5.4.5 Effect of the Inclination of the Retaining Wall

In Fig. 5.16 is shown the effect of the angle of inclination of the back face of the wall β on the expected value of d_A. The value of $E[d_A]$ increases slightly as the wall deviates from the vertical (i.e., as β decreases). A tendency for $E[d_A]$ to converge to approximately 0.45H as $\bar{a}_h$ increases can be seen in Fig. 5.16.

5.4.6 Effect of the Inclination of the Backfill

The effect of the angle of the backfill i with respect to the horizontal direction on the expected value of d_A is shown in Fig. 5.17. $E[d_A]$ can be seen to increase considerably as i increases.

CHAPTER 6

COMPARATIVE STUDY

6.1 Comparison Between Model Tests and Present Procedure

The present moment equilibrium method of determining the active earth thrust against a retaining wall is compared with values determined by model tests. Model tests performed by Mononobe and Matsuo (1929) and Jacobsen (1939) are used for this purpose.

Mononobe and Matsuo (1929) performed model tests of a retaining wall to determine the mangitude of the active earth thrust during an earthquake. They used a 4 ft. x 4 ft. x 9 ft. box fitted with a metal line and filled with a uniform, clean, dry, river sand. The square ends of the box were hinged at the bottom edge and were allowed to rotate after the backfill was placed. The pressure on the square end was measured 4.5 ft. above the hinge. The box was vibrated horizontally by an eccentric mass to simulate an earthquake.

Mononobe and Matsuo's model test results and the approximate conditions of the test are presented in Fig. 6.1.

Jacobsen (1939) performed similar model tests on a smaller wall having a height equal to 3 ft. The model test results and approximate conditions of the tests are presented in Fig. 6.2.

In Figs. 6.1 and 6.2, the solid line represents the active earth pressure determined for the single-layer model of the moment equilibrium method. The values were obtained from Eqn. (4.5). The

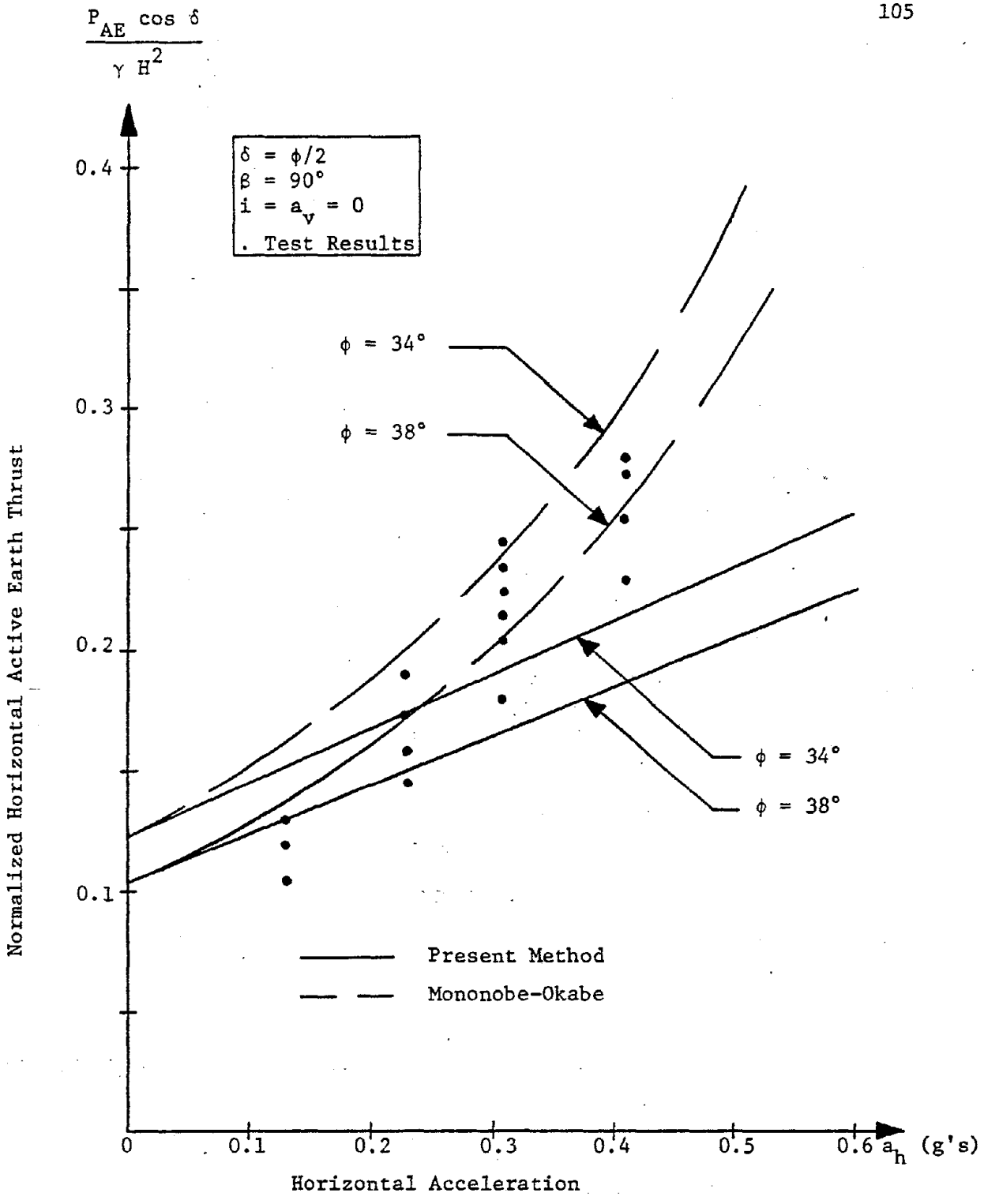

FIGURE 6.1 THE ACTIVE EARTH THRUST AGAINST A MODEL RETAINING WALL (*after* Mononobe and Matsuo, 1929)

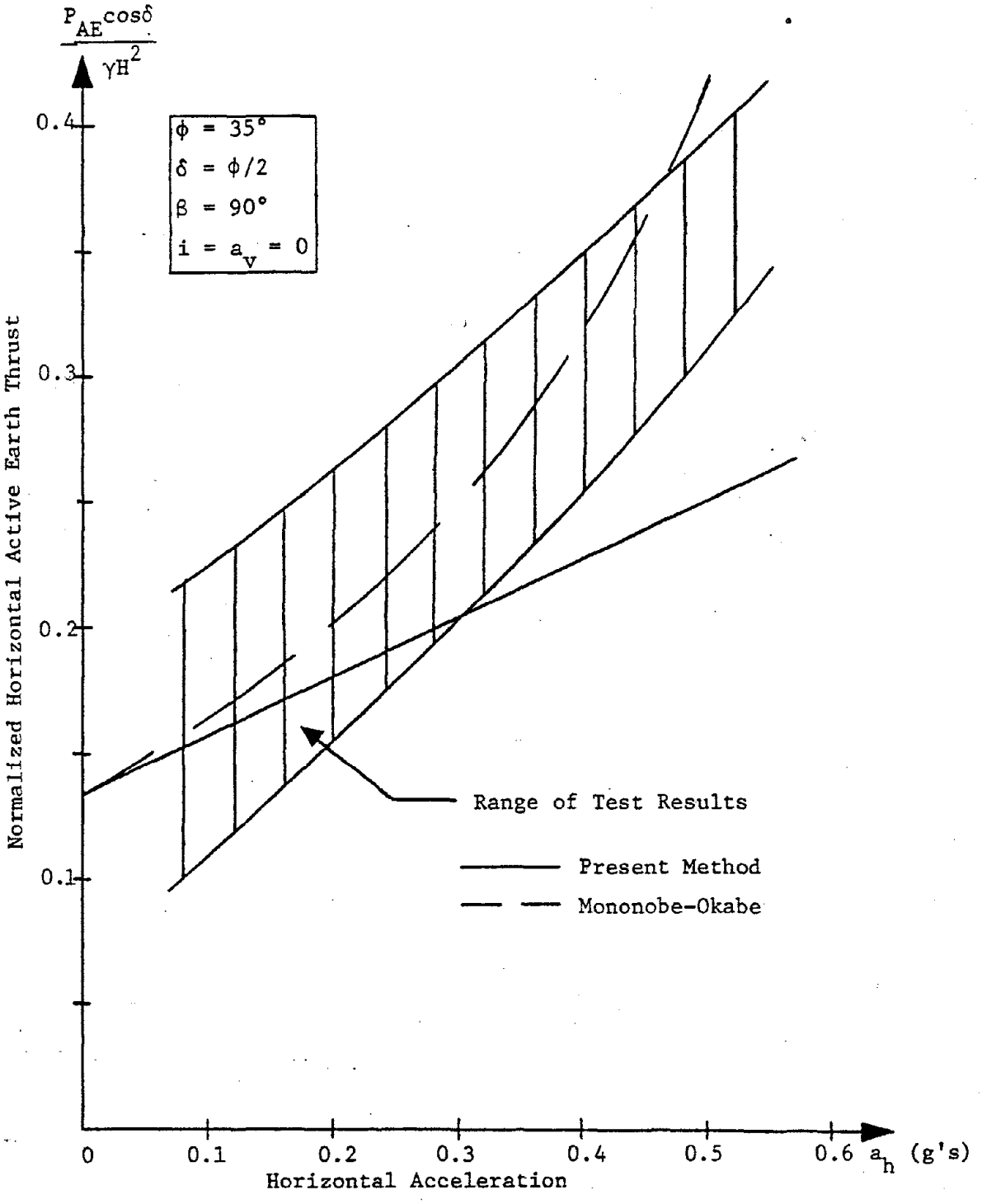

FIGURE 6.2 THE ACTIVE EARTH THRUST AGAINST A MODEL RETAINING WALL (after Jacobsen, 1939)

dashed line represents values of the active earth thrust determined from Mononobe-Okabe's method (Eqn. 1.2).

From Figs. 6.1 and 6.2, it is seen that the present method underestimates the active earth thrust against a retaining wall, while the Mononobe-Okabe method seems to fit the model test data rather well.

6.2 Comparison Between the Mononobe-Okabe Method and Present Procedure

The Mononobe-Okabe analysis of a retaining wall and its backfill is the most commonly used method of examining the effects of an earthquake on the earth thrust against the wall. However, it has several limitations that are not present in the developed procedure.

The first limitation of the Mononobe-Okabe method is that it does not accurately determine the point of application of the earth thrust. The static component is assumed to act at one-third the height of the wall above the base; the dynamic component is assumed to act at the midpoint of the wall. As a consequence of these assumptions, the retaining wall is not in moment equilibrium and, therefore, an impossible situation is analyzed.

In addition, for certain conditions, the Mononobe-Okabe method does not always provide a value for the earth thrust. If the quantity $\phi-\theta-i$ is negative in which ϕ denotes the angle of internal friction of the backfill, θ denotes the rotation of the acceleration and is equal to $\tan^{-1}(\frac{a_h}{1+a_v})$, and i denotes the slope of the backfill; Mononobe-Okabe's method cannot be evaluated. Therefore, there exists

a value of the maximum ground acceleration beyond which the Mononobe-Okabe method cannot be applied.

The limit of applicability of the Mononobe-Okabe method is illustrated in Fig. 6.3. The retaining wall examined is inclined 20 degrees from the vertical, the backfill is inclined 10 degrees from the horizontal, the angle of internal friction of the backfill material is equal to 35 degrees, and the angle of soil-wall friction is equal to one-third ϕ (i.e., $\beta = 70°$, $i = 10°$, $\phi = 35°$, and $\delta = \frac{1}{3}\phi$). The vertical component of the maximum ground acceleration is assumed to be directed upward and equal to two-thirds the horizontal component (i.e., $a_v = -\frac{2}{3} a_h$).

The solid line in Fig. 6.3 represents the active earth thrust obtained for the moment equilibrium method (Eqn. (4.5)), while the dashed line represents the active earth thrust found from Mononobe-Okabe's method (Eqn. (1.2)). The limiting value of the maximum horizontal ground acceleration beyond which the Mononobe-Okabe method cannot be applied, can be seen to be approximately 0.35g. However, the moment equilibrium method seemed to be applicable beyond this point.

Finally, the last limitation of the Mononobe-Okabe method is that the most critical condition is assumed to occur when the vertical component of the acceleration is directed upward. An upward directed acceleration maximizes the angle of rotation of the acceleration field θ from zero for the static case to $\tan^{-1}(\frac{a_h}{1+a_v})$ for a given earthquake. However, this does not always provide the critical value

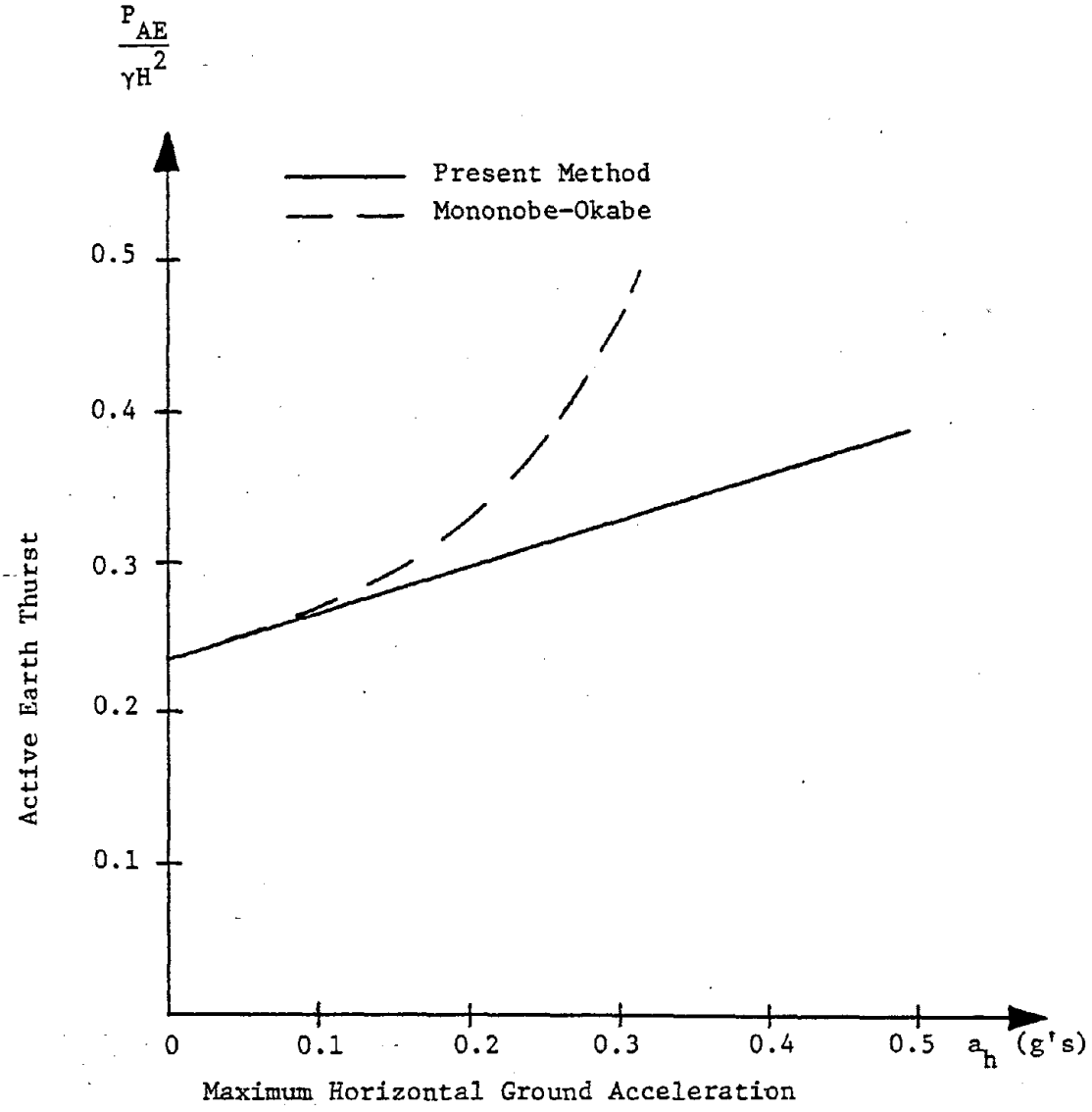

FIGURE 6.3 LIMITATION OF THE MONONOBE-OKABE ANALYSIS FOR DETERMINING THE ACTIVE EARTH THRUST

of the active earth thrust, a downward directed component of equal magnitude may provide the critical value.

The dependence of the active earth thrust on the direction of the vertical acceleration component is illustrated using a vertical retaining wall with a horizontal backfill. The angle of internal friction of the backfill material ϕ is equal to 35 degrees and the angle of soil-wall friction is assumed to be one-third ϕ (i.e., $\beta = 10°$, $i = 0°$, $\phi = 35°$, and $\delta = \frac{1}{3}\phi$). The active earth thrust obtained using the moment equilibrium and Mononobe-Okabe methods are denoted by the solid and dashed lines, respectively, in Fig. 6.4.

The Mononobe-Okabe method has the downward directed vertical acceleration being the critical case for a_h between zero and 0.4g. However, an upward directed acceleration is the critical case for a_h greater than 0.4g.

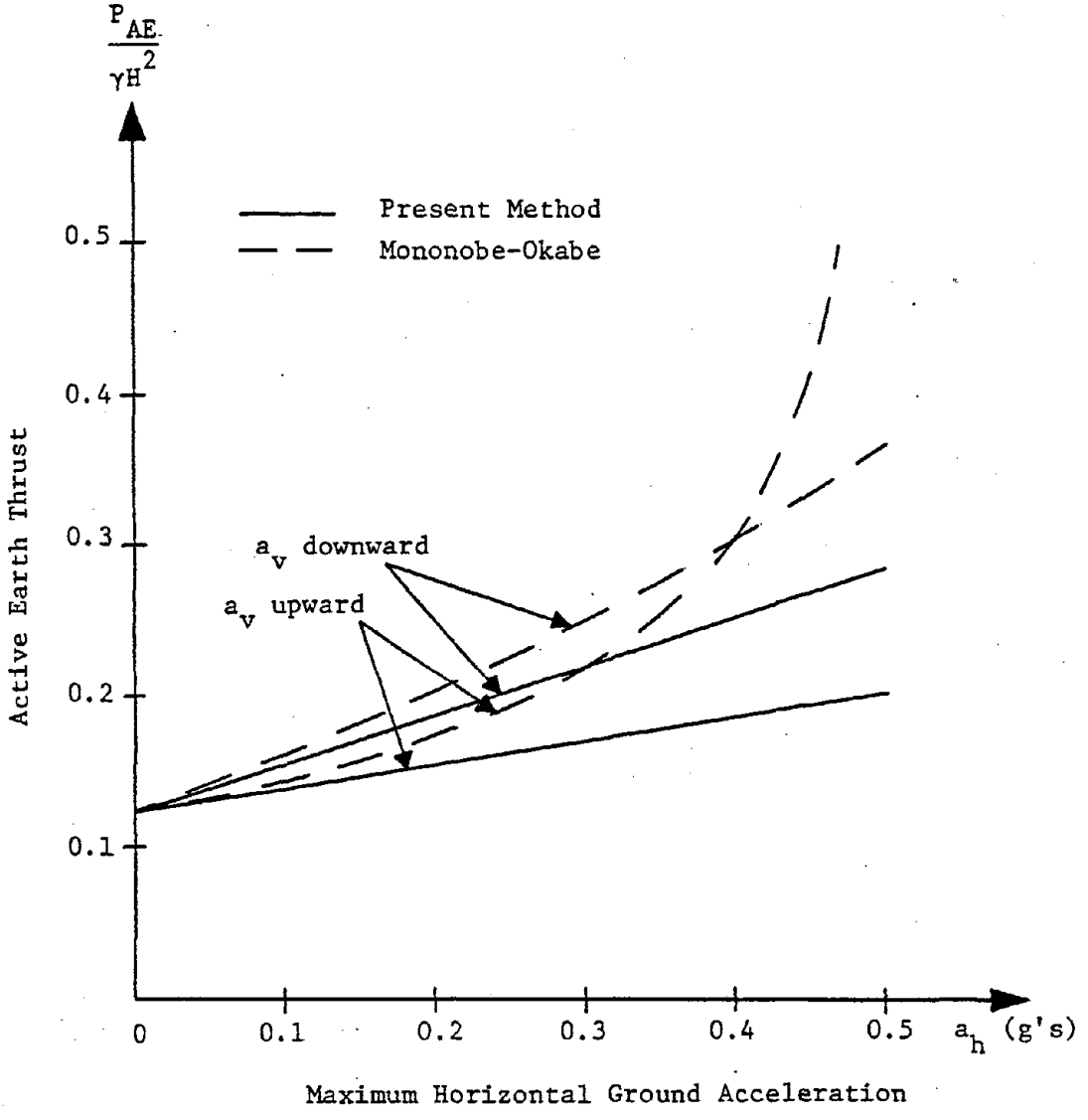

FIGURE 6.4 LIMITATION OF THE MONONOBE-OKABE ANALYSIS FOR DETERMINING THE ACTIVE EARTH THRUST

CHAPTER 7

DISCUSSION

In general, measured or inferred parameters that are used in geotechnical engineering practice exhibit some degree of variation in their numerical values. This variation causes uncertainty in the results of the analysis which in turn affects the solution given to the problem at hand.

For statistically homogeneous soils, the uncertainty associated with the variability of soil parameters has been accounted for by treating soil parameters as random variables (Lumb, 1970; Asaoka and A-Grivas, 1981a; etc.). The central tendency and degree of variation of parameters of such media are described in terms of the mean values and variances, respectively.

The uncertainty associated with the functions of random variables was examined in Chapter 2. Due to the complexity of expressions encountered in geotechnical engineering, an exact evaluation of the variability of functions of random soil parameters may often be impractical or even impossible to obtain. Thus, of necessity, one must employ some of the approximate methods that are available in order to achieve this task.

The comparison of the available approximate methods given in Section 2.5 indicated that the two-point estimate method provides more accurate estimates of a function of a random variable than the series approximation method. This accuracy may be increased further by including a third point in the discrete approximation of the involved

random variable.

The inherent variability of a soil mass often involves a depth dependent trend in the values of random soil parameters. In the case of natural deposits, this trend and its associated randomness can be attributed mainly to the nature of the geological processes involved in the formation of the deposits. A similar trend often exists in the variability of soil parameters within layers of man-made earth structures (e.g., water content of embankments or fills, etc.).

An important function used to describe the depth dependent characteristic of soil parameters is its autocorrelation function. This describes the correlation between values of the parameter at different locations within the soil mass and is expressed analytically in terms of a smooth exponential function of the ratio of the distance between two points within which the parameter shows relatively strong correlation.

The methods of estimating the correlation length that were reviewed in Sections 3.4.1 and 3.4.2, i.e., the average mean-crossing distance method and the moving average method, respectively, did not consider the depth dependent nature of soil parameters. This was accounted for through the quasi-stationary autoregressive method presented in Section 3.4.3.

All three methods were applied to a case study involving actual data of the undrained shear strength of a natural soil deposit. From Table 3.9, it is seen that the average mean-crossings

distance method provided the most inconsistent estimates of the correlation length. In one case (i.e., Borehold B-1), an estimate was impossible to obtain as the depth variation of the value of the undrained shear strength crossed its mean value line only once.

The shortcomings of the average mean-crossings distance method are illustrated in the case study associated with Borehole B-1. From Fig. 7.1(a), it is seen that the mean value is constant and intersects the trace of S_u found from the test data only once. Thus, the correlation length cannot be estimated. If the mean value of S_u was represented as a linearly increasing function of depth, as shown in Fig. 7.1(b), the trace of S_u would be equal to its mean value four times allowing then an estimate to be made of its correlation length.

From Table 3.9, it is seen that the moving average method is a better procedure for determining the correlation length than the average mean-crossings distance method. However, this method resulted in a considerable variation in the estimated correlation lengths in both sets of borings. The variation in the estimated thickness of an independent layer, determined using Eqn. (3.5), was found for both sites to be approximately 25 percent. This large amount of variation is attributed to the unrealistic assumption of a constant mean value of S_u with depth.

The quasi-stationary autoregressive method was found to

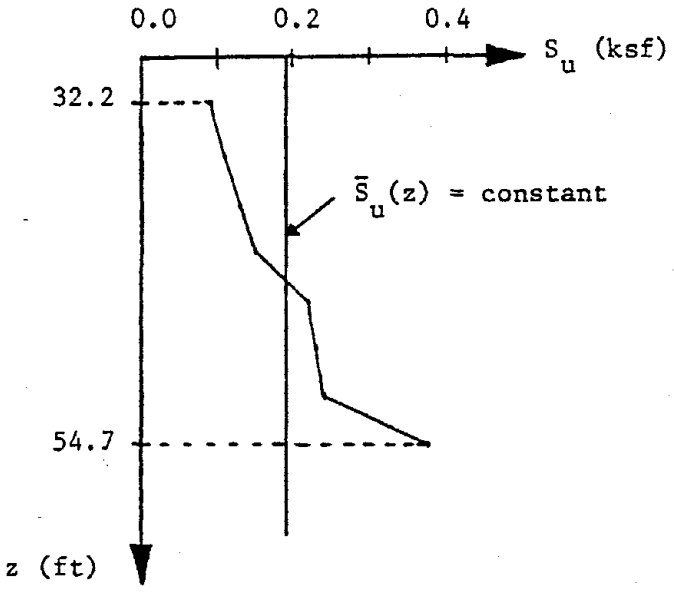

(a) Constant Mean with Depth

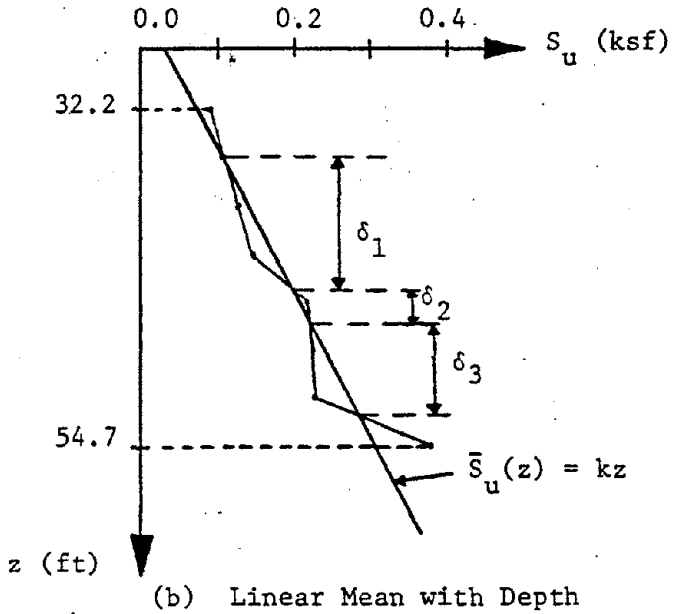

(b) Linear Mean with Depth

FIGURE 7.1 TWO MEAN VALUE FUNCTIONS OF THE UNDRAINED SHEAR STRENGTH FOR BOREHOLE B-1

provide the most consistent estimates of the correlation length of the undrained shear strength as can be seen in Table 3.9. The thickness of an independent layer d_i was found at both sites to vary by only 5 percent. This is due to the proper representation of the mean value of S_u as a linear function of depth.

In the quasi-stationary autoregressive method, the estimate of the correlation length depends on the location of the origin of the depth axis. In this study, the origin was placed at the ground surface (approximately 50 feet above the top of the clay layer) and the correlation lengths for boreholes A-1 and A-2 were equal to 4.6 ft. and 4.5 ft., respectively. Using the same data but placing the depth origin at the mudline (approximately 25 feet above the top of the clay layer), Asaoka and A-Grivas (1981b) found the correlation lengths at boreholes A-1 and A-2 to be equal to 4.0 ft. and 10.2 ft., respectively.

The effect of the location of the depth origin is shown schematically in Fig. 7.2. Point O denotes the location of the depth origin at the ground surface; Point O' denotes the location of the depth origin for the "best fit" of the data; and point O" denotes the location of the depth origin at the mudline. Lines OA, O'A', and O"A" represent the mean value $\bar{S}_u(z)$ of the undrained shear strength with depth for each of these cases (i.e., OA = $\bar{S}_u(z)$ for $z = 0$ at the ground surface, etc.).

The quasi-stationary autoregressive approach requires that the mean value of the soil parameter is equal to zero at the origin

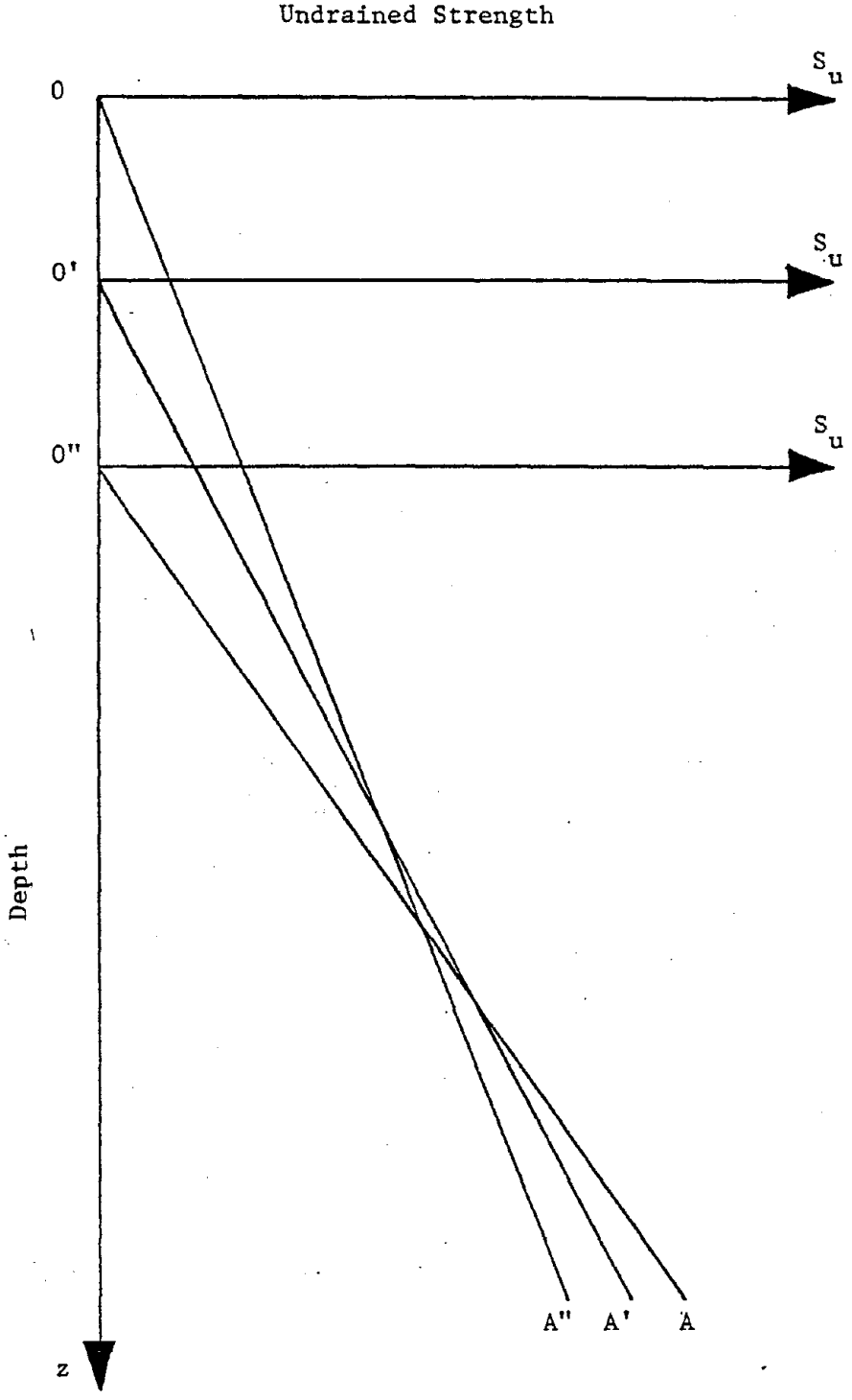

FIGURE 7.2 DEPENDENCE OF THE MEAN VALUE OF UNDRAINED STRENGTH ON THE ORIGIN

(i.e., $\bar{S}_u(z=0) = 0$). Thus, for any assumed origin, a linear representation of $\bar{S}_u(z)$ that passes through the origin can be made so that an estimate of the correlation length is obtained. The resulting values of the correlation length will vary depending on the location of the origin. The "true" or "best fit" correlation length can be found by locating the origin at point 0', as is shown in Fig. 7.2

The estimates of the correlation length obtained in this study were presented in Table 7.1. For comparison purposes, the same table lists the values of the correlation length obtained by Matsuo and Asaoka (1977) for marine clays found in Japan. It can be seen from Table 7.1 that all values obtained are within a reasonable range.

The vertical variability of the ϕ-parameter of strength of the backfill material was used to describe the force system on a retaining wall (Chapter 4). Employing all three equations of equilibrium, the active earth thrust against a retaining wall P_{AE} and its point of application d_A were determined. The results obtained for the parametric study are presented in Figs. 5.2 through 5.17. In Figs. 5.2 through 5.6, it is seen that the expected value of P_{AE} is independent of the number of layers of the backfill material, while it is linearly dependent on the value of the maximum horizontal acceleration. In Figs. 5.7 through 5.12, it can be seen that the coefficient of variation of P_{AE} is dependent on the number of layers the backfill material is considered to be comprised of. The multi-layer model provides higher values of the coefficient of

TABLE 7.1

REPORTED VALUES OF THE CORRELATION LENGTH OF THE UNDRAINED SHEAR STRENGTH OF CLAYS

METHOD	CORRELATION LENGTH, ℓ, m
Average Mean-Crossings Distance Method	$0.8 < \ell < 2.5$
Moving Average Method	$1.0 < \ell < 3.0$
Quasi-Stationary Auto-regressive Method	$1.0 < \ell < 2.5$
Matsuo and Asaoka (1977)	$0.5 < \ell < 1.5$

variation of P_{AE} than does the single-layer one. In Figs. 5.13 through 5.17, it can be seen that the expected value of the point of application of P_{AE} (i.e., $E[d_A]$) is dependent on the type of model assumed for the backfill. The single-layer backfill model provides higher values of $E[d_A]$ than the multi-layer one.

CHAPTER 8

SUMMARY AND CONCLUSIONS

A procedure was developed for the determination of the force system acting on rigid retaining walls located in an earthquake environment. It was based on a quasi-static Coulomb type analysis that satisfied the additional requirement of equilibrium of moments and, at the same time, accounted for two important uncertainties: the spatial variability of the strength of the backfill material and the randomness in the value of the seismic loading. The latter was introduced in terms of the maximum horizontal ground acceleration expected to be experienced at the site of the retaining wall during an earthquake.

As a part of this study, an investigation was made of the statistical techniques capable of describing characteristics of functions of random soil properties (case of statistically homogeneous soil deposits). In all cases examined, it was found that the "point estimates method" was more accurate and easier to implement than the "series approximation method". A similar investigation was made of procedures currently available for the description of the spatial (vertical) variability of soil properties (case of heterogeneous soil deposits). It was found that the "quasi-stationary autoregressive method" provided a better description of the vertical variability of soil properties than the "average mean-crossings distance method" and the "moving average method", especially for

the commonly encountered situations of soil properties that exhibit a trend (e.g., increase) with depth. The quasi-stationary autoregressive method was subsequently employed in this study to describe the vertical variability of the strength of cohesionless backfill materials. This resulted to two distinct but equivalent models for the backfill of retaining walls: one, involving a single-layer medium and, another, consisting of an equivalent multi-layer system.

Finally, the effect of material, loading and model parameters on the force system against a retaining wall located in an earthquake prone area was examined in a case study and the results were presented in a series of figures and tables.

On the basis of the analysis and results obtained in this study, the following conclusions can be drawn:

1. The point estimate method provides a better approximation for the statistical moments of a function of random variables than the series expansion method. Moreover, it is applicable to situations where the series approximation method is impractical or impossible to employ.
2. The accuracy of the point estimate method in estimating the statistical moments of a function of random variables is improved by using three points in the discrete approximation of the input variables.

3. Among all methods considered, the quasi-stationary autoregressive procedure provides the best description of the vertical variability of a soil parameter that increases with depth.
4. The single- and multi-layer models of the backfill material provide identical values for the active earth thrust against a retaining wall.
5. The single layer model of the backfill results in a position for the point of application of the active earth thrust that is slightly lower than that provided by the multi-layer model.
6. The expected value of the active earth thrust against a retaining wall depends on: the magnitude and direction of the maximum ground acceleration; the magnitude of the angle of internal friction of the backfill material; the angle of inclination of the back face of the wall; and the slope of the backfill.
7. The expected value of the point of application of the active earth thrust depends on: the assumed model of the backfill; the magnitude and direction of the maximum ground acceleration; the magnitude of the angle of soil-wall friction; and the slope of the backfill.

8. The coefficient of variation of the active earth thrust depends on: the statistical moments of the angle of internal friction of the backfill material and maximum ground acceleration; the magnitude of the angle of soil wall friction; and the angle of inclination of the back face of the wall.
9. The inclusion of the equilibrium of moments in analyzing the force system on a retaining wall enables the determination of the point of application of the earth thrust. It produces a lower limit for the value of the active earth thrust against the wall as compared to model test results.

CHAPTER 9

REFERENCES

1. Alonso, E.E. (1976), "Risk Analysis of Slopes and its Application to Slopes in Canadian Sensitive Clays", Geotechnique, Vol. 26, No. 3, pp. 453-472.

2. Asaoka, A. and A-Grivas, D. (1981a), "Short-Term Reliability of Slopes Under Static and Seismic Conditions", Transportation Research Record 809, "Frost Action and Risk Assessment in Soil Mechanics".

3. Asaoka, A. and A-Grivas, D. (1981b), "Spatial Variability of the Undrained Strength of Soft Clays", Submitted for Publication in the Canadian Geotechnical Journal.

4. Benjamin, J.R. and Cornell, C.A. (1970), Probability, Statistics, and Decision for Civil Engineers, McGraw-Hill Book Co., Inc., New York.

5. Cox, D.R. and Miller, H.D. (1965), The Theory of Stochastic Processes, Methuem and Co., Ltd., London.

6. Dubrova, G.A. (1963), "Interaction of Soil and Structures", Izd. "Rochnoy Transport", Moscow.

7. Hahn, G.T. and Shapiro, S.S. (1967), Statistical Models in Engineering, John Wiley and Sons, New York.

8. Harr, M.E. (1977), Mechanics of Particulate Media - A Probabilistic Approach, McGraw-Hill Book Co., Inc., New York.

9. Harrop-Williams, K. (1980), "Reliability of Geotechnical Systems", Ph.D. Dissertation, Department of Civil Engineering, Rensselaer Polytechnic Institute, Troy, New York.

10. Hooper, J.A. and Butler, F.G. (1966), "Some Numerical Results Concerning the Shear Strength of London Clays", Geotechnique, Vol. 16, No. 4, pp. 282-304.

11. Howland, J.D. (1981), "A Simplified Procedure for Reliability Analysis in Geotechnical Engineering", Ph.D. Dissertation, Department of Civil Engineering, Rensselaer Polytechnic Institute, Troy, New York.

12. Ichihara, M. (1965), "Dynamic Earth Pressure Measured by a New Testing Apparatus", Proceedings, 6th International Conference on Soil Mechanics and Foundation Engineering, Montreal, Canada, Vol. 2, September, pp. 386-390.

13. Lambe, T.W. and Whitman, R.V. (1969), Soil Mechanics, John Wiley and Sons, New York.

14. Lumb, P. (1966), "The Variability of Natural Soils", Canadian Geotechnical Journal, Vol. 3, No. 2, pp. 74-97.

15. Lumb, P. (1970), "Safety Factors and Probabilistic Distribution of Soil Strength", Canadian Geotechnical Journal, Vol. 7, No. 3, pp. 225-242.

16. Matsuo, H. and Ohara, S. (1960), "Lateral Earth Pressures and Stability of Quay Walls During Earthquakes", Proceedings, 2nd World Conference on Earthquake Engineering, Tokyo, Japan, Vol. 1.

17. Matsuo, M. and Asaoka, A. (1977), "Probability Models of Undrained Strength of Marine Clay Layer", Soils and Foundations, Vol. 17, No. 3, September, pp. 53-68.

18. McGuffey, V., Iori, J., Kyfor, Z. and A-Grivas, D. (1981), "The Use of Point Estimate for Probability Moments in Geotechnical Engineering", Transportation Research Record 809, "Frost Action and Risk Assessment in Soil Mechanics".

19. Mononobe, N. (1929), "Earthquake-Proof Construction of Masonry Dams", Proceedings, World Engineering Conference, Vol. 9.

20. Mononobe, N. and Matsuo, H. (1929), "On the Determination of Earth Pressure During Earthquake", Proceedings, World Engineering Conference, Vol. 9.

21. Nazarian, H.N. and Hadijian, A.H. (1979), "Earthquake-Induced Lateral Soil Pressure on Structures", Journal of the Geotechnical Engineering Division, ASCE, Vol. 105, No. GT9, September, pp. 1049-1066.

22. Newmark, N.M. (1965), "Effects of Earthquakes on Dams and Embankments", Geotechnique, Vol. 15, No. 2, pp. 139-160.

23. Okabe, S. (1926), "General Theory of Earth Pressure", Journal of the Japanese Society of Civil Engineers, Vol. 12, No. 1, January.

24. Papoulis, A. (1965), Probability, Random Variables, and Stochastic Processes, McGraw-Hill Book Co., Inc., New York.

25. Prakash, S. and Basavanna, B.M. (1969), "Earth Pressure Distribution Behind Retaining Wall During Earthquakes", Proceedings, 4th World Conference on Earthquake Engineering, Santiago, Chile, Vol. 3, January, pp. 133-148.

26. Prakash, S. and Nandakumaran, P. (1973), "Dynamic Earth Pressure Distribution on Rigid Walls", Symposium, Behavior of Earth and Earth Structures under Earthquakes and Dynamic Loads, March, pp. 11-16.

27. Prakash, S. and Nandakumaran, P. (1979), "Earth Pressures During Earthquakes", U.S. Earthquake Engineering Conference, Stanford, California, pp. 613-622.

28. Rice, S.O. (1944), "Mathematical Analysis of Random Noise", Bell System Technical Journal, Vol. 23, p. 282, Vol. 24, p. 46.

29. Richard, R. and Elms, D.G. (1979), "Seismic Behavior of Gravity Retaining Walls", Journal of the Geotechnical Engineering Division, ASCE, Vol. 105, No. GT4, April, pp. 449-464.

30. Rosenblueth, E. (1975), "Point Estimates for Probability Moments", Proceedings, National Academy of Science, U.S.A., Vol. 72, No. 10, October, Mathematics, pp. 3812-3814.

31. Saran, S. and Prakash, S. (1977), "Effect of Wall Movement on Lateral Earth Pressure", Proceedings, 6th World Conference on Earthquake Engineering, India, Vol. 3, pp. 2371-2372.

32. Seed, H.B. and Whitman, R.V. (1970), "Design of Earth Retaining Structures for Dynamic Loads", Specialty Conference on Lateral Stresses in the Ground and Design of Earth-Retaining Structures, ASCE, Cornell University, pp. 103-147.

33. Sharma, S.K. (1975), "Seismic Stability of Earth Dams and Embankments", Geotechnique, Vol. 25, No. 4, pp. 743-761.

34. Terzaghi, K. (1936), "A Fundamental Fallacy in Earth Pressure Computations", Journal of Boston Society of Civil Engineers, April, pp. 78-79.

35. Tarzaghi, K. (1941), "General Wedge Theory of Earth Pressure", Transactions of American Society of Civil Engineers, Paper No. 20099, 106, pp. 68-97.

36. Tschebotarioff, G.P. (1951), Soil Mechanics, Foundations, and Earth Structures, McGraw-Hill Book Co., Inc., New York.

37. Vanmarcke, E.H. (1977), "Probabilistic Modeling of Soil Profiles", Journal of the Geotechnical Engineering Division, ASCE, Vol. 103, No. GT11, November, pp. 1227-1246.

38. Vlavianos, G.J. (1981), "Convention and Probabilistic Evaluations of Seismic Safety of Rigid Retaining Walls", M.S. Thesis, Department of Civil Engineering, Rensselaer Polytechnic Institute, Troy, New York.

APPENDIX

APPENDIX

COMPUTER PROGRAMS

The following is a listing of computer programs developed in the course of this study. The programs are written in BASIC for the Radio Shack TRS-80 Micro Computer. Together with each program are given a brief description and an illustrative example showing both the display and the required input.

The listed programs can be divided into three basic categories; one, those dealing with the statistical description of random variables; two, those dealing with methods of determining the correlation length of soil parameters; and finally, those dealing with the determination of the earth thrust against retaining walls.

Title MOMENTS (Statistical Moments and Pearson's K)

Description:

This program determines the mean value μ_x, variance σ_x^2, coeff. of variation V, coeff. of skewness α_3, coeff. of kurtosis α_4 and Pearson's K criterion of a set of N data points of a random variable x, in which

$$\mu_x = \frac{1}{N} \sum_{i=1}^{N} (x_i)$$

$$\sigma_x^2 = \frac{1}{(N-1)} \sum_{i=1}^{N} (x_i - \mu_x)^2$$

$$V_x = \sigma_x / \mu_x$$

$$\alpha_3 = \frac{1}{N} \sum_{i=1}^{N} (x_i - \mu_x)^3 / \sigma_x^3$$

$$\alpha_4 = \frac{1}{N} \sum_{i=1}^{N} (x_i - \mu_x)^4 / \sigma_x^4$$

$$K = \frac{\alpha_3^2 (\alpha_4 + 3)^2}{4(2\alpha_4 - 3\alpha_3^2 - 6)(4\alpha_4 - 3\alpha_3^2)}$$

Example: N = 5 x_i = 1, 3, 4, 6, & 7

	Input	Display	Note		Input	Display	Note
1	RUN	NO DATA PTS=		11		MEAN X = 4.2	
2	5 ENTER	VALUE=		12	ENTER	VARIANCE = 5.7	
3	1 ENTER	VALUE=		13	ENTER	COEF VAR=5.68E-01	
4	4 ENTER	VALUE=		14	ENTER	SKEWNESS=9.88E-02	
5	6 ENTER	VALUE=		15	ENTER	KURTOSIS=1.101	
6	7 ENTER			16	ENTER	K=-2.45E-03	
7				17			
8				18			
9				19			
10				20			

Title MOMENTS

Memory content			Line number	Statements
A	1	N	10	CLEAR:INPUT "NO DATA PTS="; A
B	2	counter	20	FOR B = 1 TO A
C	3	μ_x	30	INPUT "VALUE="; J
D	4	σ_x^2	40	C=C+J:A(B+11)=J:NEXTB
E	5	V_x	50	C=C/B
F	6	α_3	60	FOR B = 1 TO A
G	7	α_4	70	H=A(B+11)-C:I=H*H
H	8	$x_i-\mu_x$	80	D=D+I:F=F+H*I:G=G+I*I:NEXTB
I	9	$(x_i-\mu_x)^2$	90	D=D/(A-1):E= $\sqrt{D}$/C
J	10	α_3^2	100	F=F/A/D↑1.5:G=G/A/D/D
K	11	K criterion	110	J=F*F:K=J*(G+3)↑2/4/
L	12			(2*G-3*J-6)/(4*G-3*J)
M	13		120	PRINT "MEAN X="; C
N	14		130	PRINT "VARIANCE="; D
O	15		140	PRINT "COEF VAR="; E
P	16		150	PRINT "SKEWNES="; F
Q	17		160	PRINT "KURTOSIS="; G
R	18		170	PRINT "K="; K
S	19		180	END
T	20			
U	21			
V	22			
W	23			
X	24			
Y	25			
Z	26			

Title CORCOEF (Correlation Coefficient)

Description:

This program determines the mean values, $\bar{x}$ and $\bar{y}$; variances, σ_x^2 and σ_y^2; coeff. of variation, V_x and V_y; and correlation coefficient ρ_{xy} of a set of N pairs of data points for the random variables x and y, in which

$$\bar{x} = \frac{1}{N} \sum_{i=1}^{N} (x_i)$$

$$\sigma_x^2 = \frac{1}{N-1} \sum_{i=1}^{N} (x_i - \bar{x})^2$$

$$V_x = \sigma_x / \bar{x}$$

$$\bar{y} = \frac{1}{N} \sum_{i=1}^{N} (y_i)$$

$$\sigma_y^2 = \frac{1}{N-1} \sum_{i=1}^{N} (y_i - \bar{y})^2$$

$$V_y = \sigma_y / \bar{y}$$

$$\rho_{xy} = \left(\frac{1}{N} \sum_{i=1}^{N} (x_i - \bar{x})(y_i - \bar{y})\right) / \sigma_x \sigma_y$$

Example: N = 5

x	y
1.4	6.0
1.7	5.4
1.0	5.8
1.3	6.2
1.5	6.1

	Input	Display	Note		Input	Display	Note
1	RUN	NO DATA SETS=		11	1.5 ENTER	VALUE OF Y=	
2	5 ENTER	VALUE OF X=		12	6.1 ENTER		
3	1.4 ENTER	VALUE OF Y=		13		MEAN VALUE X=1.38	
4	6.0 ENTER	VALUE OF X=		14	ENTER	VARIANCE X=0.067	
5	1.7 ENTER	VALUE OF Y=		15	ENTER	COE VAR X=1.88E-01	
6	5.4 ENTER	VALUE OF X=		16	ENTER	MEAN VALUE Y=5.9	
7	1.0 ENTER	VALUE OF Y=		17	ENTER	VARIANCE Y=0.1	
8	5.8 ENTER	VALUE OF X=		18	ENTER	COE VAR Y=5.36E-02	
9	1.3 ENTER	VALUE OF Y=		19	ENTER	COR COE=3.67E-01	
10	6.2 ENTER	VALUE OF X=		20			

Title	CORCOEFF		
Memory content		Line number	Statements
A 1	N	10	CLEAR:INPUT"NO OF DATA SETS="; A
B 2	counter	20	FOR B = 1 TO A
C 3	x_i	30	INPUT "VALUE OF X="; C
D 4	Σx_i	40	D=D+C:E=E+C*C
E 5	Σx_i^2	50	INPUT "VALUE OF Y="; F
F 6	y_i	60	G=G+F:H=H+F*F:I=I+C*F
G 7	Σy_i	70	NEXT B
H 8	Σy_i^2	80	J=D/A:K=(E-D*D/A)/(A-1):L=$\sqrt{K}$/J
I 9	$\Sigma x_i y_i$	90	M=G/A:N=(H-G*G/A)/(A-1):O=$\sqrt{N}$/M
J 10	$\bar{x}$	100	P=(A*I-D*G)/ $\sqrt{}$((A*E-D*D)*(A*H-G*G))
K 11	σ_x^2	110	PRINT "MEAN VALUE X="; J
L 12	V_x	120	PRINT "VARIANCE X="; K
M 13	$\bar{y}$	130	PRINT "COE VAR X="; L
N 14	σ_y^2	140	PRINT "MEAN VALUE Y="; M
O 15	V_y	150	PRINT "VARIANCE Y="; N
P 16	ρ_{xy}	160	PRINT "COE VAR Y="; O
Q 17		170	PRINT "COR COE="; P
R 18		180	END
S 19			
T 20			
U 21			
V 22			
W 23			
X 24			
Y 25			
Z 26			

Title PEM-1 (Point Estimate Method - 1 Variable)

Description:

The point estimate method is used to evaluate the statistical moment of a function of one random variable. Probabilities P_+ and P_- at points x_+ and x_- are equal to

$$P_+ = \frac{1}{2}\left(1 + \left(1 - \frac{1}{1 \pm \left(\frac{\alpha_3}{2}\right)^2}\right)^{1/2}\right)$$

$$P_- = 1 - P_+$$

and

$$x_+ = \bar{x} + \sigma_x (P_+/P_-)^{1/2}$$

$$x_- = \bar{x} - \sigma_x (P_-/P_+)^{1/2}$$

in which $\bar{x}$ is the mean, σ_x is the standard deviation, and α_3 is the coefficient of skewness of x. The expected value and coefficient of variation of function $y = y(x)$ are equal to

$$E[y] = P_+ y(x_+) + P_- y(x_-)$$

$$V_y = \left(P_+ y(x_+)^2 + P_- y(x_-)^2 - E[y]^2\right)^{1/2} / E[y].$$

Example:

$y = x^2 + 3x - 4$ (Line 200 of PEM-1 contains this function)

$\bar{x} = 4$

$\sigma_x = 1.5$

$\alpha_3 = 0.5$

	Input	Display	Note		Input	Display	Note
1	RUN	MEAN=		11			
2	4 ENTER	SID.=		12			
3	1.5 ENTER	SKEWNESS=		13			
4	.5 ENTER			14			
5		35.063 5.027E-01	$\bar{y}$, V_y	15			
6				16			
7				17			
8				18			
9				19			
10				20			

Title	

		Memory content	Line number	Statements
A	1	α_3	10	INPUT "MEAN="; W,"STD. DEV.="; S,
B	2			"SKEWNESS="; A
C	3		20	P = 0.5*(1+√(1-1/(1+(A/2)↑2)))
D	4		30	Q = 1 - P
E	5		40	X = W+S*√(P/Q)
F	6	$y(x_+)$ & $y(x_-)$	50	Y = W-S*√(Q/P)
G	7		60	Z = X:GOSUB200
H	8		70	M = P*F:V=P*F*F
I	9		80	Z = Y:GOSUB200
J	10		90	M=M+Q*F:V=√(V+Q*F*F-M*M)/M
K	11		100	PRINT M,V
L	12		110	END
M	13	E[y]	200	F = Z ↑ 2 + 3&z - 4
N	14		210	RETURN
O	15			
P	16	P_+		
Q	17	P_-		
R	18			
S	19	σ		
T	20			
U	21			
V	22	V_y		
W	23	$\bar{x}$		
X	24	x_+		
Y	25	x_-		
Z	26	Temp. x_+, x_-		

Title PEM-2 (Point Estimate Method - 2 Variables)

Description:

The expected value and coefficient of variation of a function of two correlated random variables are determined using the point estimate method. If $\bar{x}_1$, σ_1 and $\bar{x}_2$, σ_2 are the mean values and standard deviations of x_1 and x_2, respectively and ρ is their correlation coefficient, one has

$$P_{++} = P_{--} = (1+P)/4$$
$$P_{+-} = P_{-+} = (1-P)/4$$
$$x_{1+} = \bar{x}_1 + \sigma_1$$
$$x_{1-} = \bar{x}_1 - \sigma_1$$
$$x_{2+} = \bar{x}_2 + \sigma_2$$
$$x_{2-} = \bar{x}_2 - \sigma_2$$

The statistical moments of $y = y(x_1,x_2)$ are found from the following expression:

$$E[y^n] = P_{++}\, y_{++}^n + P_{+-}\, y_{+-}^n + P_{-+}\, y_{-+}^n + P_{--}\, y_{--}^n$$

in which $y_{++} = y(x_{1+},x_{2+})$, $y_{+-} = y(x_{1+}, x_{2-})$, etc.

Example: $y = \dfrac{x_1 + 2x_2}{3}$ (Line 200 of PEM-2 contains this function)

$\bar{x}_1 = 4.0$

$\sigma_1 = 1.5$

$\bar{x}_2 = 6.0$

$\sigma_2 = 1.0$

$\rho = 0.5$

	Input	Display	Note		Input	Display	Note
1	RUN	MEAN VALUES=		11			
2	4 ENTER	?		12			
3	6 ENTER	STD. DEVS.=		13			
4	1.5 ENTER	?		14			
5	1 ENTER	CORR. COEFF=		15			
6	.5 ENTER			16			
7		5.333 1.90E-01	$\bar{y}$, V_y	17			
8				18			
9				19			
10				20			

Title PEM-2

Memory content			Line number	Statements
A	1	$\bar{x}_1$	10	CLEAR:INPUT "MEAN VALUES="; A, B,
B	2	$\bar{x}_2$		"STD. DEVS.="; C, D," CORR.
C	3	σ_1		COEF.="; E
D	4	σ_2	20	F=(1+E)/4:G=(1-E)/4
E	5	ρ	30	H=A+C:I=A-C:J=B+D:K=B-D
F	6	P_{++}	40	L=H:M=J:N=F:GOSUB200
G	7	P_{+-}	50	GOSUB300
H	8	x_{1+}	60	M=K:N=G:GOSUB200
I	9	x_{1-}	70	GOSUB300
J	10	x_{2+}	80	L=I:M=J:GOSUB200
K	11	x_{2-}	90	GOSUB300
L	12	Dummy for x_1	100	M=K:N=F:GOSUB200
M	13	Dummy for x_2	110	GOSUB300
N	14	Dummy for P	120	Q=√(Q-P^2)/P
O	15	$y(x_1,x_2)$	130	PRINT P, Q
P	16	$\bar{y}$	140	END
Q	17	V_y	200	0 = (L + 2M)/3
R	18		210	RETURN
S	19		300	P = P + 0 * N
T	20		310	Q = Q + 0 ^ 2 * N
U	21		320	RETURN
V	22			
W	23			
X	24			
Y	25			
Z	26			

Title PEM-3 (Three-Point Estimate Method)

Description:

The three-point estimate method is used to evaluate the statistical moments of a function of one random variable. The probabilities P_-, P_o and P_+ at points x_-, $\bar{x}$, and x_+, respectively are

$$P_o = 1 - \frac{1}{\alpha_4 - \alpha_3^2}$$

$$P_- = \frac{1}{\alpha_4 - \alpha_3^2}\left\{4 + \frac{\alpha_3^2}{\alpha_4 - \alpha_3^2} \pm \left[\frac{4\alpha_3^2}{\alpha_4 - \alpha_3^2} + \left(\frac{\alpha_3^2}{\alpha_4 - \alpha_3^2}\right)^2\right]^{1/2}\right\}^{-1}$$

$$P_+ = \frac{1}{\alpha_4 - \alpha_3^2} - P_-$$

and

$$x_+ = \bar{x} + \sigma_x \left[P_+\left(1 + \frac{P_+}{P_-}\right)\right]^{-1/2}$$

$$x_- = \bar{x} - \frac{P_+}{P_-}(x_+ - \bar{x})$$

in which $\bar{x}$ is the mean, σ_x is the standard deviation, α_3 is the coefficient of skewness, and α_4 is the coefficient of kurtosis of x. The expected value and coefficient of variation of the function y = y(x) are

$$E[y] = P_+ y(x_+) + P_o y(\bar{x}) + P_- y(x_-)$$

$$V_y = \left(P_+ y(x_+)^2 + P_o y(\bar{x})^2 + P_- y(x_-)\right)^{1/2} / E[y]$$

Example: $y(x) = e^{-3x}$ (Line 200 of PEM-3 contains this function)

$\bar{x} = 0.0$

$\sigma_x = 1.0$

$\alpha_3 = 0.0$

$\alpha_4 = 2.14$

	Input	Display	Note		Input	Display	Note
1	RUN	MEAN=		11			
2	0.ENTER	STD. DEV=		12			
3	1 ENTER	SKEWNESS=		13			
4	0.ENTER	KURTOSIS=		14			
5	2.14ENTER			15			
6		19.35 1.746	$\bar{y}$, V_y	16			
7				17			
8				18			
9				19			
10				20			

Title PEM-3

Memory content			Line number	Statements
A	1	$\bar{x}$	10	CLEAR:INPUT "MEAN="; A," STD.
B	2	σ_x		DEV="; B,"SKEWNESS="; C,
C	3	α_3; α_3^2		"KURTOSIS="; D
D	4	α_4; $\alpha_4 - \alpha_3^2$	20	L=1:IFC>1 LET L=1
E	5	P_o	30	C=C*C:D=D-C:E=1-1/D
F	6	P_-	40	F=2/D/(4+C/D+L*√(4*C/D
G	7	P_+		+ (C/D)^2))
H	8	x_+	50	G = 1/D-F
I	9		60	H = A+B/√(G*(1+G/F))
J	10	Σy; $\bar{y}$	70	I = A-G/F*(H-A)
K	11	Σy^2; V_y	80	M = A:N=E:GOSUB200
L	12	dummy	90	M = H:N=G:GOSUB200
M	13	dummy x	100	M = I:N=F:GOSUB200
N	14	dummy P	110	K = √(K-J*J)/J
O	15	y	120	PRINT J,K
P	16		130	END
Q	17		200	O = EXP(-3*M)
R	18		210	J = J+O*N
S	19		220	K = K+O*O*N
T	20		230	RETURN
U	21			
V	22			
W	23			
X	24			
Y	25			
Z	26			

Title AMCDM (Average Mean-Crossings Distance Method)

Description:

This program finds the correlation length ℓ using the average mean-crossings distance method. The points of intersection of $x(z)$ and $\bar{x}(z)$ denoted by C are found by making linear extrapolation of $x(z)$ between the data points x_i and x_{i-1} at uniform sampling intervals Δz_o. The correlation length is found to be equal to

$$\ell = \frac{C_m - C_o}{m}$$

in which C_m and C_o are the depths of the last and first mean-crossings and m is the number of intervals between crossings.

Example: N = 5 x_i = 1.7, 1.0, 2.3, 2.0, 1.5

Δz_o = 1.0

	Input	Display	Note		Input	Display	Note
1	RUN	NO OF SAMPLES=		11			
2	5 ENTER	PROP VALUE=		12			
3	1.7 ENTER	PROP VALUE=		13			
4	1.0 ENTER	PROP VALUE=		14			
5	2.3 ENTER	PROP VALUE=		15			
6	2.0 ENTER	PROP VALUE=		16			
7	1.5 ENTER			17			
8		1.8 2.	ℓ m	18			
9				19			
10				20			

Title AMCDM

		Memory content	Line number	Statements
A	1	counter	10	CLEAR:INPUT "No. of Samples="; B
B	2	No. of samples	20	FOR A = 10 TO B + 9
C	3	mean value	30 40	INPUT "PROP VALUE="; A(A) C = C+A(A)
D	4	depth of first crossing	50	NEXT A
E	5	No. of δ_i = m	60	C = C/B:E = -1
F	6	Depth of crossing	70	FOR A = 11 TO B + 9
G	7	$z_n - D$	80	IF (A(A-1)-C)*(A(A)-C)>0 GO TO 130
H	8	Δz_o	90	IF A(A-1) = A(A) GO TO 130
I	9	corr. length = ℓ	100	F = (C-A(A-1))/(A(A)-A(A-1))+A-2
J	10	A(10) Soil Prop Pt1	110	IF E = -1 LET D = F
K	11	A(11) Soil Prop Pt2	120	E = E + 1
L	12	:	130	NEXT A
M	13	.	140	G = F - D
N	14	.	150	IF G=0 PRINT "Only one crossing": GO TO 190
O	15	A(B+9)=Soil Prop at Point B	160	INPUT "Sample Distance="; H
P	16		170	I = G/E*H
Q	17		180	PRINT I, E
R	18		190	END
S	19			
T	20			
U	21			
V	22			
W	23			
X	24			
Y	25			
Z	26			

Title MAM (Moving Average Method)

Description:

This program uses the moving average method to determine the correlation length ℓ of a set of data. The correlation length is found by minimizing the error between the variance reduction function (i.e., $\Gamma(k) = \sigma_k/\sigma_1$) and its best fit (i.e., $\Gamma^2(k) = k^*/k$). For N data points, k^* is given by

$$k^* = \text{Min}\left[\frac{1}{N-2}\sum_{k=1}^{N-1}\left(\frac{\sigma_k^2}{\sigma_1^2} - \frac{k^*}{k}\right)^2\right]$$

The correlation length is found to be equal to

$$\ell = 2\Delta z_o \{\ell n[(k^*+1)/(k^*-1)]\}$$

where Δz_o is the distance between adjacent samples.

Example:

x	; Δz_o = 1.0
1.7	
1.0	
1.9	
2.3	
1.6	

	Input	Display	Note		Input	Display	Note
1	RUN	NO OF SAMPLES=		11			
2	5 ENTER	PROP VALUE=		12			
3	1.7 ENTER	PROP VALUE=		13			
4	1.0 ENTER	PROP VALUE=		14			
5	1.9 ENTER	PROP VALUE=		15			
6	2.3 ENTER	PROP VALUE=		16			
7	1.6 ENTER			17			
8		SAMPLE DISTANCE=		18			
9	1. ENTER			19			
10		1.2 8.34E-01	k^*, ℓ	20			

Title	

Memory content			Line number	Statements
A	1	counter for R; slope: ℓ	10	CLEAR:INPUT "No. of Samples="; B
B	2	No. of Samples; counter: Δz_o	20	FOR A=26 TO B + 25
C	3	counter of n	30	INPUT "Soil Property="; A(A)
D	4	$\Sigma \bar{r}_i$; K^*	40	NEXT A
E	5	$\Sigma \bar{r}_i^2$; Error	50	FOR C = 1 TO 15:BEEP C
F	6	counter; counter for K*	60	IF B=C LET C=C-1:GO TO 180
G	7	i+n; n_{max}	70	D = 0:E = 0
H	8	Σr_i, Error min.	80	FOR F = 1 TO B-C+1
I	9	K^*_{min}	90	G = C+F-1:H=0
J	10	$r^2(1)$	100	FOR A = F TO G
K	11	$r^2(2)$	110	H = H + A(A+25)
L	12	$r^2(3)$	120	NEXT A
M	13	$r^2(4)$	130	D=D+H/C:E=E+(H/C)^2
N	14	$r^2(5)$	140	NEXT F
O	15	$r^2(6)$	150	A(C+9)=(E-D^2/(B-C+1))/(B-C)
P	16	$r^2(7)$	160	IF C<>1LET A(C+9)=A(C+9)/J
Q	17	$r^2(8)$	170	NEXT C
R	18	Soil Property Pt 1	180	G = C:B=11:J=1:H=9
S	19	Soil Property Pt 2	190	FOR F=1 TO 20:BEEP 2
T	20	.	200	D = 1.0+2*F:A=-1:E=0
U	21	.	210	IF D=B-9 LET B=B+1 GO TO 230
V	22	.	220	E=A(B)-(A(A-1)-A(B))*(D-B+10):E=(1-E)^2:A=0
W	23	R(B) Soil Prop PtB	230	FOR C = 2 TO G
X	24		240	IFC<DLETE=E+(1-A(C+(9)^2:A=A+1:GOTO260
Y	25		250	E=E+(ABS(A(C+9)-D/C))^2:A=A+1
Z	26		260	NEXT C
			270	IF H>=E/A LET H=E/A:I=D
			280	NEXT F
			290	BEEP15:INPUT "Sample Distance="; B
			300	A=2*B/LN((I+1)/(I-1))
			310	PRINT I,A
			320	END

Title QSARM

Description:

This program uses the quasi-stationary autoregressive method to evaluate the correlation length ℓ of a set of data. The modeling parameters β_o and β_1 are determined by the least squared error method of the data. The correlation length is found to be equal to

$$\ell = \frac{\Delta z_o}{\ell n|\beta_1|}$$

where z_o is the distance between adjacent samples

Example:

x	z
1.7	2
1.0	3
1.9	4
2.3	5
1.6	6

, $\Delta z_o = 1.0$

	Input	Display	Note		Input	Display	Note
1	RUN	NO OF SAMPLES=		11	6 ENTER	PROP VALUE=	
2	5 ENTER	z=		12	1.6 ENTER		
3	2 ENTER	PROP VALUE=		13		SAMPLE DISTANCE=	
4	1.7 ENTER	z=		14	1. ENTER		
5	3 ENTER	PROP VALUE=		15		5.46E-01 4.21E-02	β_1, β_o
6	1.0 ENTER	z=		16	ENTER	1.65 9.	ℓ, H
7	4 ENTER	PROP VALUE=		17			
8	1.9 ENTER	z=		18			
9	5 ENTER	PROP VALUE=		19			
10	2.3 ENTER	z=		20			

Title QSARM

	Memory content		Line number	Statements
A	1	Σu_i	10	CLEAR:INPUT "No of Samples="; N
B	2	Σu_i^2	20	FOR K=1 TO N
C	3	Σu_{i-1}	30	INPUT "Z="; z, "PROP VALUE="; P
D	4	Σu_{i-1}, u_i	40	V = P/Z
E	5	Working Space	50	A=A+U:B=B+U*U
F	6	β_1	60	N = N + 1
G	7	β_o	70	IF K=1 GO TO 100
H	8	Δz_o	80	C = C + U
I	9	Correlation Length	90	D = D + U*V
J	10	Thickness of Soil	100	V=U:BEEP2:NEXT K
K	11	counter	110	A=A-U:B=B-U*U:N=N-1
L	12		120	E=N*B-A*A
M	13		130	F=(N*D-A*C)/E
N	14	Number of Points	140	G=(B*C-A*D)/E
O	15		150	INPUT "SAMPLE DIST.="; H
P	16	Soil Property	160	I=-H/LNABS(F):J=H*N
Q	17		170	PRINT F,G:PRINT I,J
R	18		180	END
S	19			
T	20			
U	21	$P/z = u_i$		
V	22	u_{i-1}		
W	23			
X	24			
Y	25			
Z	26	Depth		

Title COULOMB (Coulomb Method-Active)

Description:

This program finds the active earth thrust against a retaining wall using Coulomb's Theory, i.e.,

$$P_A = \frac{1}{2}\frac{\gamma H^2}{\tan\theta}\left[\frac{\csc\beta\,\sin(\beta-\phi)}{\{\sin(\beta+\delta)\}^{1/2} + \{\frac{\sin(\phi-\delta)\sin(\phi-i)}{\sin(\beta-i)}\}^{1/2}}\right]^2$$

in which P_A = active earth thrust,
γ = unit weight of the backfill,
H = height of the retaining wall,
ϕ = angle of internal friction of backfill,
δ = angle of wall friction
β = inclination of wall from the vertical, and
i = inclination of backfill.

Example: H = 10 ft.
ϕ = 30°
δ = 10°
γ = 100 pcf
β = 5°
i = 0°

	Input	Display	Note		Input	Display	Note
1	RUN	H=		11			
2	10 ENTER	PHI=		12			
3	30 ENTER	DELTA=		13			
4	10 ENTER	UNIT WGT=		14			
5	100 ENTER	BETA=		15			
6	5 ENTER	I=		16			
7	0 ENTER			17			
8		COULOMB.PA=858.8	P_A	18			
9				19			
10				20			

Title COULOMB

Memory content			Line number	Statements
A	1	H	10	INPUT "H="; A "PHI="; B, "DELTA=";
B	2	ϕ		C, "UNIT WGT=", D, "BETA=", E,
C	3	δ		"I=",; F
D	4	γ	20	G=SIN(E-B)/COSE
E	5	β	30	H=$\sqrt{}$ SIN(E+C)
F	6	i	40	IF E-F<0 PRINT "NO SOLUTION
G	7	csc β sin($\beta-\phi$)		POSSIBLE":GO TO 80
H	8	sin($\beta+\delta$)	50	I= (SIN(B+C)*SIN(B-F)/SIN(E-F))
I	9	$\frac{\sin(\phi+\delta)\sin(\phi-i)}{\sin(\beta-i)}$	60	J=D*A*A/2*(G*H*I)*(G*H*I)
J	10	P_A	70	PRINT "COULOMB,PA=",J
K	11		80	END
L	12			
M	13			
N	14			
O	15			
P	16			
Q	17			
R	18			
S	19			
T	20			
U	21			
V	22			
W	23			
X	24			
Y	25			
Z	26			

Title M-O (Mononobe-Okabe Method)

Description:

This program determines the active earth thrust P_{AE} against a retaining wall for seismic conditions using Mononobe-Okabe's method. The expression for P_{AE} is

$$P_{AE} = \frac{1}{2} \gamma H^2 (1+k_v) \cdot K_{AE}$$

in which

$$K_{AE} = \frac{\cos^2(\phi-\theta-\beta)}{\cos\theta \cos^2\beta \cos(\delta+\beta+\theta) \left[1 + \frac{\sin(\phi+\delta)\sin(\phi-\theta-i)}{\cos(\delta+\beta+\theta)\cos(i-\beta)}\right]^2}$$

P_{AE} = the seismic active earth thrust,
γ = the unit weight of the backfill,
H = the height of the retaining wall,
k_v = the vertical component of the ground acceleration,
k_h = the horizontal component of the ground acceleration,
ϕ = the angle of internal friction of backfill,
β = inclination of wall from the vertical,
i = inclination of backfill,
δ = the angle of wall friction, and
$\theta = \tan^{-1}\left(\frac{k_h}{1+k_v}\right)$.

Example: γ = 100 pcf; $\beta = 5°$; H = 10 ft.; $i = 0°$; $\phi = 30°$; $a_h = 0.2g$; $\delta = 10°$; $a_v = 0.0g$

	Input	Display	Note		Input	Display	Note
1	RUN	H=		11			
2	10 ENTER	PHI=		12			
3	30 ENTER	DELTA=		13			
4	10 ENTER	BETA=		14			
5	5 ENTER	I=		15			
6	0 ENTER	VERT ACC=		16			
7	0 ENTER	HORZ ACC=		17			
8	2 ENTER	UNIT WGT=		18			
9	100 ENTER			19			
10		M-O,PAE=2469.	P_{AE}	20			

Title M-O

Memory content			Line number	Statements
A	1	H	10	INPUT"H=";A,"PHI=";B,"DELTA=";C,"BETA="
B	2	ϕ		D,"I=";E,"VERT ACC=";F,"HORZ ACC=";G
C	3	δ	20	INPUT "UNIT WGT=";H
D	4	β	30	I = ATN (G/(1+F))
E	5	i	40	IF B-I-E<0 GO TO 120
F	6	k_v	50	J = COS(B-I-D)^2
G	7	k_h	60	J=J/COSI/COSD^2/COS(C+D+I)
H	8	γ	70	K=SIN(B+C)*SIN(B-I-E)
I	9	θ	80	K=K/COS(C+D+I)/COS(E-D)
J	10	K_{AE}	90	K=(1+$\sqrt{}$ K)^2:J=J/K
K	11	Working space	100	L=H/2*A^2*(1+F)*J
L	12	P_{AE}	110	PRINT "M-O, PAE="; L : GO TO 130
M	13		120	PRINT "NO SOLUTION POSSIBLE"
N	14		130	END
O	15			
P	16			
Q	17			
R	18			
S	19			
T	20			
U	21			
V	22			
W	23			
X	24			
Y	25			
Z	26			

Title SLM (Single Layer Model of Wall Backfill)

Description:

This program determines $E[P_{AE}]$, V_{PAE}, and $E[d_A]$ for a retaining wall in which the backfill is considered to consist of one layer and its ϕ strength parameter is a r.v. with mean $\bar{\phi}$ and variance σ^2/n_i. The ground acceleration is also a r.v. The parameters are defined as follows:

H = height of wall,
γ = unit weight of backfill material,
δ = angle of wall friction,
β = inclination of retaining wall ($\beta \neq 90°$),
i = inclination of backfill,
a_h = horizontal acceleration,
a_v = vertical acceleration, and
$\theta = 45° + \bar{\phi}/2$, angle of failure plane.

Example:

H = 10 ft.
γ = 100 pcf
$\bar{\phi}$ = 30°
V_ϕ = .20
δ = 10°
β = 85°
i = 0°
a_h = 0.2g
a_v = 0.0g
V_i = .10
n_i = 4

	Input	Display	Note		Input	Display	Note
1	RUN	H=		11	.1 ENTER	VERT/HORZ=	
2	10 ENTER	PHI=		12	0 ENTER		
3	30 ENTER	VPHI=		13		2319. 7.80E-02	$E[P_{AE}], V_D$
4	.2 ENTER	NI=		14	ENTER	4.304	$E[d_A]$
5	4 ENTER	DELTA=		15			
6	10 ENTER	BETA=		16			
7	85 ENTER	I=		17			
8	0 ENTER	UNIT WGT=		18			
9	100 ENTER	HORZ ACC=		19			
10	.2 ENTER	VACC=		20			

Title SLM

Memory content			Line number	Statements
A	1	height H	10	INPUT"H=";A,"PHI=";B,"VPHI=";C,NI=";D
B	2	$\bar{\phi}$	20	INPUT"DELTA=";E,"BETA=",F,"I=";G,"UNIT WGT=";H
C	3	V_{ϕ}	30	INPUT"HORZ ACC=";I,"VACC=";J,"VERT/HORZ=";K
D	4	n_i	40	L = 45+B/2
E	5	δ	50	M=B*(1+C/√D):N=B*(1-C/√D):O=I*(1+J):P=I*(1-J)
F	6	β	60	Q=TANF:R=TANG:S=TANL
G	7	i	70	M=TAN(L-M):N=TAN(L-N)
H	8	γ	80	T=TAN(F-E):V=SIN(F-E)
I	9	$\bar{a}_h$; PEM counter	90	W=H*A*A/2/U*(1*S/Q)*(1+R/Q)/(S-R)
J	10	V_a; PEM counter	100	X=0:Y=0:Z=I:BEEP3
K	11	a_v/a_h	110	FOR I = 13 TO 14
L	12	θ	120	FOR J = 15 TO 16
M	13	ϕ_+ $\tan(\theta-\phi_+)$	130	V=W*(A/J)+(1+A(J)*K)*A(I))/(1+A(I)/T)
N	14	ϕ_-; $\tan(\theta-\phi_-)$	140	X=X+V/4:Y=Y+V*V/4
O	15	a_{h+}	150	NEXT J
P	16	a_{h-}	160	NEXT I
Q	17	$\tan\beta$	170	Z=A/3*(W*Z/X*(1+S/Q)+(1+1/S/T)
R	18	tani		*(1-S/Q+R*(S+Q)/Q/(S-R)))/(1+1/Q/T)
S	19	$\tan\theta$		
T	20	$\tan(\beta-\delta)$	180	V=√(Y-X*X)/X
U	21	$\sin(\beta-\delta)$	190	PRINT X,V:PRINT Z
V	22	$P_{AE(PEM)}$	200	END
W	23	Weight of wedge		
X	24	ΣV		
Y	25	ΣV^2; V_P		
Z	26	d_A		